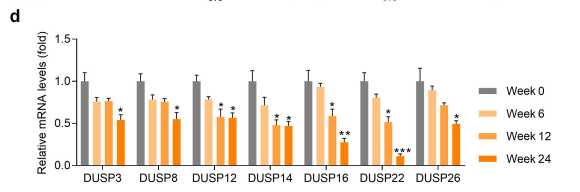
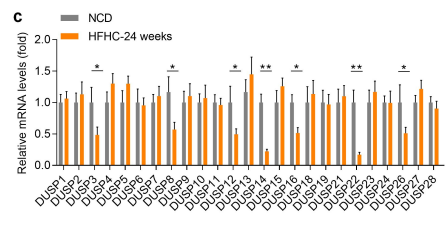
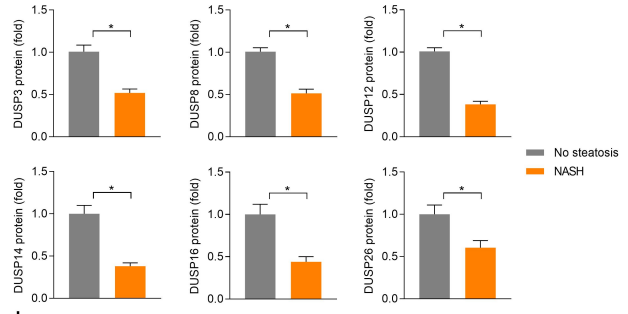
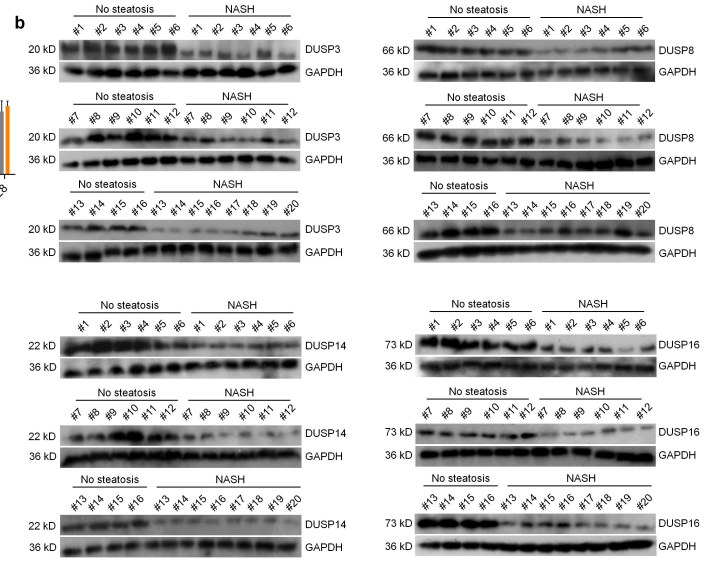
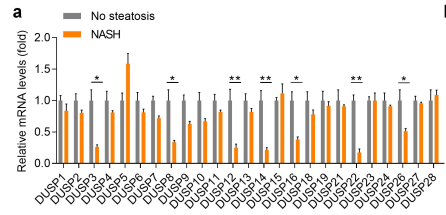


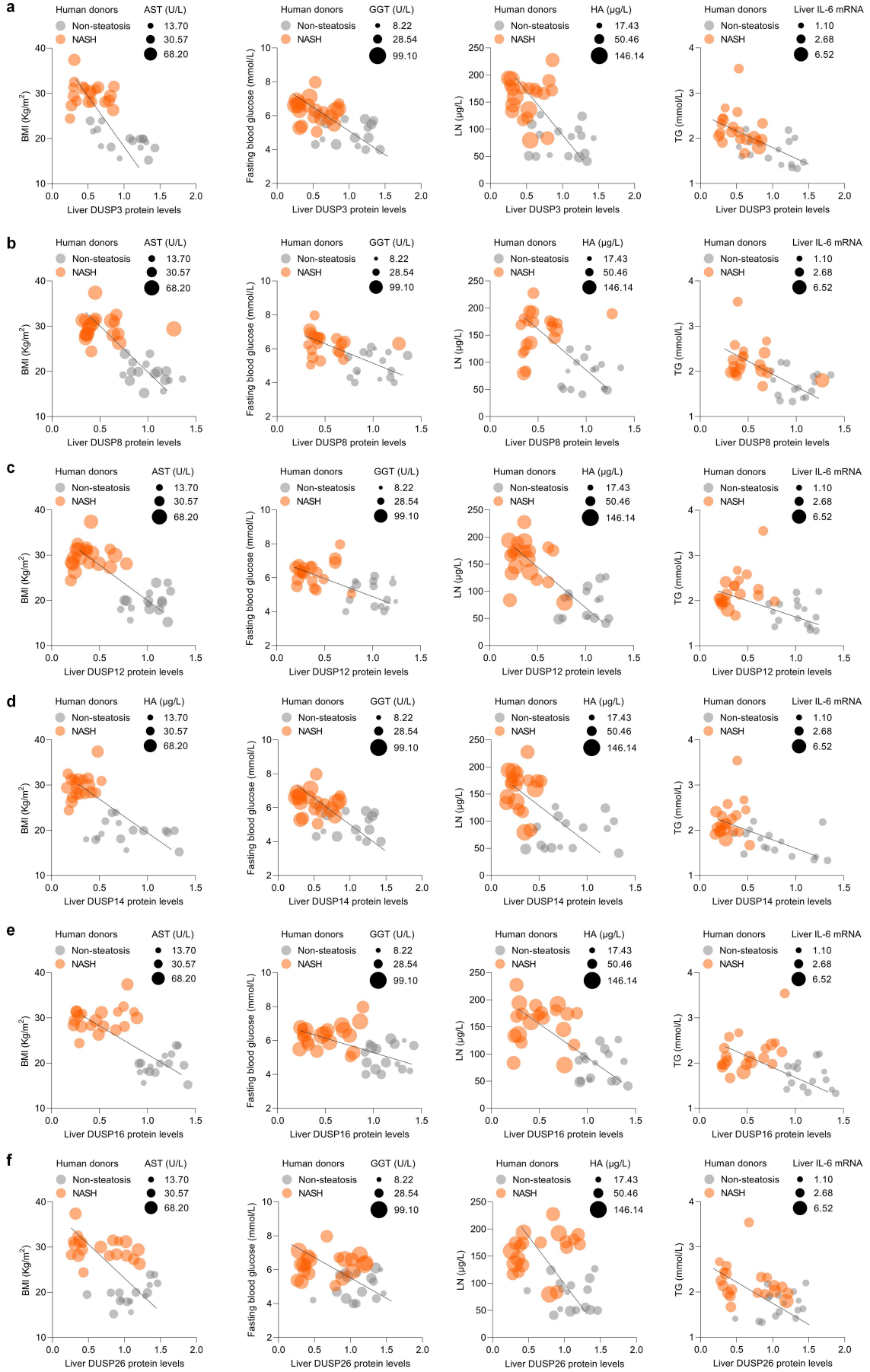
SUPPLEMENTARY INFORMATION for:

**Hepatocyte phosphatase DUSP22 mitigates NASH-HCC progression
by targeting FAK**

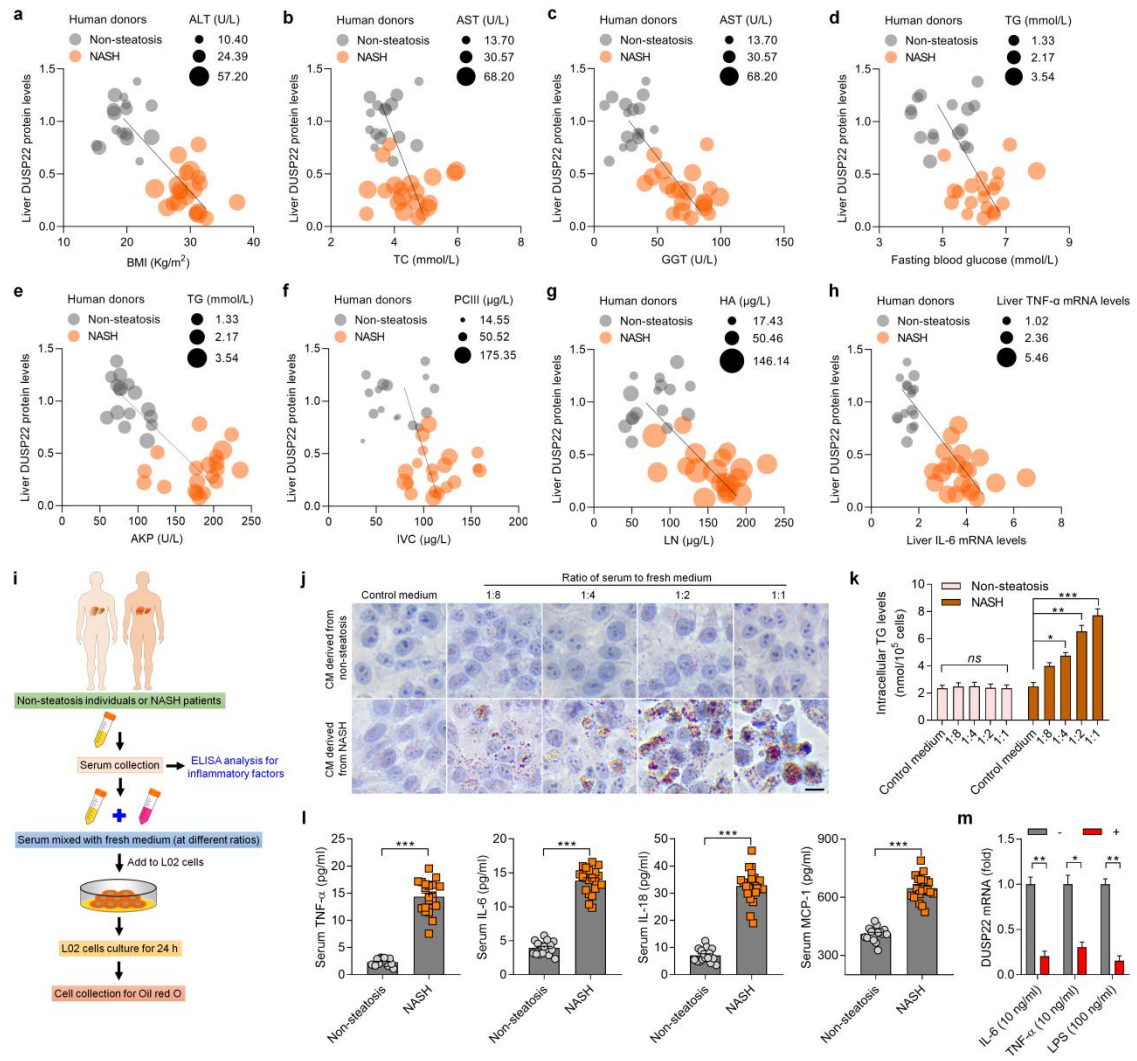
Ge et al.



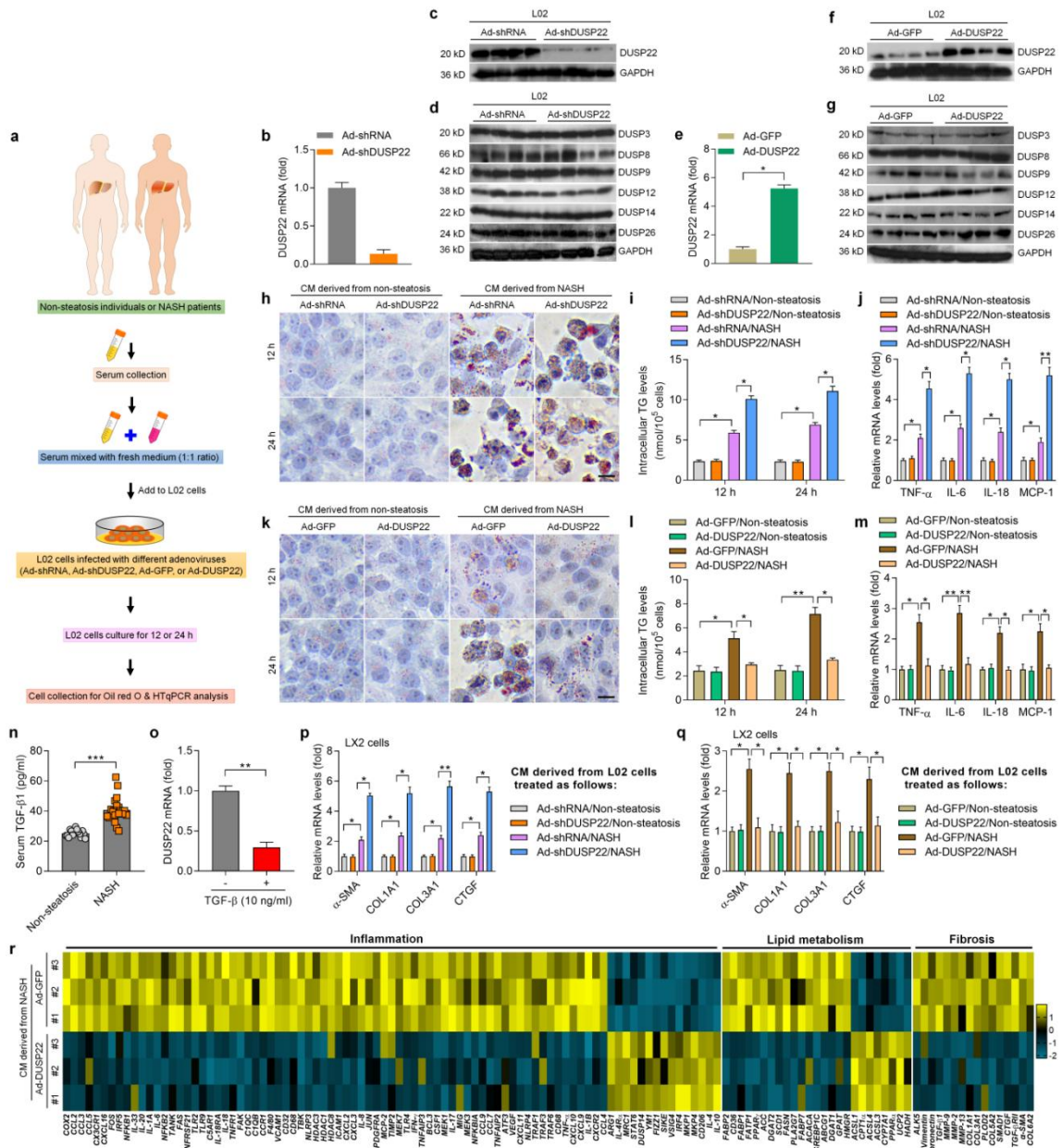
Supplementary Figure 1. DUSPs expression changes in clinical NASH patients and HFHC-induced mouse models. **a** RT-qPCR analysis for the mRNA expression levels of DUSPs family members in livers from individuals without (No steatosis; n=16) or with NASH (n=20) (* P <0.05 and ** P <0.01). **b** Western blotting results for DUSP3, DUSP8, DUSP12, DUSP14, DUSP16 and DUSP26 protein expression liver in livers from individuals without (No steatosis; n=16) or with NASH (n=20) (* P <0.05). **c** RT-qPCR analysis for the mRNA expression levels of DUSPs family members in livers isolated from mice fed with NCD or HFHC for 24 weeks (n=6 per group) (* P <0.05 and ** P <0.01). **d** RT-qPCR analysis for hepatic DUSP3, DUSP8, DUSP12, DUSP14, DUSP16, UDSP22 and DUSP26 gene expression levels of HFHC-treated mice at the shown time points (n=8 per group) (* P <0.05, ** P <0.01 and *** P <0.001). Data are expressed as mean \pm SEM from at least three independent experiments. For statistical analysis, **a-c** were conducted by two-tailed Student's t -test; **d** was performed by one-way ANOVA.



Supplementary Figure 2. Correlation analysis between the expression of several DUSPs family members with clinical NASH severity. a-f Pearson correlation analysis showing the correlations between human liver (a) DUSP3, (b) DUSP8, (c) DUSP12, (d) DUSP14, (e) DUSP16 and (f) DUSP26 protein expression levels and body mass index (BMI), fasting blood glucose levels, serum laminin (LN) and serum TG levels. n=36 subjects per parameter. Correlations were performed using Spearman's rank correlation coefficient analysis.

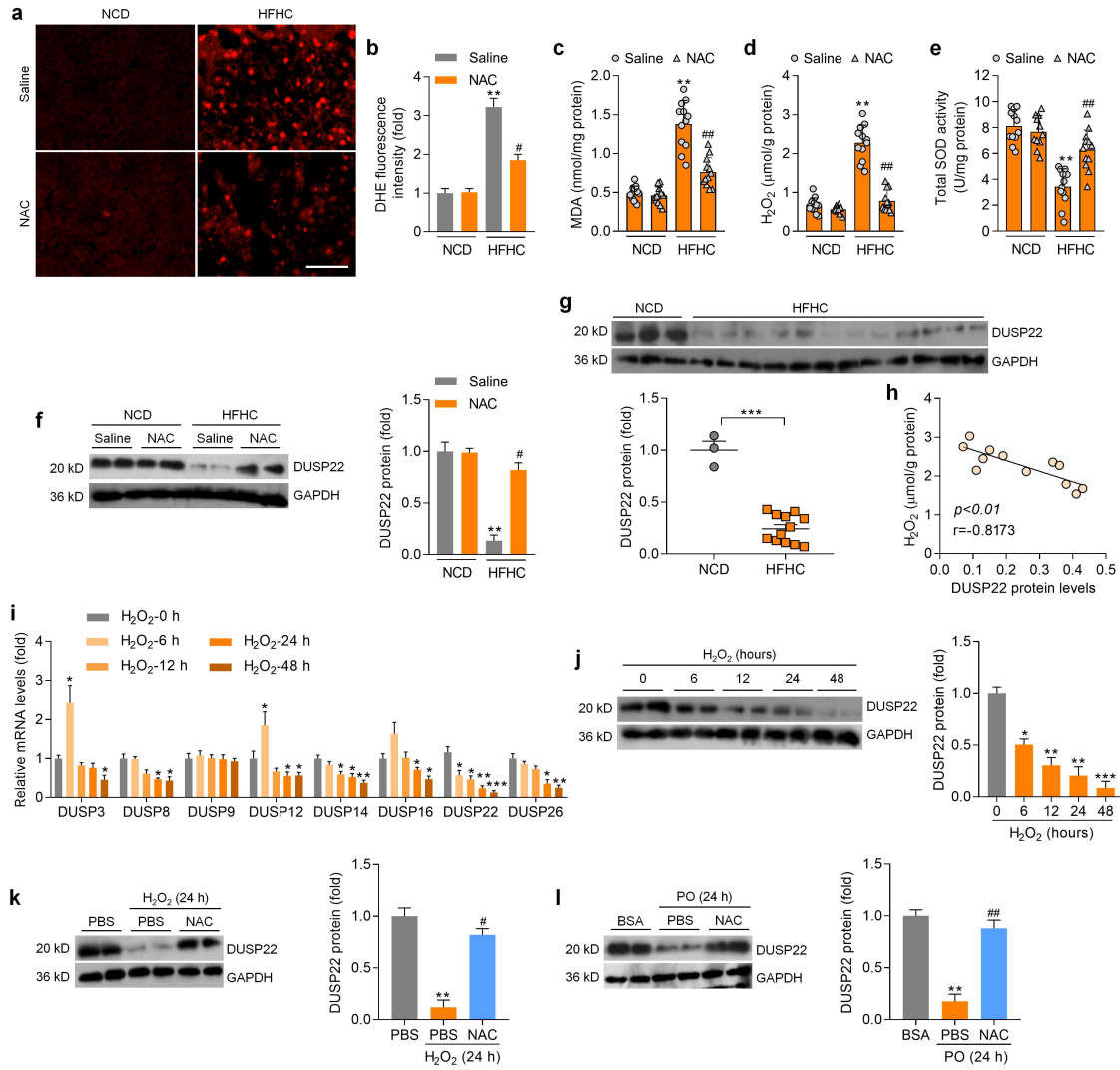


Supplementary Figure 3. DUSP22 is negatively correlated with NASH severity in human patients. a-h Pearson correlation analysis showing the correlations between human liver DUSP22 protein expression levels and (a) BMI, (b) serum TC levels, (c) serum γ -glutamyl transpeptidase (GGT) contents, (d) fasting blood glucose concentrations, (e) serum alkaline phosphatase (AKP) activities, (f) collagen Type IV (IVC), (g) serum LN, and (h) liver IL-6 mRNA expression levels. n=36 subjects per parameter. **i** Scheme showing the L02 cell culture in serum collected from NASH patients or Non-steatosis individuals. **j** Representative Oil red O staining images and **k** intracellular TG contents in L02 cells after 24 h culture in the conditional medium mixed with different ratios of serum from NASH or Non-steatosis individuals and fresh medium as shown. Fresh medium only was served as control (n=5 per group, with 10 images per group; Scale bar, 25 μ m) (* P <0.05, ** P <0.01 and *** P <0.001; *ns*, no significant difference). **l** Examination of inflammatory factors including TNF- α , IL-6, IL-18 and MCP-1 in serum collected from NASH or Non-steatosis individuals (n=36 subjects in total) (*** P <0.001). **m** RT-qPCR results for DUSP22 mRNA expression levels in L02 cells exposed to IL-6 (10 ng/ml), TNF- α (10 ng/ml) or LPS (100 ng/ml) for 24 h (n=4 per group) (* P <0.05 and ** P <0.01). Data are expressed as mean \pm SEM from at least three independent experiments. For statistical analysis, correlations in **a-h** were performed using Spearman's rank correlation coefficient analysis; **k-m** were conducted by two-tailed Student's *t*-test.

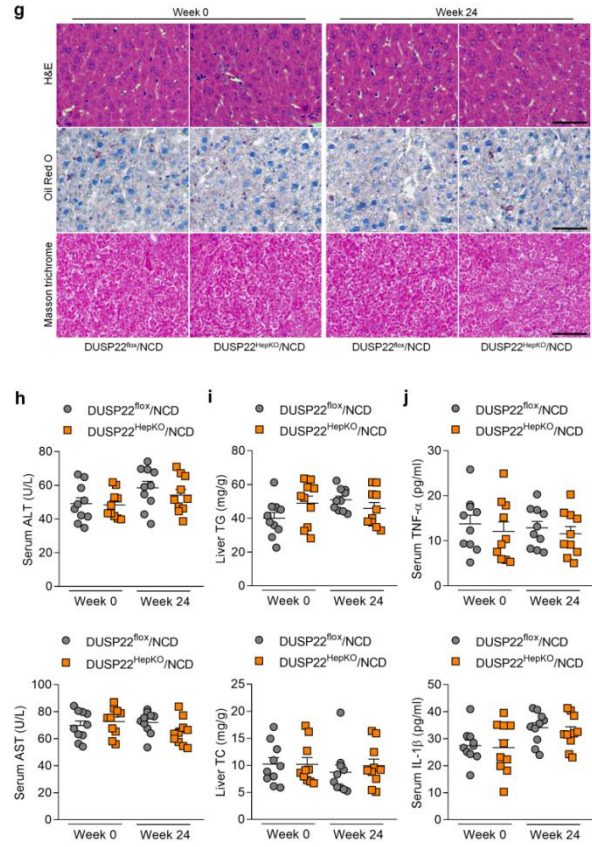
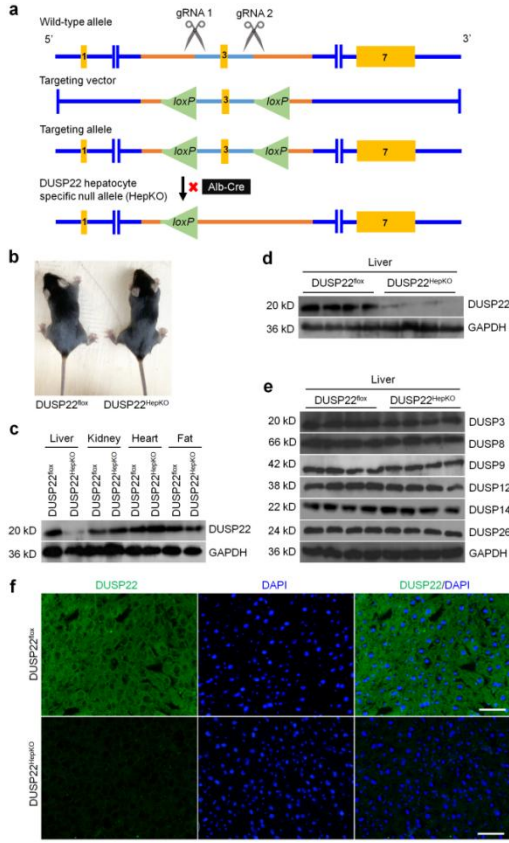


Supplementary Figure 4. Hepatocyte DUSP22 expression mitigates lipid deposition, inflammation and fibrosis *in vitro*. **a** Scheme showing the L02 cell culture in serum collected from NASH patients or Non-steatosis individuals after transfection with adenovirus-loaded short hairpin RNA targeting DUSP22 (Ad-shDUSP22) or adenovirus-loaded full-length DUSP22 sequences (Ad-DUSP22) for 24 h. Ad-shRNA and Ad-GFP were used as the corresponding controls. **b-d** (**b**) RT-qPCR and (**c**) western blotting analysis for mRNA and/or protein expression levels of DUSP22, (**d**) DUSP3, DUSP8, DUSP9, DUSP12, DUSP14 and DUSP26 in L02 cells transfected with Ad-shDUSP22 or Ad-shRNA for 24 h (n=4 per group). **e-g** (**e**) RT-qPCR and (**f**) western blotting analysis for mRNA and/or protein expression levels DUSP22, (**g**) DUSP3, DUSP8, DUSP9, DUSP12, DUSP14 and DUSP26 in L02 cells transfected with Ad-DUSP22 or Ad-GFP for 24 h (n=4 per group). **h,i** (**h**) Representative Oil red O staining images, and (**i**) intracellular TG contents in L02 cells that were transfected with Ad-shDUSP22 or Ad-shRNA after culture in the conditional medium (CM) mixed with NASH or Non-steatosis serum and fresh medium (1:1 ratio) for 12 or 24 h (n=5 per group, with 10 images per group; Scale bar, 25 μ m) (* P <0.05). **j** RT-qPCR results for inflammatory factors TNF- α , IL-6, IL-18 and MCP-1 in L02 cells transfected with Ad-shDUSP22 or Ad-shRNA after culture in the CM mixed with NASH or Non-steatosis serum and fresh medium (1:1 ratio) for 24 h (n=4 per group) (* P <0.05 and ** P <0.01). **k,l** (**k**) Representative Oil red O staining images, and (**l**) intracellular TG contents in L02 cells that were transfected with Ad-DUSP22 or Ad-GFP post culture in the CM mixed with NASH or Non-steatosis serum and fresh medium (1:1 ratio) for 12 or 24 h (n=5 per group, with 10 images per group; Scale bar, 25 μ m) (* P <0.05 and ** P <0.01). **m** RT-qPCR results for inflammatory factors TNF- α , IL-6, IL-18 and MCP-1 in L02 cells transfected with Ad-DUSP22 or Ad-GFP after culture in the CM mixed with NASH or Non-steatosis serum and fresh medium (1:1 ratio) for 24 h (n=4 per group) (* P <0.05 and ** P <0.01). **n** Assessment of TGF- β 1 in serum collected from NASH or Non-steatosis individuals (n=36 subjects in total) (** P <0.001). **o** RT-qPCR results for DUSP22 mRNA expression levels in L02 cells exposed to TGF- β 1 (10 ng/ml) for 24 h (n=4 per group) (** P <0.01). **p,q** CM was collected from L02 cells that were transfected with (**p**) Ad-shDUSP22, Ad-shRNA, (**q**) Ad-DUSP22 or Ad-GFP as shown after culture in the medium mixed with NASH or Non-steatosis serum and fresh medium (1:1 ratio) for 24 h (n=4 per group), and was then used for LX2 cell culture for another 24 h through mixing with fresh medium (1:1 ratio) (n=4 per group) (* P <0.05 and ** P <0.01). **r** HTqPCR analysis showing the alteration of inflammation (left) and lipid metabolism (middle) related genes expression in L02 cells treated as explained in (**m**), and the expression changes of fibrosis-related genes (right) in LX2 cells treated as described in (**q**) (n=3 per group). Data are expressed as mean \pm SEM from at least three

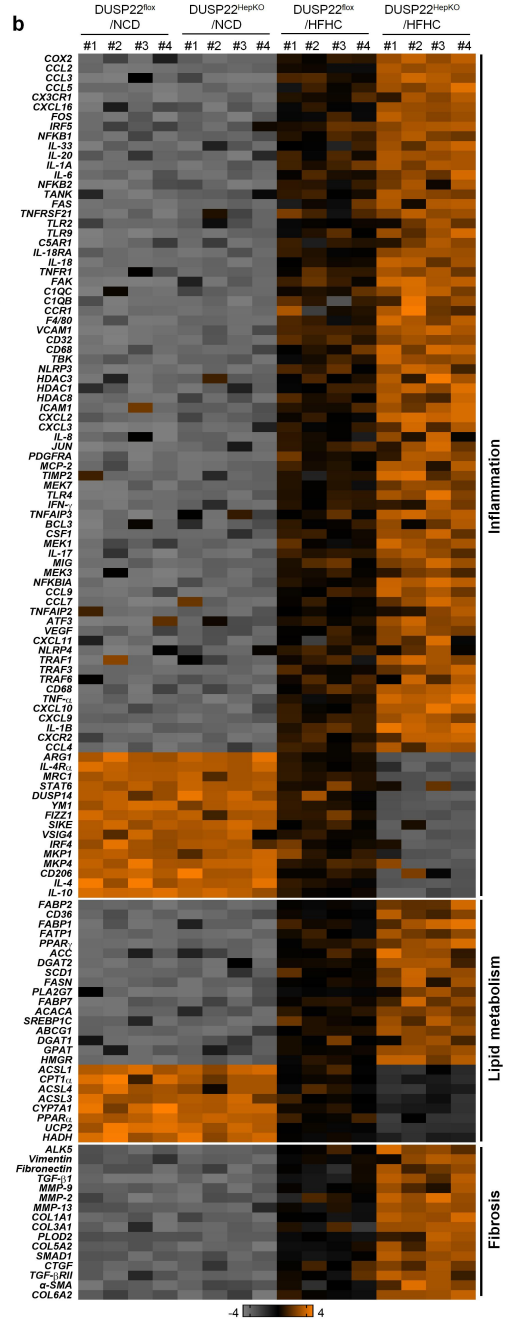
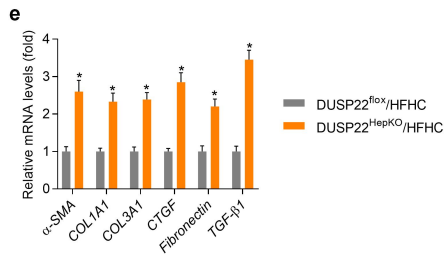
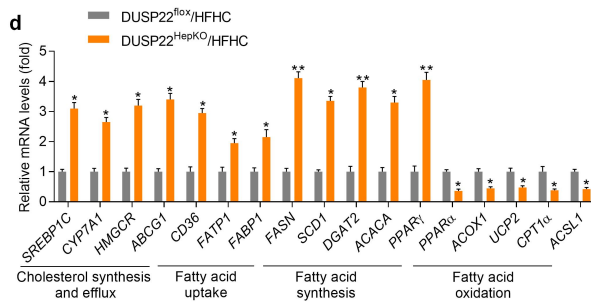
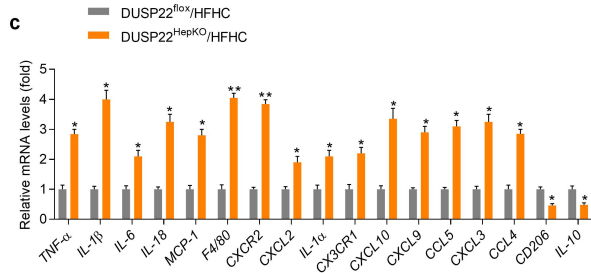
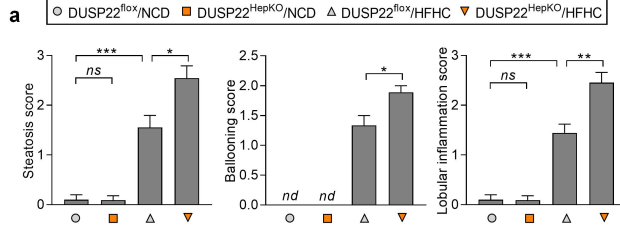
independent experiments. Statistical analysis were performed by two-tailed Student's *t*-test.



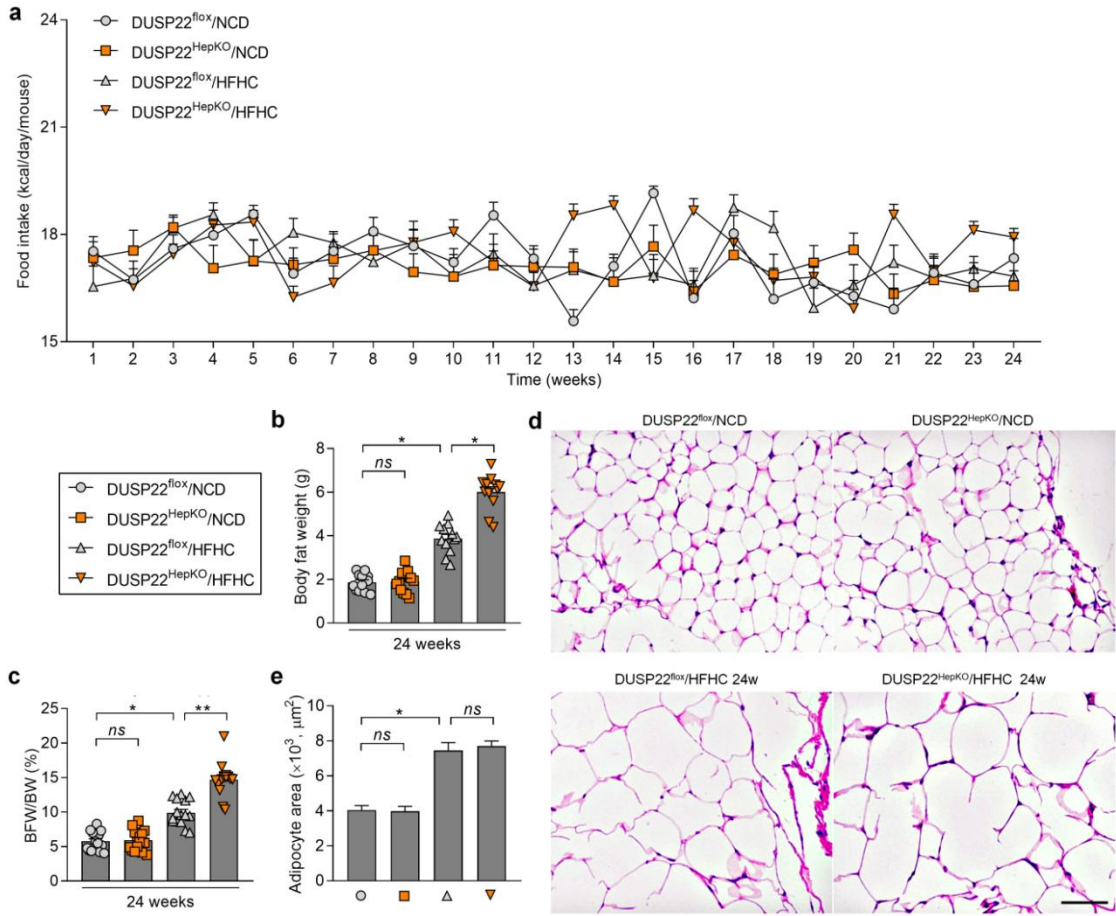
Supplementary Figure 5. ROS production negatively mediates DUSP22 expression during HFHC. **a** Representative image of DHE staining on the fresh frozen liver sections of WT mice after a 24-week HFHC feeding with or without NAC (N-acetyl-cysteine) administration (n=6 mice/group; Scale bar, 50 μ m). **b** Quantification for DHE fluorescent intensity in the liver samples of mice from the shown groups of mice (n=6 mice per group) (** P <0.01 versus the NCD/Saline group; # P <0.05 versus the HFHC/Saline group). **c-e** Examination for **(c)** MDA levels, **(d)** H₂O₂ contents, and **(e)** total SOD activity in liver tissues from the indicated groups of mice (n=11 or 12 mice per group) (** P <0.01 versus the NCD/Saline group; ## P <0.01 versus the HFHC/Saline group). **f** Representative western blotting analysis and quantification of DUSP22 protein expression in livers of the shown groups of mice (n=4 mice per group) (** P <0.01 versus the NCD/Saline group; # P <0.05 versus the HFHC/Saline group). **g** Representative western blotting analysis for DUSP22 in liver samples from NCD-fed mice (n=3) or 24-week HFHC-treated mice (n=12) (** P <0.001). **h** Pearson correlation analysis showing the correlation between hepatic DUSP22 protein expression levels and H₂O₂ contents from HFHC group of mice. **i** The mouse primary hepatocytes were incubated with H₂O₂ (100 μ M) for 6, 12, 24 or 48 h, and were then collected for RT-qPCR analysis of DUSP3, DUSP8, DUSP9, DUSP12, DUSP14, DUSP16, UDSP22 and DUSP26 gene expression levels (n=6 per group) (* P <0.05, ** P <0.01 and *** P <0.001 versus the H₂O₂-0 h group). **j** Protein expression of DUSP22 by western blotting analysis in mouse primary hepatocytes treated with H₂O₂ (100 μ M) for 6, 12, 24 or 48 h (n=4 per group) (* P <0.05, ** P <0.01 and *** P <0.001 versus the H₂O₂-0 h group). **k,l** Western blotting analysis for protein expression of DUSP22 in mouse primary hepatocytes treated with **(k)** H₂O₂ (100 μ M) or **(l)** PO (0.4 mM PA and 0.8 mM OA) for 24 h in the presence or absence of NAC (5 mM). PBS was used as control (n=4 per group) (** P <0.01 versus the PBS or BSA group; # P <0.05 and ## P <0.01 versus the H₂O₂/PBS or PO/PBS group). Data are expressed as mean \pm SEM from at least three independent experiments. For statistical analysis, **b-g**, **k** and **l** were conducted by two-tailed Student's *t*-test; **i** and **j** were performed by one-way ANOVA.



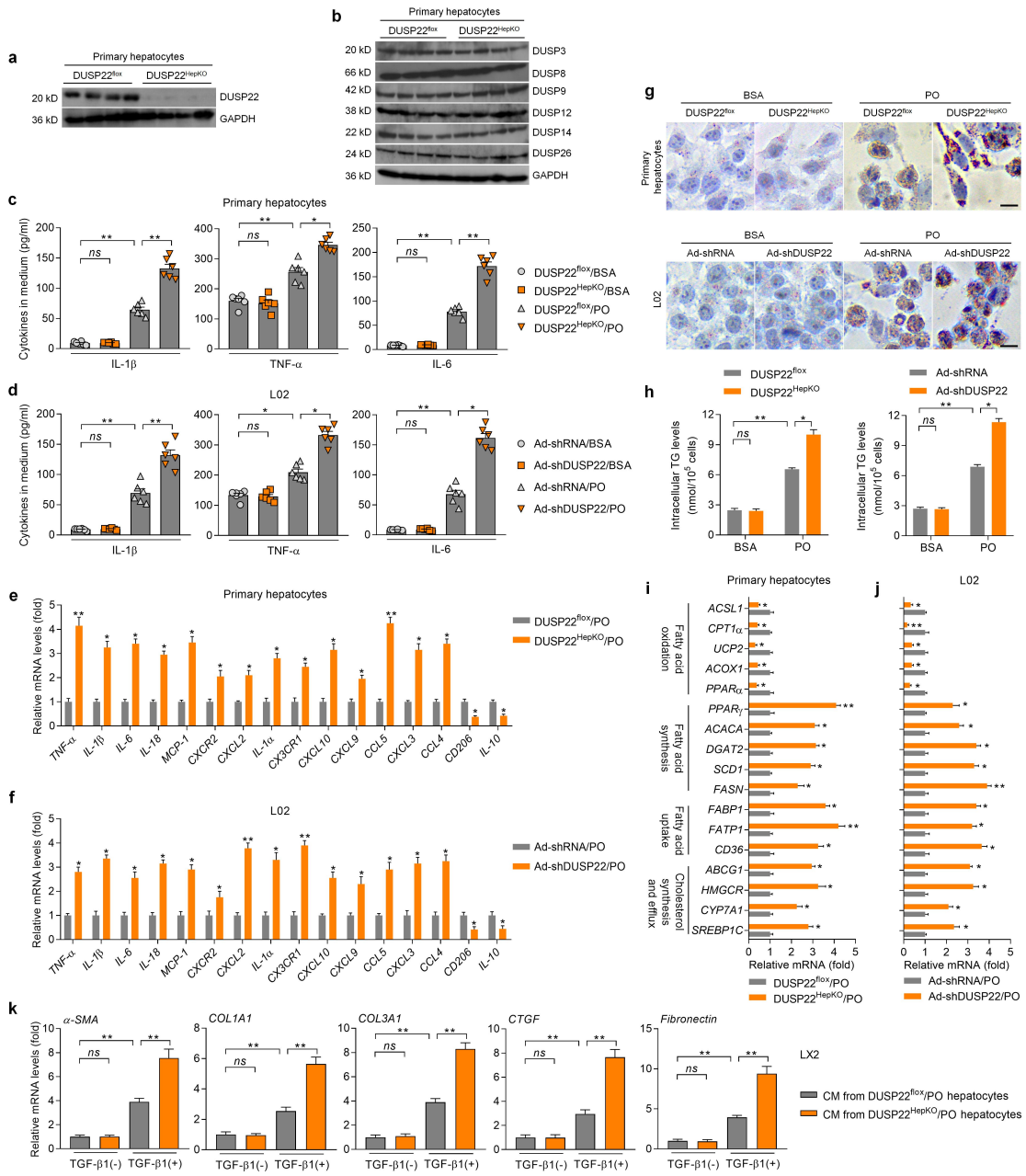
Supplementary Figure 6. Construction of hepatocyte-specific DUSP22 knockout mice. **a** Schematic workflow showing the establishment of the hepatocyte-specific DUSP22-knockout (DUSP22^{HepKO}) mouse strain. **b** Images of 8-week-old male DUSP22^{fllox} and DUSP22^{HepKO} mice. **c** Western blot showing DUSP22 expression in liver, kidney, heart, and fat of the indicated mice (n=3 mice per group). **d,e** Western blot showing **(d)** DUSP22, **(e)** DUSP3, DUSP8, DUSP9, DUSP12, DUSP14 and DUSP26 expression in liver from DUSP22^{fllox} and DUSP22^{HepKO} mice (n=4 mice per group). **f** Representative immunofluorescence images of DUSP22 (green) in the livers of mice from the DUSP22^{fllox} and DUSP22^{HepKO} mice, and nuclei were stained with DAPI (blue) (n=3 mice per group, with 10 images for each mouse; Scale bars, 40 μ m). **g** H&E staining of liver sections from DUSP22^{fllox} and DUSP22^{HepKO} mice at 0 and 24 weeks of NCD feeding (n=8 mice per group, with 10 images for each mouse; Scale bars, 50 μ m). **h-j** Quantification for **(h)** serum ALT and AST contents, **(i)** liver TG and TC levels, and **(j)** serum TNF- α and IL-1 β concentrations in DUSP22^{fllox} and DUSP22^{HepKO} mice at 0 and 24 weeks of NCD feeding (n=10 per group). Data are expressed as mean \pm SEM from at least three independent experiments. For statistical analysis, **h-j** were performed by one-way ANOVA.



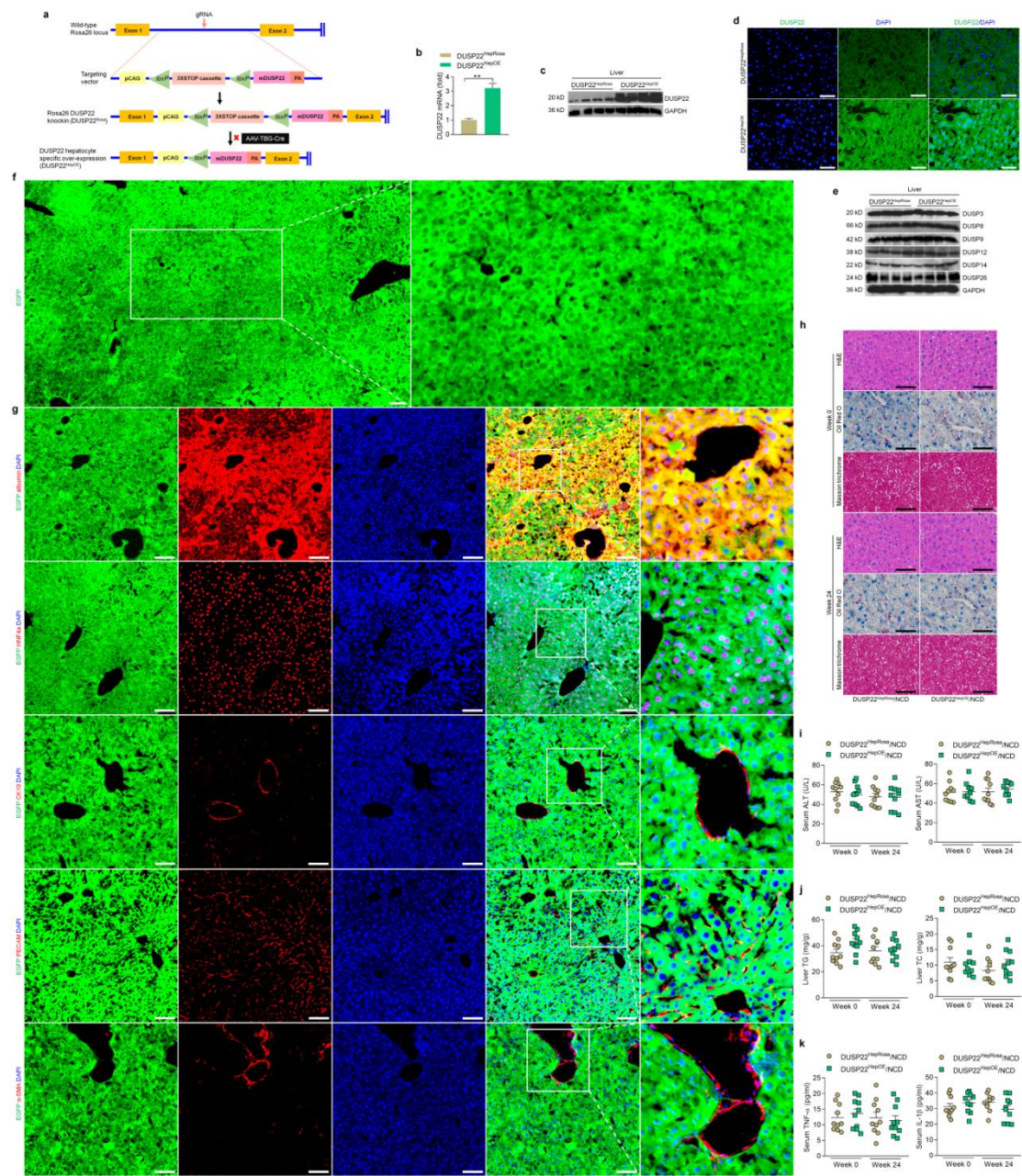
Supplementary Figure 7. Hepatocyte-specific DUSP22 deficiency exacerbates HFHC-induced steatohepatitis. **a** Quantification for steatosis score, ballooning score and lobular inflammation score of each group of mice as shown (n=10 or 11 mice per group) (* P <0.05, ** P <0.01 and *** P <0.001; *ns*, no significant difference). **b** High-throughput real-time PCR (HTqPCR) analysis indicating the inflammation-, lipid metabolism- and fibrosis-related genes expression alteration in liver of DUSP22^{fllox} and DUSP22^{HepKO} mice fed with a NCD or a HFHC for 24 weeks (n=4 mice per group). **c** RT-qPCR analysis for the mRNA expression levels of inflammation-related genes including pro-inflammatory factors (TNF- α , IL-1 β , IL-6, IL-18, MCP-1, F4/80, CXCR2, CXCL2, IL-1 α , CX3CR1, CXCL10, CXCL9, CCL5, CXCL3 and CCL4) and anti-inflammatory molecules (CD206 and IL-10) in liver tissues from DUSP22^{fllox} and DUSP22^{HepKO} groups of mice after a 24-week HFHC feeding (n=4 mice per group) (* P <0.05 and ** P <0.01 versus the DUSP22^{fllox}/HFHC group). **d** RT-qPCR analysis of mRNA levels for lipid metabolism-related genes in the livers of HFHC-fed DUSP22^{fllox} and DUSP22^{HepKO} mice, including genes associated with cholesterol synthesis and efflux (SREBP1C, CYP7A1, HMGCR and ABCG1), fatty acid uptake (CD36, FATP1 and FABP1), fatty acid synthesis (FASN, SCD1, DGAT2, ACACA and PPAR γ) and fatty acid oxidation (PPAR α , ACOX1, UCP2, CPT1 α and ACSL1) (n=4 mice per group) (* P <0.05 and ** P <0.01 versus the DUSP22^{fllox}/HFHC group). **e** RT-qPCR analysis for mRNA levels of fibrosis markers, including α -SMA, COL1A1, COL3A1, CTGF, Fibronectin and TGF- β 1, in the livers of the indicated mice fed a HFHC for 24 weeks (n=4 mice per group) (* P <0.05 versus the DUSP22^{fllox}/HFHC group). Data are expressed as mean \pm SEM from at least three independent experiments. For statistical analysis, **a** and **b** were performed by one-way ANOVA; **c-e** were conducted by two-tailed Student's *t*-test.



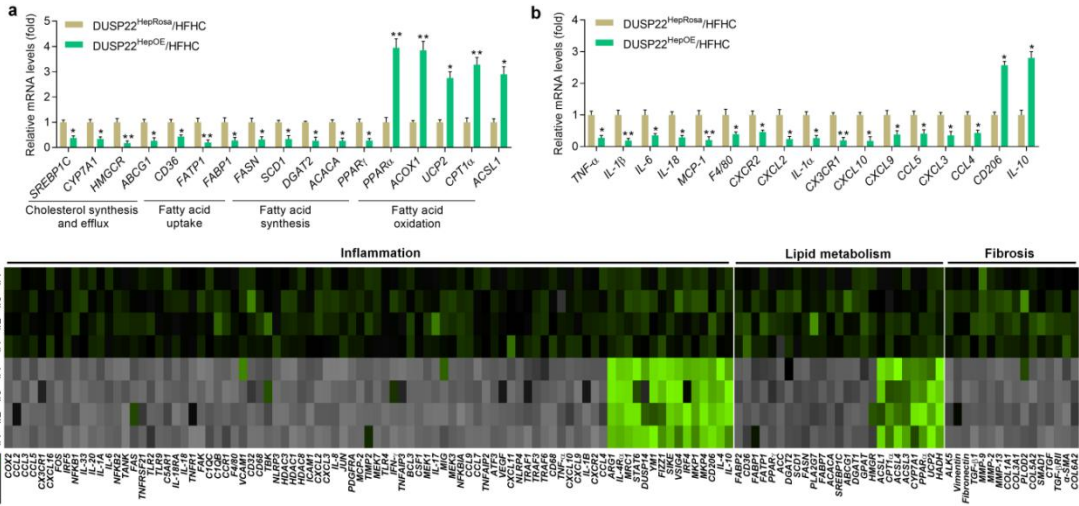
Supplementary Figure 8. Hepatocyte-specific DUSP22 knockout promotes weight gain of adipose tissue to accelerate HFHC-induced NASH pathologies. **a** Records of food intake (Kcal/day/per mice) of the shown groups of mice in a 24-weeks NCD or HFHC feeding (n=15 mice per group). **b,c** Measurements of **(b)** body fat weight (BFW) and **(c)** the ratio of BFW/BW (n=15 mice per group) (* P <0.05 and ** P <0.01; *ns*, no significant difference). **d** Representative images of H&E staining of the white adipose tissue (WAT) sections of mice from the DUSP22^{fl^{ox}} and DUSP22^{Hep^{KO}} groups fed with a NCD or HFHC for 24 weeks (n=8 mice per group, with 10 images for each mouse; Scale bars, 100 μ m). **e** Quantification for the adipocyte area (μ m²) following **(d)** (n=8 mice per group) (* P <0.05; *ns*, no significant difference). Data are expressed as mean \pm SEM from at least three independent experiments. Statistical analysis were performed by one-way ANOVA.



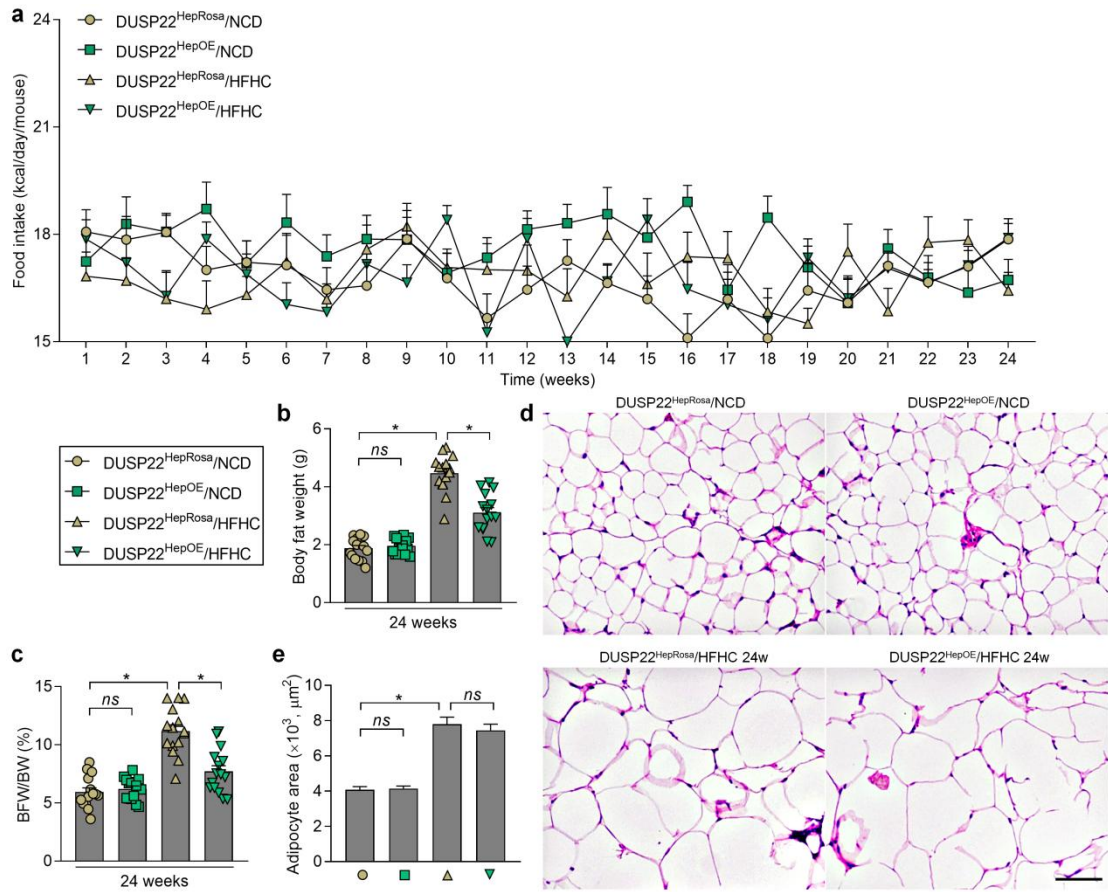
Supplementary Figure 9. DUSP22 decreases aggravate inflammation, lipid deposition and fibrosis *in vitro*. **a,b** Western blot showing (a) DUSP22, (b) DUSP3, DUSP8, DUSP9, DUSP12, DUSP14 and DUSP26 protein expression levels in the isolated primary hepatocytes from DUSP22^{fllox} and DUSP22^{HepKO} mice (n=4 per group). **c** The concentrations of IL-1 β , TNF- α and IL-6 in the culture medium of primary hepatocytes that were isolated from DUSP22^{fllox} and DUSP22^{HepKO} mice. The hepatocytes were treated with PO (0.4 mM PA and 0.8 mM OA) for 24 h. The medium was then collected for ELISA analysis (n=6 per group) (* P <0.05 and ** P <0.01; *ns*, no significant difference). **d** The concentrations of IL-1 β , TNF- α and IL-6 in the medium of L02 cells transfected with Ad-shDUSP22 or Ad-shRNA after 24 h PO (0.4 mM PA and 0.8 mM OA) treatment (n=6 per group) (* P <0.05 and ** P <0.01; *ns*, no significant difference). **e** RT-qPCR analysis for the mRNA expression levels of inflammation-related genes in the isolated primary hepatocytes as shown after PO (0.4 mM PA and 0.8 mM OA) incubation for 24 h (n=4 per group) (* P <0.05 and ** P <0.01 versus the DUSP22^{fllox}/PO group). **f** RT-qPCR analysis for the mRNA expression levels of inflammation-related genes in L02 cells with knockdown of DUSP22 after PO (0.4 mM PA and 0.8 mM OA) treatment for 24 h (n=4 per group) (* P <0.05 and ** P <0.01 versus the Ad-shRNA/PO group). **g** Representative Oil red O staining images of the primary DUSP22^{fllox} and DUSP22^{HepKO} hepatocytes (top) and L02 cells transfected with shRNA or shDUSP22 (bottom) after PO (0.4 mM PA and 0.8 mM OA) treatment for 24 h (n=5 per group, with 10 images per group; Scale bar, 25 μ m). **h** Intracellular TG contents in the primary DUSP22^{fllox} and DUSP22^{HepKO} hepatocytes (left) and L02 cells with or without DUSP22 knockdown (right) after PO (0.4 mM PA and 0.8 mM OA) incubation for 24 h (n=5 per group) (* P <0.05 and ** P <0.01; *ns*, no significant difference). **i,j** RT-qPCR analysis of mRNA levels for lipid metabolism-related genes in the (i) primary DUSP22^{fllox} and DUSP22^{HepKO} hepatocytes (* P <0.05 and ** P <0.01 versus the DUSP22^{fllox}/PO group), and (j) L02 cells transfected with shRNA or shDUSP22 after PO (0.4 mM PA and 0.8 mM OA) exposure for 24 h (* P <0.05 and ** P <0.01 versus the Ad-shRNA/PO group) (n=4 per group). **k** RT-qPCR analysis of fibrosis-related genes α -SMA, COL1A1, COL3A1, CTGF and Fibronectin expression levels in 24 h TGF- β 1 (10 ng/ml)-treated human hepatic stellate cell (HSC) line LX2 cells incubated with fresh medium that was mixed with CM from (e) at 1:1 ratio (n=4 per group) (** P <0.01; *ns*, no significant difference). Data are expressed as mean \pm SEM from at least three independent experiments. For statistical analysis, **c**, **d**, **h** and **k** were conducted by one-way ANOVA; **e**, **f**, **i** and **j** were performed by two-tailed Student's *t*-test.



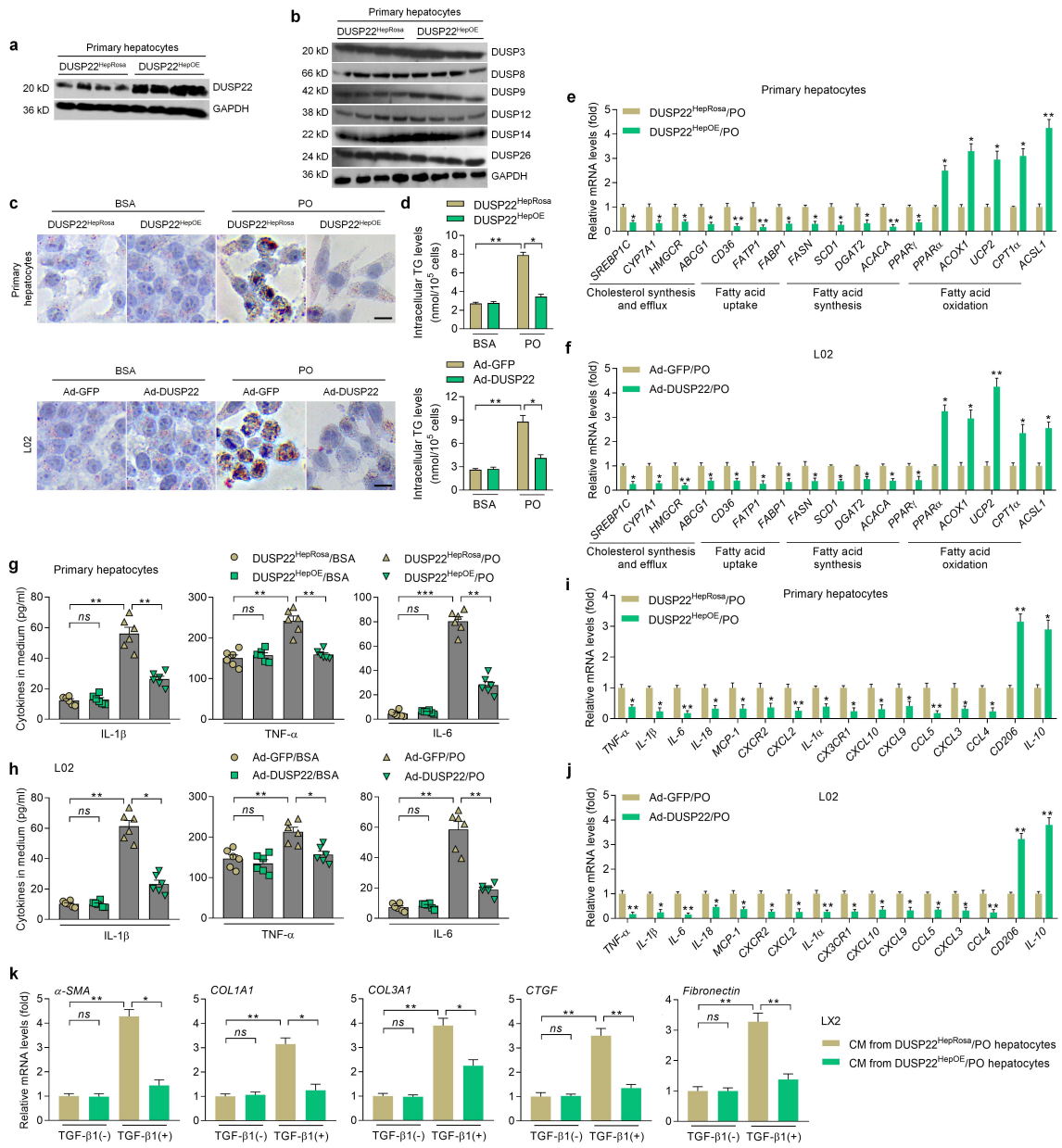
Supplementary Figure 10. Construction of hepatocyte-specific DUSP22 over-expression mice. **a** Scheme showing the establishment of hepatocyte-specific DUSP22 over-expression (DUSP22^{HepOE}) mouse strain. **b,c** **(b)** RT-qPCR and **(c)** western blot showing DUSP22 expression in liver from DUSP22^{HepRosa} and DUSP22^{HepOE} mice (n=4 mice per group) (***P*<0.01). **d** Representative immunofluorescence images of DUSP22 (green) in the livers of mice from DUSP22^{HepRosa} and DUSP22^{HepOE} mice, and nuclei were stained with DAPI (blue) (n=3 mice per group, with 10 images for each mouse; Scale bars, 40 μ m). **e** Western blot showing DUSP3, DUSP8, DUSP9, DUSP12, DUSP14 and DUSP26 protein expression in liver from DUSP22^{HepRosa} and DUSP22^{HepOE} mice (n=4 mice per group). **f** Fluorescence view of the adult liver from 32-week-old AAV-TBG-Cre;Rosa26^{DUSP22}-EGFP mice (n=3 mice per group, with 10 images for each mouse; Scale bars, 100 μ m). **g** Immunostaining for EGFP, Albumin, HNF4a, CK19, PECAM and α -SMA on liver sections showing DUSP22-expressing hepatocytes in 32-week-old AAV-TBG-Cre;Rosa26^{DUSP22}-EGFP mice (n=3 mice per group, with 10 images for each mouse; Scale bars, 40 μ m). **h** H&E staining of liver sections from DUSP22^{HepRosa} and DUSP22^{HepOE} mice at 0 and 24 weeks of NCD feeding (n=8 mice per group, with 10 images for each mouse; Scale bars, 50 μ m). **i-k** Quantification for **(i)** serum ALT and AST contents, **(j)** liver TG and TC levels, and **(k)** serum TNF- α and IL-1 β concentrations in DUSP22^{HepRosa} and DUSP22^{HepOE} mice at 0 and 24 weeks of NCD feeding (n=10 per group). Data are expressed as mean \pm SEM from at least three independent experiments. Statistical analysis were performed by two-tailed Student's *t*-test.



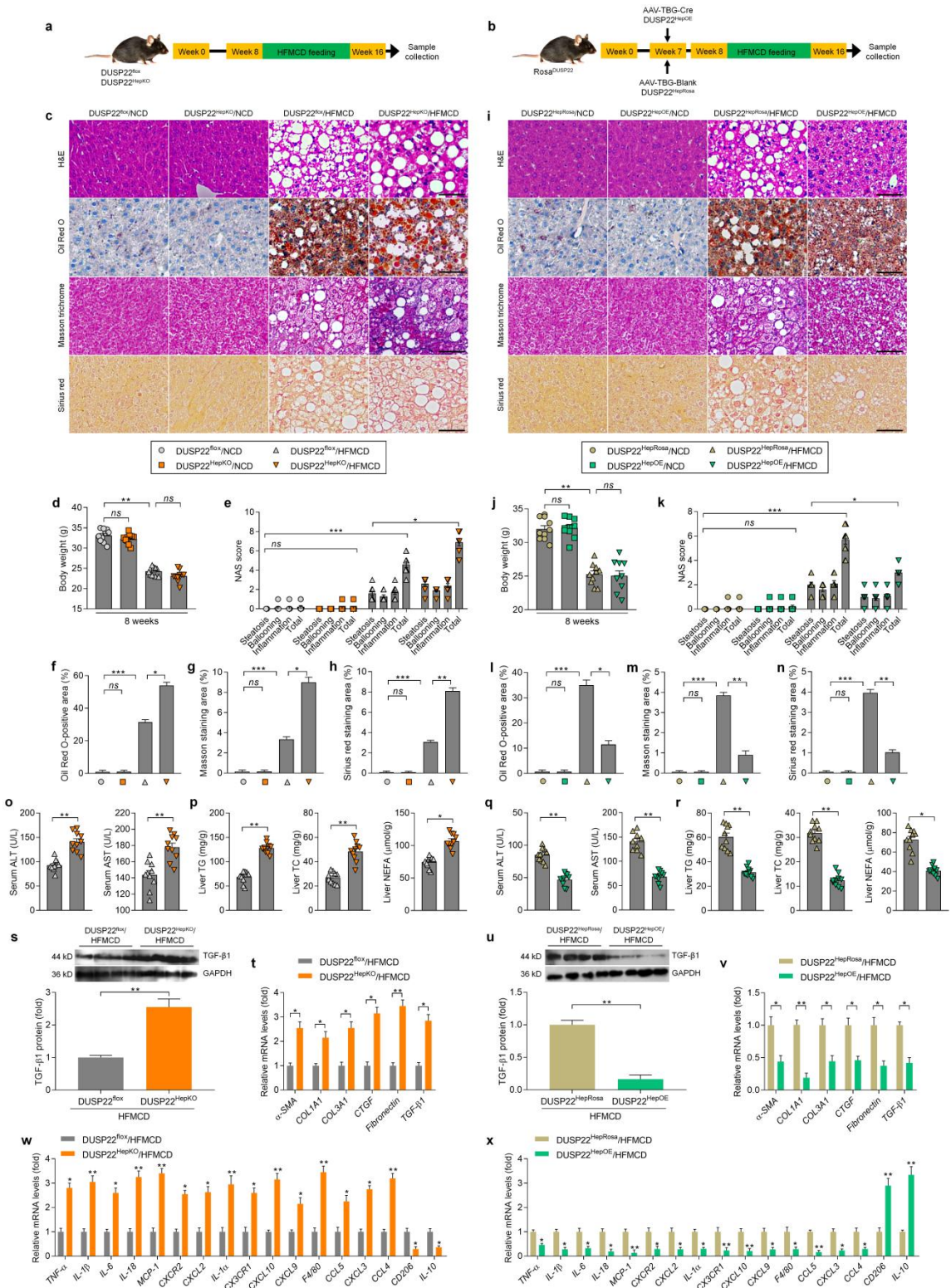
Supplementary Figure 11. Hepatocyte-specific DUSP22 over-expression mitigates HFHC-induced steatohepatitis. **a** RT-qPCR analysis of mRNA levels for lipid metabolism-related genes in the livers of a 24-week HFHC-fed DUSP22^{HepRosa} and DUSP22^{HepOE} mice (n=4 mice per group) (* P <0.05 and ** P <0.01 versus the DUSP22^{HepRosa}/HFHC group). **b** RT-qPCR analysis of mRNA levels for inflammation-associated genes in the livers of DUSP22^{HepRosa} and DUSP22^{HepOE} mice after HFHC feeding for 24 weeks (n=4 mice per group) (* P <0.05 and ** P <0.01 versus the DUSP22^{HepRosa}/HFHC group). **c** HTqPCR analysis indicating the inflammation-, lipid metabolism- and fibrosis-related genes expression alteration in liver of DUSP22^{HepRosa} and DUSP22^{HepOE} mice fed with a HFHC for 24 weeks (n=4 mice per group). Data are expressed as mean \pm SEM from at least three independent experiments. Statistical analysis were performed by two-tailed Student's t -test.



Supplementary Figure 12. Hepatocyte-specific DUSP22 over-expression ameliorates weight gain of adipose tissue to alleviate HFHC-triggered NASH pathologies. **a** Records of food intake (Kcal/day/per mice) of the shown groups of mice with a 24-week NCD or HFHC feeding (n=15 mice per group). **b,c** Measurements of **(b)** body fat weight (BFW) and **(c)** the ratio of BFW/BW (* $P < 0.05$; *ns*, no significant difference). **d** Representative images of H&E staining of the WAT sections of mice from the DUSP22^{HepRosa} and DUSP22^{HepOE} groups fed with a NCD or HFHC for 24 weeks (n=8 mice per group, with 10 images for each mouse; Scale bars, 100 μm). **e** Quantification for the adipocyte area (μm^2) following **(d)** (n=8 mice per group) (* $P < 0.05$; *ns*, no significant difference). Data are expressed as mean \pm SEM from at least three independent experiments. Statistical analysis were performed by one-way ANOVA.

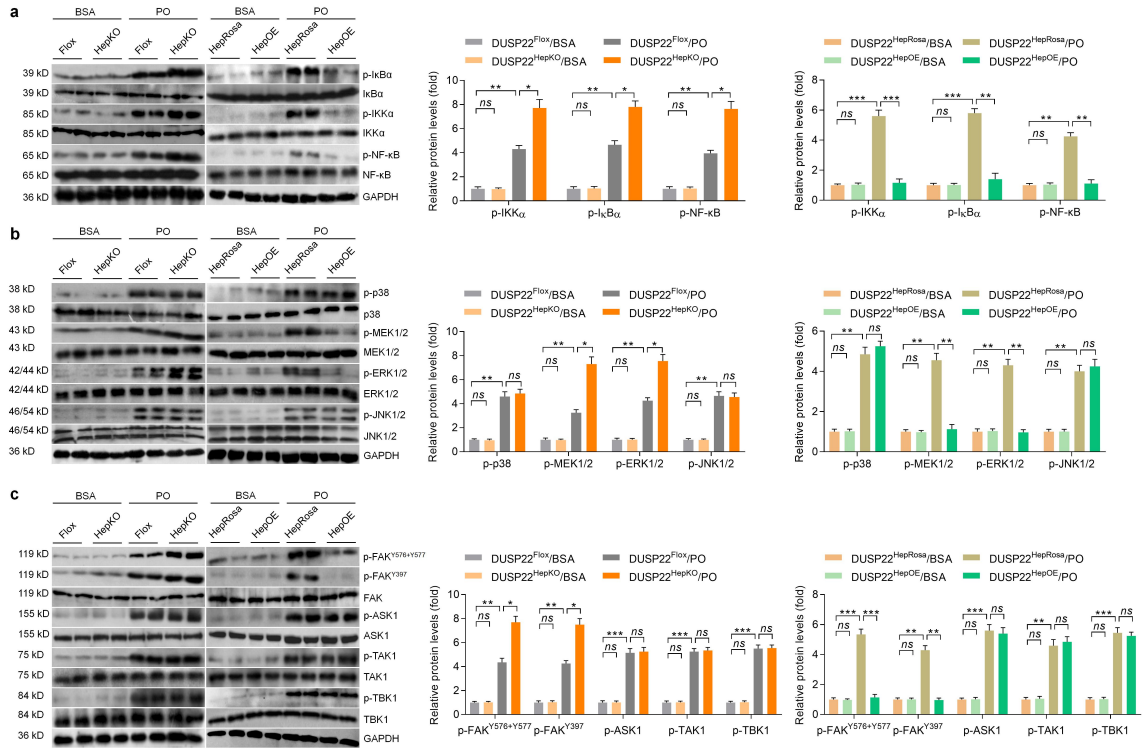


Supplementary Figure 13. Increases of DUSP22 mitigates inflammation, lipid deposition and fibrosis *in vitro*. **a,b** Western blot showing (a) DUSP22, (b) DUSP3, DUSP8, DUSP9, DUSP12, DUSP14 and DUSP26 protein expression in the isolated primary hepatocytes from DUSP22^{HepRosa} and DUSP22^{HepOE} mice (n=4 per group). **c** Representative Oil red O staining images of the primary DUSP22^{HepRosa} and DUSP22^{HepOE} hepatocytes (top) and L02 cells transfected with Ad-GFP or Ad-DUSP22 (bottom) after PO (0.4 mM PA and 0.8 mM OA) treatment for 24 h (n=5 per group, with 10 images per group; Scale bar, 25 μ m). **d** Intracellular TG contents in the primary DUSP22^{HepRosa} and DUSP22^{HepOE} hepatocytes (top) and L02 cells with or without DUSP22 over-expression (bottom) after PO (0.4 mM PA and 0.8 mM OA) incubation for 24 h (n=5 per group) (* P <0.05 and ** P <0.01). **e** RT-qPCR analysis for the mRNA expression levels of lipid metabolism-associated genes in the isolated primary hepatocytes as shown after PO (0.4 mM PA and 0.8 mM OA) exposure for 24 h (n=4 per group) (* P <0.05 and ** P <0.01 versus the DUSP22^{HepRosa}/PO group). **f** RT-qPCR analysis for the mRNA expression levels of lipid metabolism-related genes in L02 cells transfected with Ad-GFP or Ad-DUSP22 following PO (0.4 mM PA and 0.8 mM OA) treatment for 24 h (n=4 per group) (* P <0.05 and ** P <0.01 versus the Ad-GFP/PO group). **g** The concentrations of IL-1 β , TNF- α and IL-6 in the culture medium of primary hepatocytes that were isolated from DUSP22^{HepRosa} and DUSP22^{HepOE} mice. The hepatocytes were then treated with PO (0.4 mM PA and 0.8 mM OA) for 24 h. The medium was collected for ELISA assay (n=6 per group) (** P <0.01 and *** P <0.001; *ns*, no significant difference). **h** The concentrations of IL-1 β , TNF- α and IL-6 in the medium of L02 cells with or without DUSP22 over-expression post 24 h PO (0.4 mM PA and 0.8 mM OA) treatment (n=6 per group) (* P <0.05 and ** P <0.01; *ns*, no significant difference). **i,j** RT-qPCR analysis of mRNA levels for inflammation-related genes in the (i) primary hepatocytes isolated from DUSP22^{HepRosa} and DUSP22^{HepOE} mice (* P <0.05 and ** P <0.01 versus the DUSP22^{HepRosa}/PO group), and (j) L02 cells transfected with Ad-GFP or Ad-DUSP22 after PO (0.4 mM PA and 0.8 mM OA) incubation for 24 h (* P <0.05 and ** P <0.01 versus the Ad-GFP/PO group) (n=4 per group). **k** RT-qPCR analysis of fibrosis-associated genes expression levels in 24 h of TGF- β 1 (10 ng/ml)-stimulated LX2 cells that were incubated with the mix of fresh medium and CM from (e) at 1:1 ratio (n=4 per group) (* P <0.05 and ** P <0.01; *ns*, no significant difference). Data are expressed as mean \pm SEM from at least three independent experiments. For statistical analysis, **d**, **g**, **h** and **k** were conducted by one-way ANOVA; **e**, **f**, **i** and **j** were performed by two-tailed Student's *t*-test.

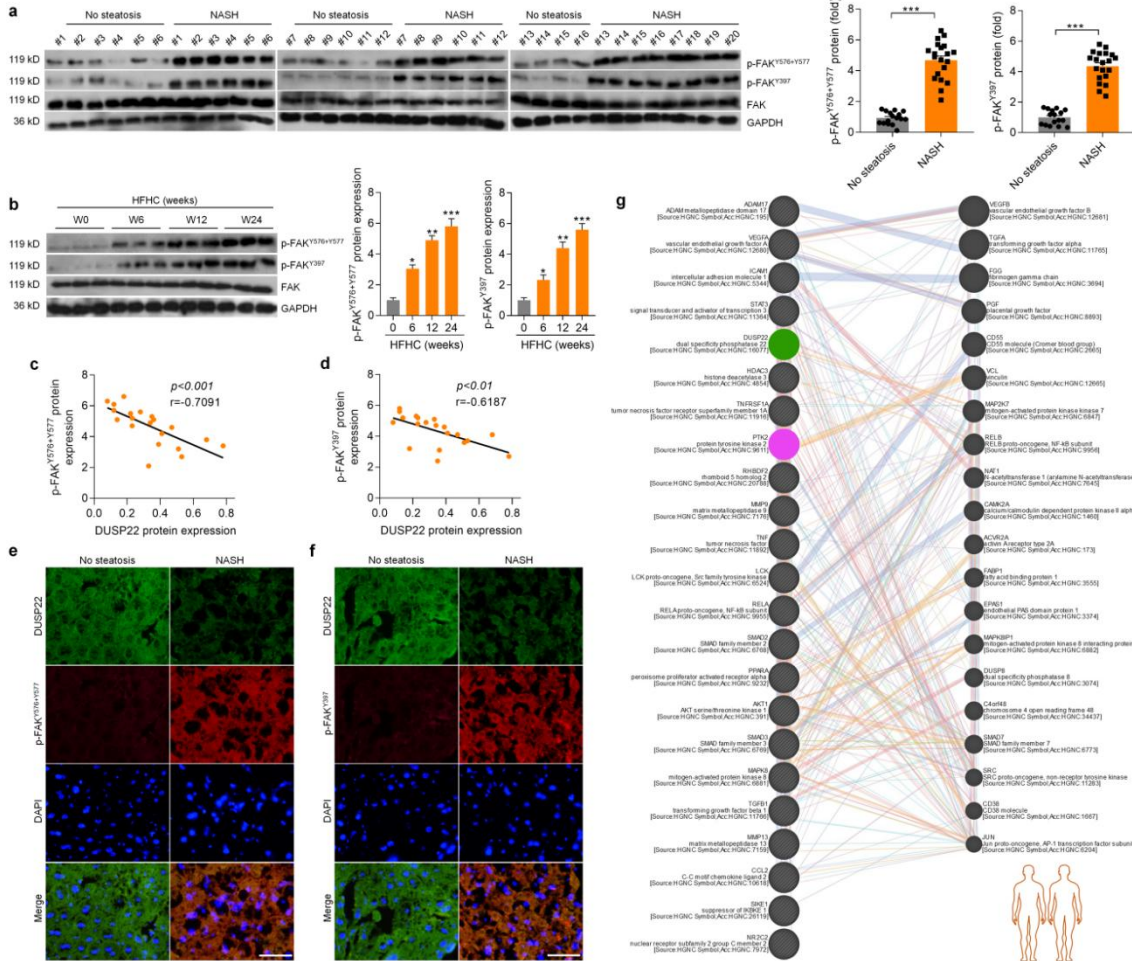


Supplementary Figure 14. Hepatocyte DUSP22 ameliorates HFMCD diet-induced NASH phenotypes *in vivo*. **a** Scheme showing hepatocyte-specific DUSP22 knockout mice with an 8-week NCD or HFMCD feeding (DUSP22^{HepKO} NCD; DUSP22^{HepKO} HFMCD). The DUSP22^{fllox} was used as control (DUSP22^{fllox} NCD; DUSP22^{fllox} HFMCD). **b** Schematic diagram of AAV-TBG-Cre-mediated DUSP22 over-expression in liver of an 8-week NCD or HFMCD diet-fed RosaDUSP22 mice (DUSP22^{HepOE} NCD; DUSP22^{HepOE} HFMCD). The AAV-TBG-blank was used as control (DUSP22^{HepRosa} NCD; DUSP22^{HepRosa} HFMCD). **c** Representative images of H&E staining, Oil Red O staining, Masson trichrome staining and Sirius red staining in liver sections from DUSP22^{fllox} and DUSP22^{HepKO} mice fed with a NCD or a HFMCD for 8 weeks (n=6 or 10 mice per group, with 10 images for each mouse; Scale bars, 50 μ m). **d** Measurements of body weights of mice from the shown groups of mice (n=10 mice per group) (* P <0.01; *ns*, no significant difference). **e-h** Results for **(e)** NAS score, **(f)** Oil Red O-positive staining, **(g)** Masson trichrome-positive staining, and **(h)** Sirius red-positive staining were analyzed and quantified in the shown groups of mice (n=6 or 10 mice per group) (* P <0.05, ** P <0.01 and *** P <0.001; *ns*, no significant difference). **i** Representative images of H&E staining, Oil Red O staining, Masson trichrome staining and Sirius red staining in liver sections from DUSP22^{HepRosa} and DUSP22^{HepOE} mice fed with a NCD or a HFMCD for 8 weeks (n=6 or 10 mice per group, with 10 images for each mouse; Scale bars, 50 μ m). **j** Measurements of body weights of mice from the indicated groups of mice (n=10 mice per group) (* P <0.01; *ns*, no significant difference). **k-n** Results for **(k)** NAS score, **(l)** Oil Red O-positive staining, **(m)** Masson trichrome-positive staining, and **(n)** Sirius red-positive staining were analyzed and quantified in the indicated groups of mice (n=6 or 10 mice per group) (* P <0.05, ** P <0.01 and *** P <0.001; *ns*, no significant difference). **o,p** Contents of **(o)** serum ALT and AST, and **(p)** liver TG, TC and NEFA were assessed in DUSP22^{fllox} and DUSP22^{HepKO} mice fed with a HFMCD for 8 weeks (n=10 mice per group) (* P <0.05 and ** P <0.01). **q,r** Contents of **(q)** serum ALT and AST, and **(r)** liver TG, TC and NEFA were assessed in DUSP22^{HepRosa} and DUSP22^{HepOE} mice fed with a HFMCD for 8 weeks (n=10 mice per group) (* P <0.05 and ** P <0.01). **s** Representative western blotting and quantification of the protein expression of TGF- β 1 in liver of DUSP22^{fllox} and DUSP22^{HepKO} mice fed with a HFMCD for 8 weeks (n=4 mice per group) (** P <0.01). **t** RT-qPCR results for mRNA levels of fibrosis-related genes in liver of the shown groups of mice (n=4 mice per group) (* P <0.05 and ** P <0.01). **u** Representative western blotting of TGF- β 1 in liver of DUSP22^{HepRosa} and DUSP22^{HepOE} mice fed with a HFMCD for 8 weeks (n=4 mice per group) (** P <0.01). **v** RT-qPCR results for mRNA levels of fibrosis-related genes in liver of the indicated groups of mice (n=4 mice per group) (* P <0.05 and ** P <0.01). **w,x** RT-qPCR results

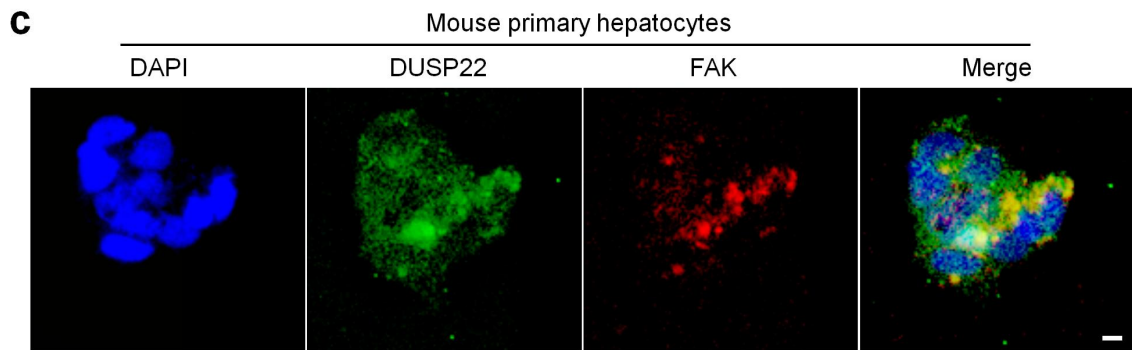
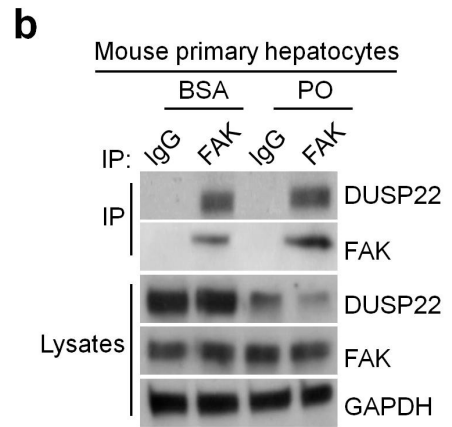
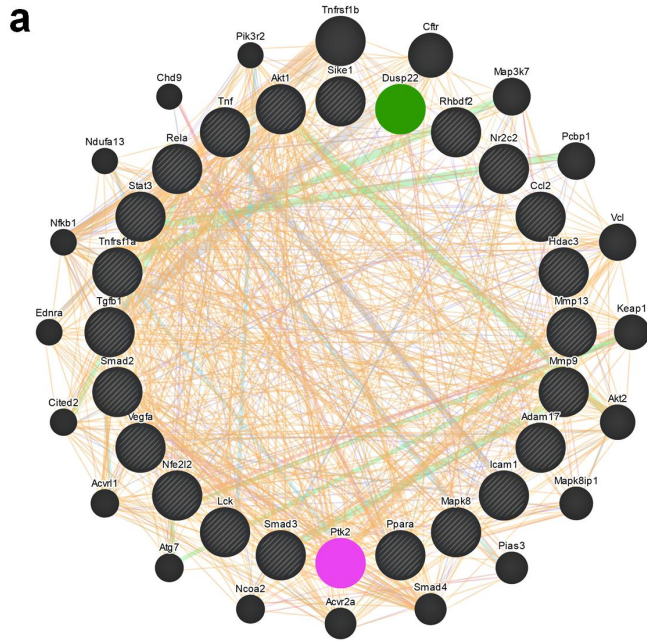
for inflammation-related genes in liver of (w) DUSP22^{fllox} and DUSP22^{HepKO} mice (* P <0.05 and ** P <0.01 versus the DUSP22^{fllox}/HFMCD group), and (x) DUSP22^{HepRosa} and DUSP22^{HepOE} mice fed with HFMCD for 8 weeks (* P <0.05 and ** P <0.01 versus the DUSP22^{HepRosa}/HFMCD group) (n=4 mice per group). Data are expressed as mean \pm SEM from at least three independent experiments. Statistical analysis were conducted by two-tailed Student's t -test.



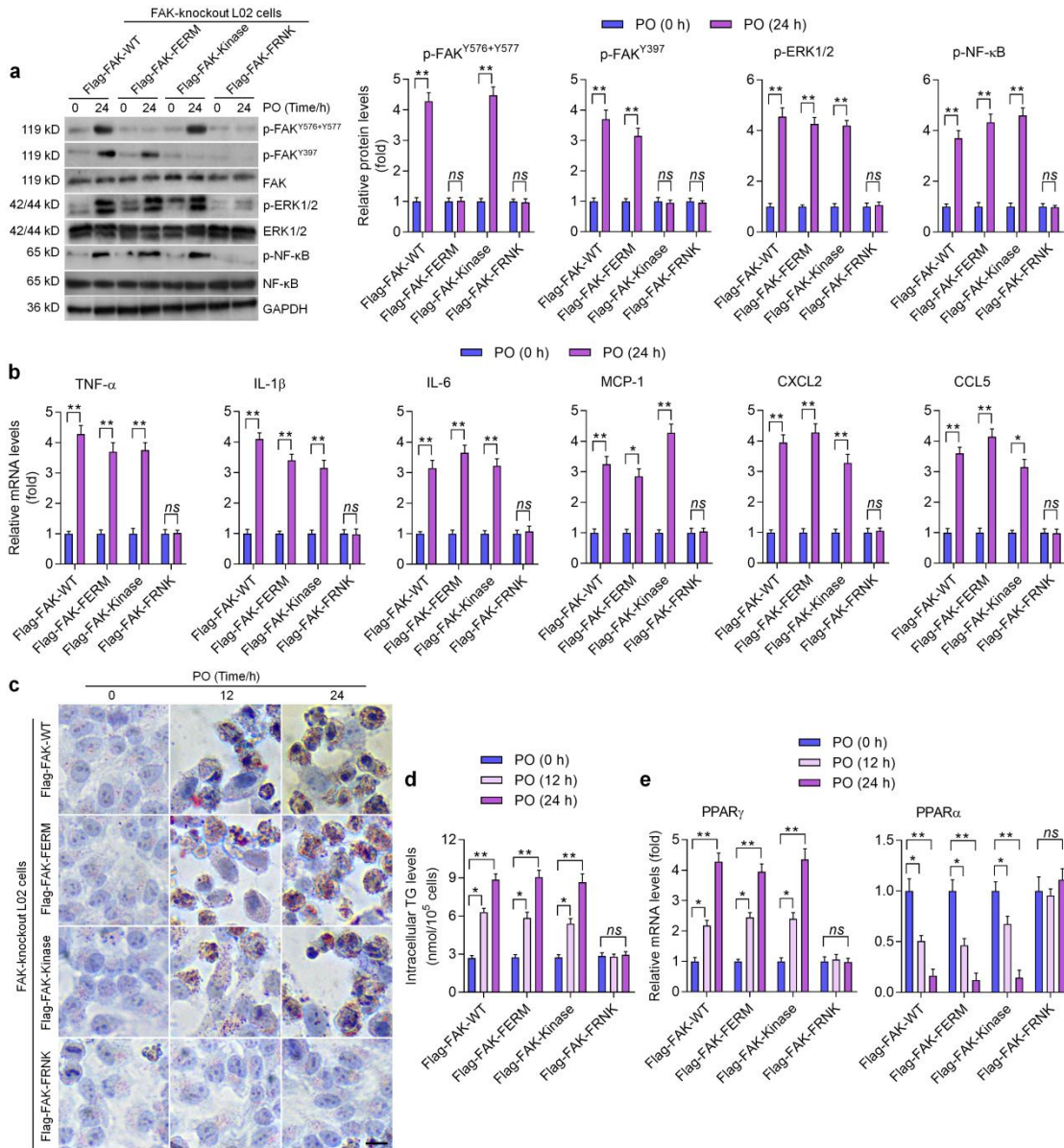
Supplementary Figure 15. DUSP22 regulates the activation of NF- κ B and FAK signaling *in vitro*. **a** Representative western blotting and quantification of the protein expression of total and phosphorylated IKK α , I κ B α and NF- κ B in the 24 h PO (0.4 mM PA and 0.8 mM OA)-treated primary hepatocytes isolated from DUSP22^{fl α} , DUSP22^{HepKO}, DUSP22^{HepRosa} and DUSP22^{HepOE} mice as shown (* P <0.05, ** P <0.01 and *** P <0.001; *ns*, no significant difference). **b** Representative western blotting of total and phosphorylated p38, MEK1/2, ERK1/2 and JNK1/2 protein expression levels in the primary hepatocytes from the mice as displayed after PO (0.4 mM PA and 0.8 mM OA) treatment for 24 h (* P <0.05 and ** P <0.01; *ns*, no significant difference). **c** Representative western blotting and quantification of the protein expression of total and phosphorylated FAK^{Y576+Y577}, FAK^{Y397}, ASK1, TAK1 and TBK1 in the primary hepatocytes from the mice as displayed after PO (0.4 mM PA and 0.8 mM OA) incubation for 24 h (* P <0.05, ** P <0.01 and *** P <0.001; *ns*, no significant difference). Data are expressed as mean \pm SEM from at least three independent experiments (n=4 per group). Statistical analysis was carried out by two-tailed Student's *t*-test.



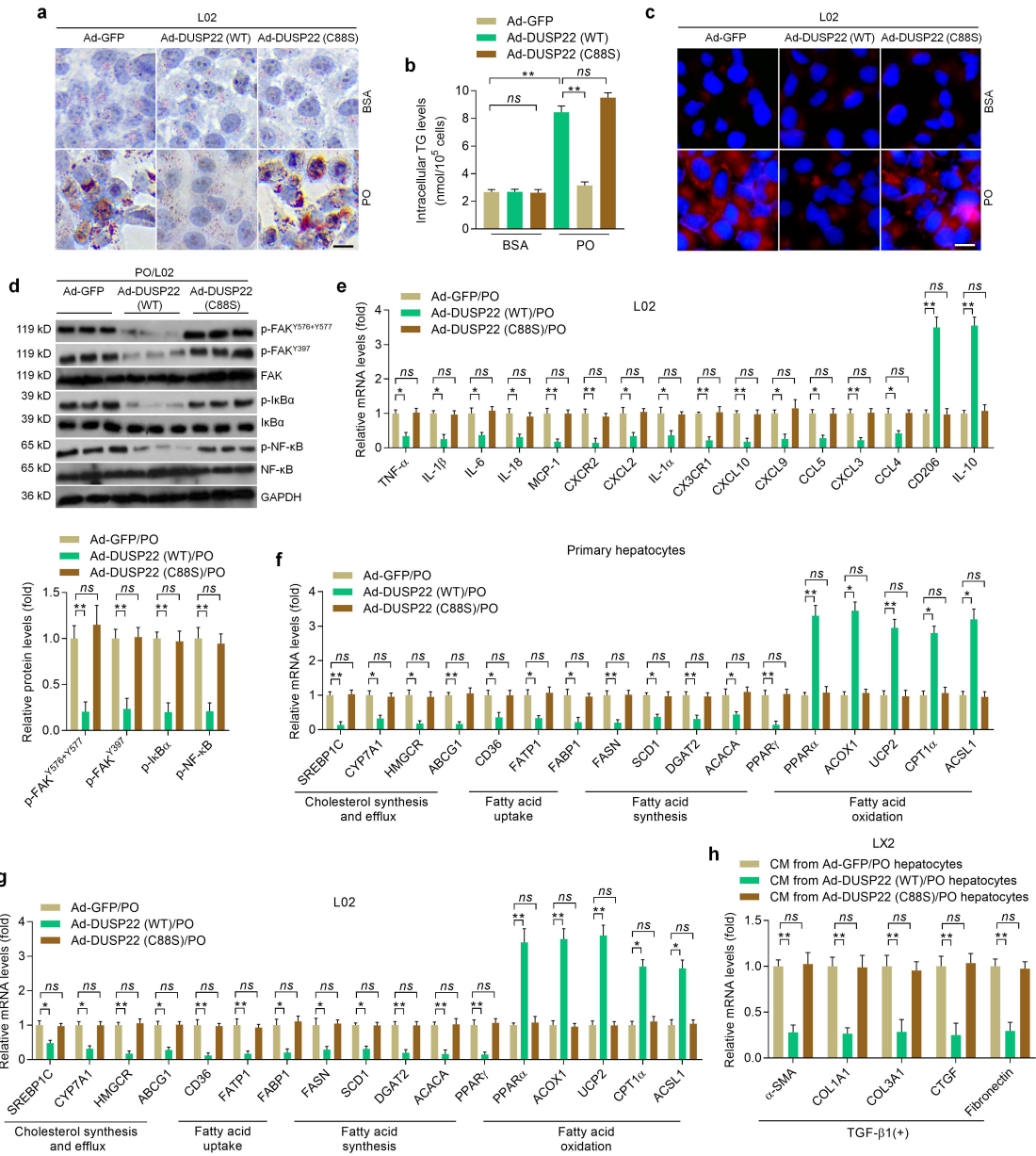
Supplementary Figure 16. FAK activation is up-regulated in livers with hepatic steatosis. **a** Representative western blotting analysis and quantification of total FAK and phosphorylated FAK^{Y576+Y577} and FAK^{Y397} protein expression in livers of individuals without (No steatosis; n=16) or with NASH (n=20) (***P*<0.001). **b** Western blotting analysis for total FAK and phosphorylated FAK^{Y576+Y577} and FAK^{Y397} protein levels in the livers of WT C57BL/6N mice fed a HFHC at the indicated time of weeks (n=3 per group) (**P*<0.05, ***P*<0.01 and ****P*<0.001 versus the expression at HFHC-0-week group). **c** Pearson comparison analysis of the correlation between DUSP22 protein level and phosphorylated FAK^{Y576+Y577} protein expression levels in NASH patients (n=20). **d** Pearson comparison analysis of the correlation between DUSP22 protein level and phosphorylated FAK^{Y397} protein expression levels in NASH patients (n=20). **e** Representative immunofluorescence images of phosphorylated FAK^{Y576+Y577} (red) and DUSP22 (green) co-expression in liver tissue of individuals with non-steatosis or NASH phenotype (n=8 per group, with 10 images for each sample; Scale bars, 50 μm). **f** Representative immunofluorescence images of phosphorylated FAK^{Y397} (red) and DUSP22 (green) co-expression in liver tissue of individuals with non-steatosis or NASH phenotype (n=8 per group, with 10 images for each sample; Scale bars, 50 μm). **g** GeneMANIA predicts the possible protein interaction network between human DUSP22 and FAK (PTK2). Data are expressed as mean ± SEM from at least three independent experiments. For statistical analysis, **a** was performed by two-tailed Student's *t*-test; **b** was performed by one-way ANOVA.



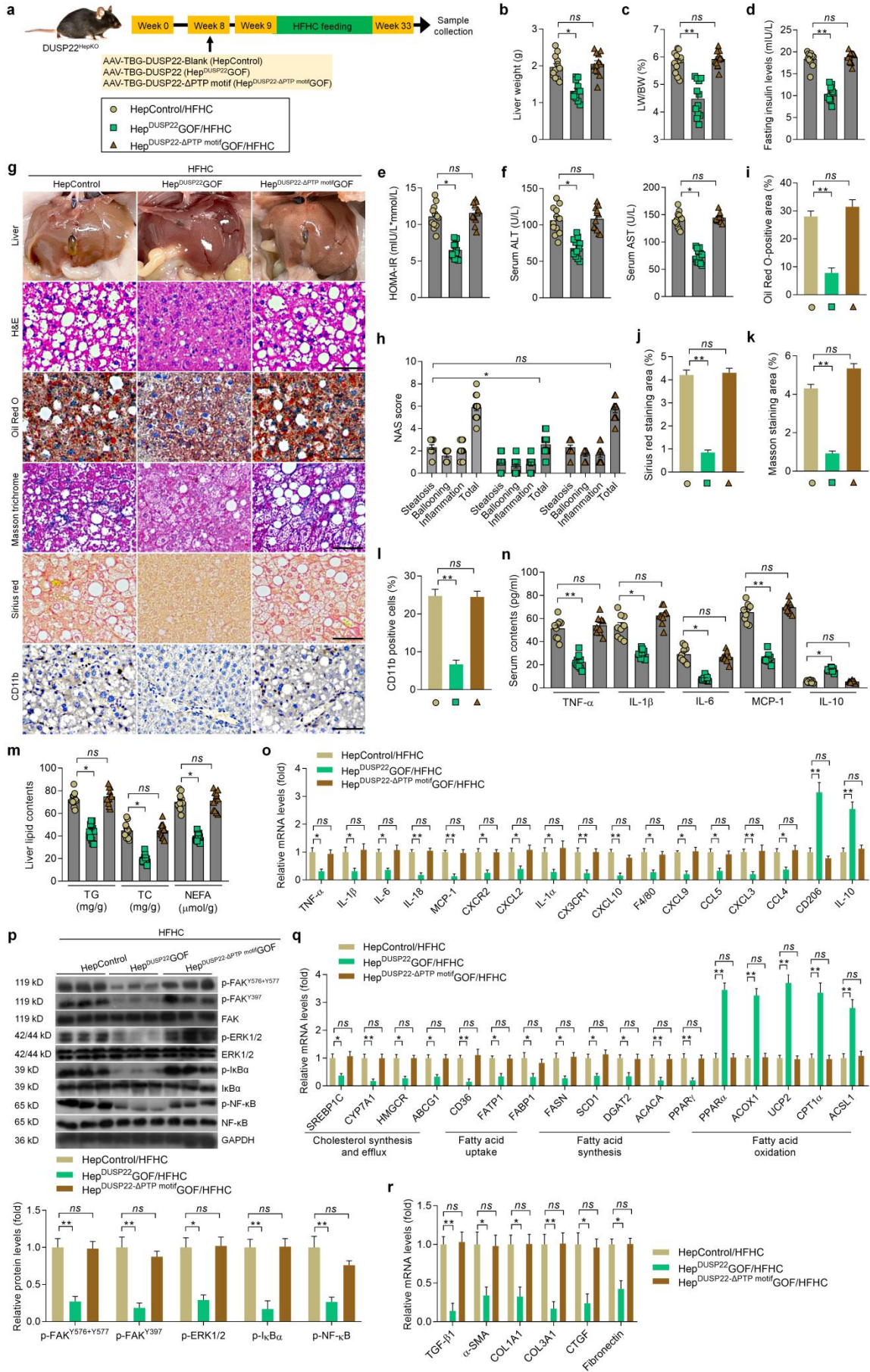
Supplementary Figure 17. DUSP22 interacts with FAK in mouse. **a** GeneMANIA predicts the possible protein interaction network between mouse DUSP22 and FAK (PTK2). **b** Results from endogenous Co-IP of DUSP22 with FAK in primary mouse hepatocytes stimulated with PO (0.4 mM PA and 0.8 mM OA) or vehicle (BSA) for 24 h. IgG was used as a control. **c** Representative immunofluorescent staining of primary mouse hepatocytes co-transfected with Flag-tagged DUSP22 (green) and HA-tagged FAK (red) after transfection for 24 h (n=10 images in total; Scale bar, 10 μ m). Data are expressed as mean \pm SEM from at least three independent experiments.



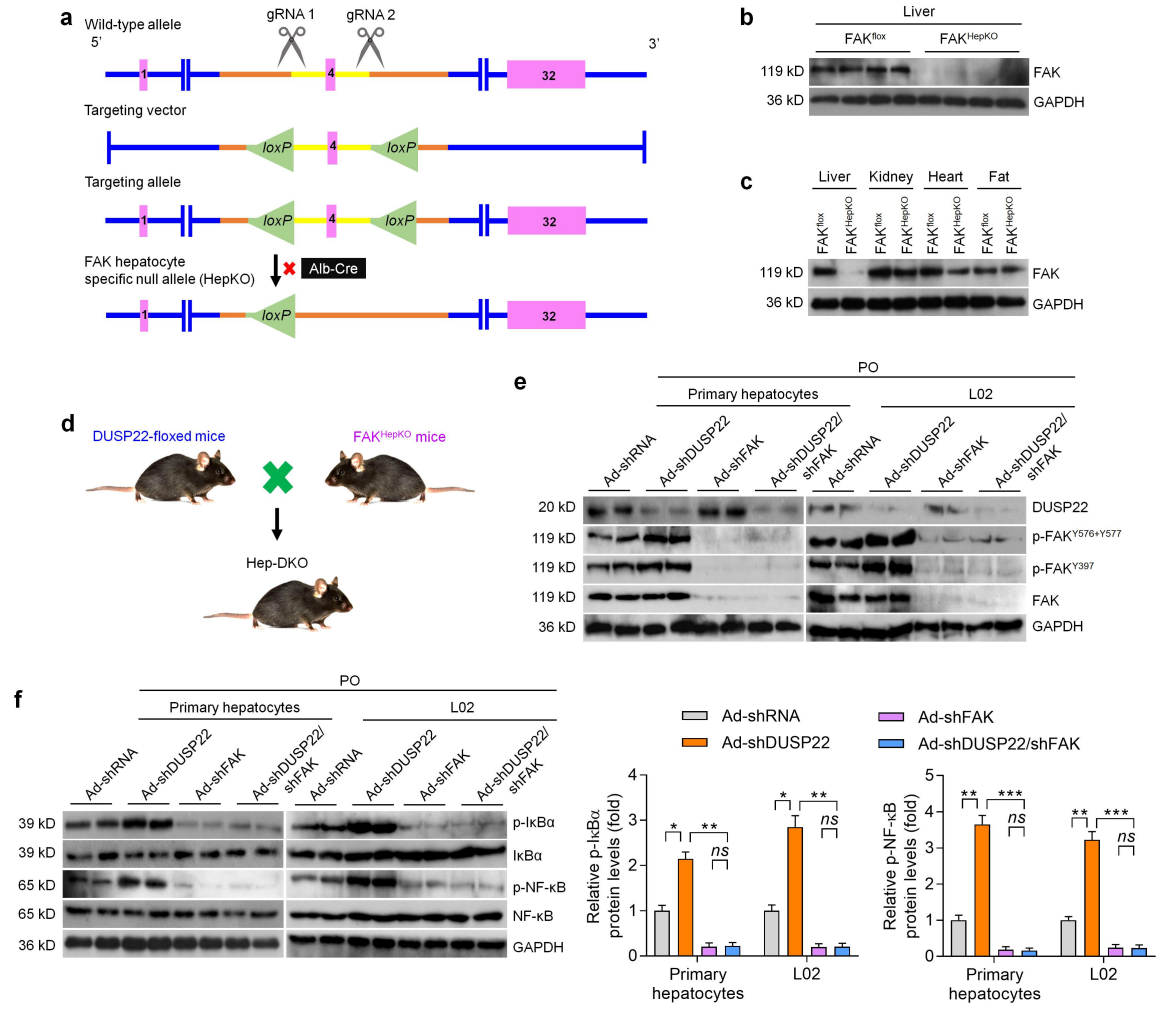
Supplementary Figure 18. Both FAK (FERM) and FAK (Kinase) promote NASH *in vitro*. **a** Representative western blot analysis of phosphorylated and total FAK, ERK1/2 and NF- κ B in the FAK-knockout L02 cells transfected with the Flag-FAK-WT, Flag-FAK-FERM, Flag-FAK-Kinase or Flag-FAK-FRNK plasmids after PO (0.4 mM PA and 0.8 mM OA) challenge for 0 h and 24 h (** P <0.01; *ns*, no significant difference). **b** RT-qPCR results for inflammation-related genes as shown in the FAK-knockout L02 cells transfected with the presented plasmids after PO (0.4 mM PA and 0.8 mM OA) incubation for 0 h and 24 h (* P <0.05 and ** P <0.01; *ns*, no significant difference). **c,d** Representative Oil red O staining images (**c**) and intracellular TG contents (**d**) in FAK-knockout L02 cell line transfected with the shown plasmids following PO (0.4 mM PA and 0.8 mM OA) treatment for 0 h, 12 h and 24 h (10 images per group; Scale bar, 25 μ m) (* P <0.05 and ** P <0.01; *ns*, no significant difference). **e** RT-qPCR results for PPAR γ and PPAR α in the FAK-knockout L02 cells transfected with the indicated plasmids after PO (0.4 mM PA and 0.8 mM OA) exposure for 0 h, 12 h and 24 h (* P <0.05 and ** P <0.01; *ns*, no significant difference). Data are expressed as mean \pm SEM from at least three independent experiments (n=4 per group). Statistical analysis were performed by two-tailed Student's *t*-test.



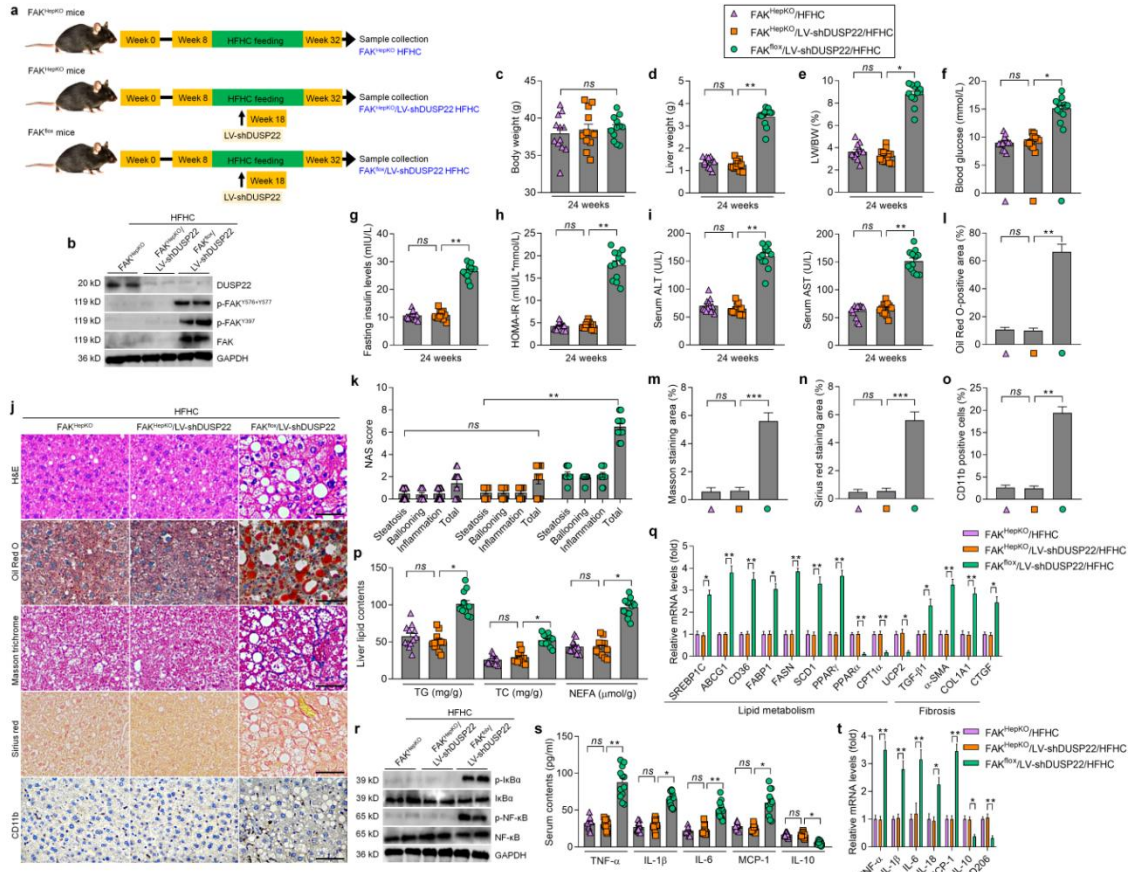
Supplementary Figure 19. DUSP22-C88S is responsible for FAK inactivation *in vitro*. **a-c** Results of **(a)** representative Oil red O staining images, **(b)** intracellular TG contents and **(c)** Nile Red staining images of 24 h BSA- or PO (0.4 mM PA and 0.8 mM OA)-treated L02 cells transfected with Ad-DUSP22 (WT) and Ad-DUSP22 (C88S) (n=4 per group, with 10 images per group; Scale bar, 25 μ m) (** P <0.01; *ns*, no significant difference). **d** Western blotting and quantification of the protein expression of total and phosphorylated FAK^{Y576+Y577}, FAK^{Y397} and NF- κ B in L02 cells transfected with Ad-GFP, Ad-DUSP22 (WT) and Ad-DUSP22 (C88S) after PO (0.4 mM PA and 0.8 mM OA) incubation for 24 h (n=3 per group). **e** RT-qPCR analysis of inflammation-related genes as exhibited in L02 cells transfected with Ad-GFP, Ad-DUSP22 (WT) and Ad-DUSP22 (C88S) in response to PO (0.4 mM PA and 0.8 mM OA) for 24 h (n=3 per group) (* P <0.05 and ** P <0.01; *ns*, no significant difference). **f,g** RT-qPCR results for lipid metabolism-associated genes as displayed in **(f)** mouse primary hepatocytes and **(g)** L02 cells transfected with Ad-GFP, Ad-DUSP22 (WT) and Ad-DUSP22 (C88S) after PO (0.4 mM PA and 0.8 mM OA) exposure for 24 h (n=3 per group) (* P <0.05 and ** P <0.01; *ns*, no significant difference). **h** RT-qPCR analysis of fibrosis-related genes as shown in LX2 cells cultured in fresh medium mixed with CM derived from **(f)** at 1:1 ratio for 24 h (n=3 per group) (** P <0.01; *ns*, no significant difference). Data are expressed as mean \pm SEM from at least three independent experiments. Statistical analysis was conducted by one-way ANOVA.



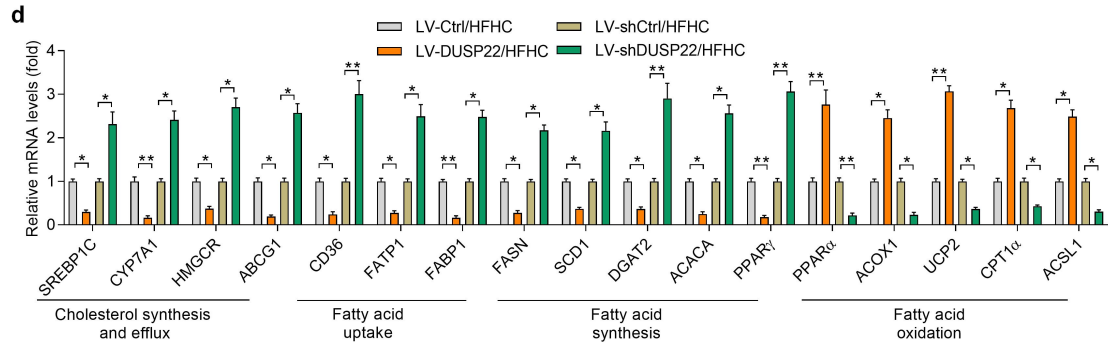
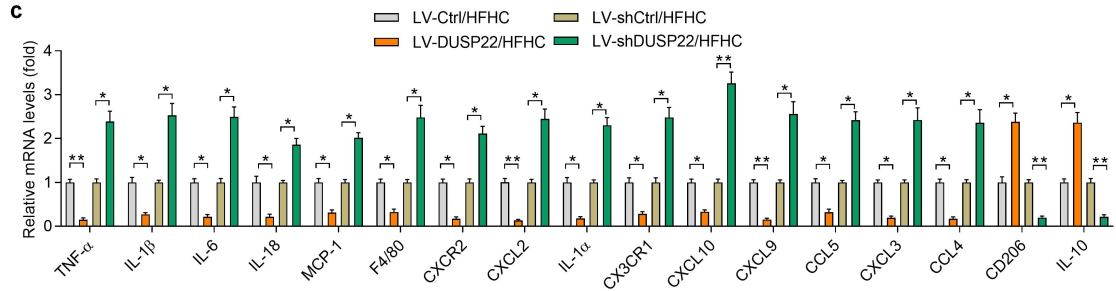
Supplementary Figure 20. DUSP22 (PTP motif) mitigates NASH *in vivo*. **a** Scheme showing AAV-TBG-DUSP22 and AAV-loaded DUSP22 with PTP-motif domain deletion (AAV-TBG-DUSP22 (Δ PTP motif))-regulated hepatocyte-specific DUSP22 gain-of-function (GOF) in liver of a 24-week HFHC-fed DUSP22^{HepKO} mice (Hep^{DUSP22}GOF/HFHC; Hep^{DUSP22- Δ PTP motif} GOF/HFHC). The AAV-TBG-blank was used as control (HepControl/HFHC). **b-f** Measurements of **(b)** liver weight, **(c)** ratio of LW/BW, **(d)** fasting insulin levels, **(e)** HOMA-IR index, and **(f)** serum ALT and AST contents in the groups of mice as shown (n=12 mice per group) (* P <0.05 and ** P <0.01; *ns*, no significant difference). **g** Representative images of liver appearance, H&E staining, Oil Red O staining, Masson trichrome staining, Sirius red staining and immunohistochemistry examination of CD11b in liver sections from HepControl, Hep^{DUSP22}GOF and Hep^{DUSP22- Δ PTP motif} mice fed with a HFHC for 24 weeks (n=6 or 12 mice per group, with 10 images for each mouse; Scale bars, 50 μ m). **h-l** Results for **(h)** NAS score, **(i)** Oil Red O-positive staining, **(j)** Sirius red-positive staining, **(k)** Masson trichrome-positive staining, and **(l)** CD11b-positive cells were analyzed and quantified (n=6 or 12 mice per group) (* P <0.05 and ** P <0.01; *ns*, no significant difference). **m** Examination for TG, TC and NEFA contents in liver of the shown groups of mice (n=12 mice per group) (* P <0.05; *ns*, no significant difference). **n** Measurements of serum concentrations of inflammatory factors TNF- α , IL-1 β , IL-6, MCP-1 and IL-10 from the indicated groups of mice (n=9 mice per group) (* P <0.05 and ** P <0.01; *ns*, no significant difference). **o** RT-qPCR analysis for mRNA levels of inflammation-associated genes in livers of the displayed groups of mice (n=4 mice per group) (* P <0.05 and ** P <0.01; *ns*, no significant difference). **p** Representative western blotting and quantification of the protein expression of total and phosphorylated FAK^{Y576+Y577}, FAK^{Y397}, I κ B α and NF- κ B in liver of the indicated groups of mice fed with a HFHC for 24 weeks (n=4 mice per group) (* P <0.05 and ** P <0.01; *ns*, no significant difference). **q** RT-qPCR analysis of mRNA levels for lipid metabolism-related genes in the liver of the shown groups of mice (n=4 mice per group) (* P <0.05 and ** P <0.01; *ns*, no significant difference). **r** RT-qPCR results for mRNA levels of fibrosis-related genes in livers of the indicated groups of mice (n=4 mice per group) (* P <0.05 and ** P <0.01; *ns*, no significant difference). Data are expressed as mean \pm SEM from at least three independent experiments. Statistical analysis was conducted by one-way ANOVA.



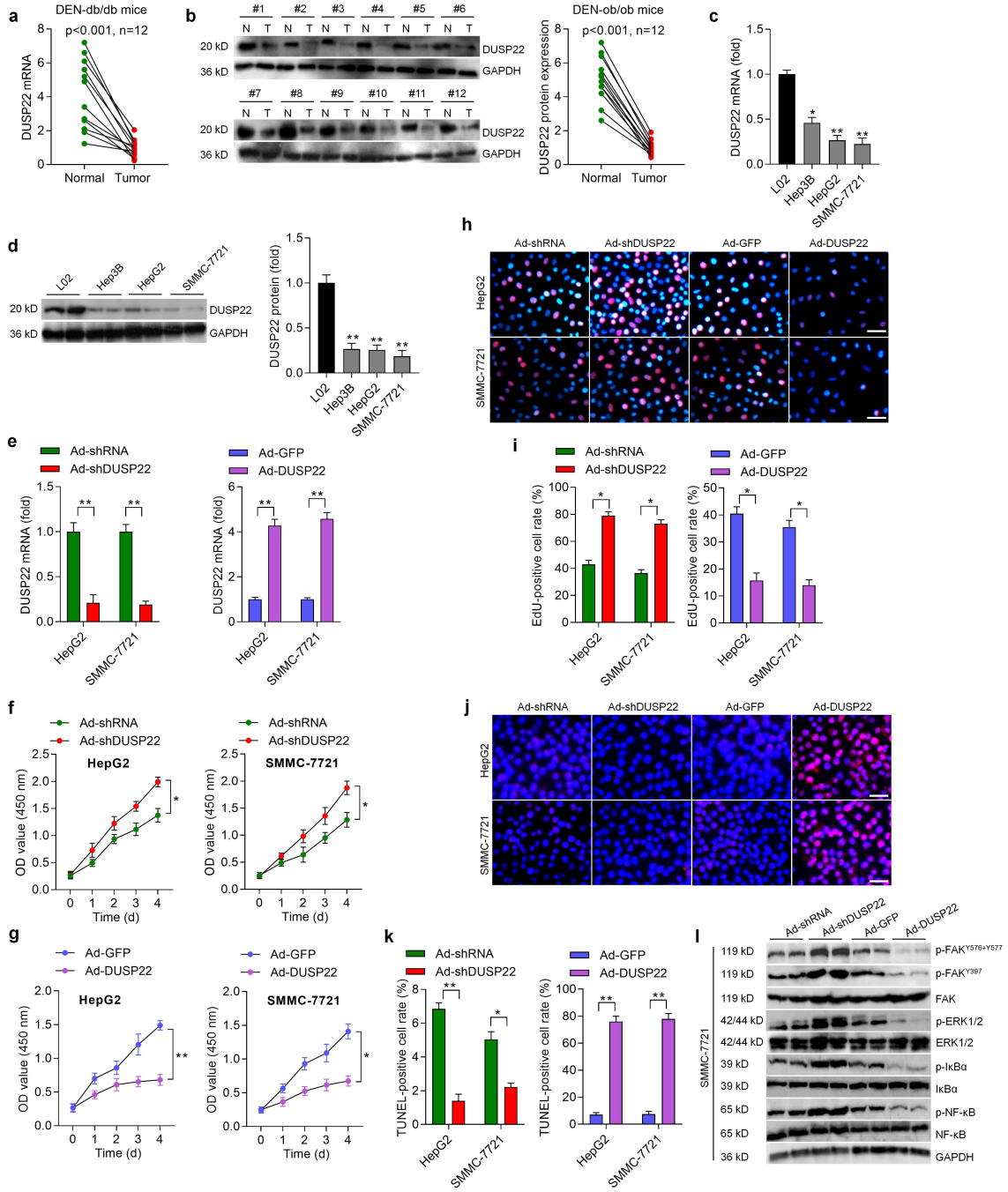
Supplementary Figure 21. Construction of hepatocyte-specific FAK knockout mice, and FAK is required for DUSP22 to restrain NF- κ B signaling *in vitro*. **a** Schematic workflow showing the establishment of the hepatocyte-specific FAK-knockout (FAK^{HepKO}) mouse strain. **b** Western blot showing FAK expression in liver from FAK^{fllox} and FAK^{HepKO} mice (n=4 mice per group). **c** Western blot showing FAK expression in liver, kidney, heart and fat of the indicated mice (n=3 mice per group). **d** Schematic diagram of the establishment of hepatocyte-specific DUSP22 and FAK double knockout (HepDKO) mouse strain. **e** Representative western blotting for the expression of DUSP22, p-FAK^{Y576+Y577}, p-FAK^{Y397} and FAK in the 24 h PO (0.4 mM PA and 0.8 mM OA)-treated primary hepatocytes or L02 cells transfected or co-transfected with Ad-shDUSP22, Ad-shFAK and Ad-shDUSP22/shFAK as shown. Cells transfected with Ad-shRNA were used as a control (n=4 per group). **f** Representative western blotting (left) and quantification (right) for the expression of total and phosphorylated I κ B α and NF- κ B in the 24 h PO (0.4 mM PA and 0.8 mM OA)-treated primary hepatocytes or L02 cells transfected or co-transfected with Ad-shDUSP22, Ad-shFAK and Ad-shDUSP22/shFAK as shown. Cells transfected with Ad-shRNA were used as a control (n=4 per group) (* P <0.05, ** P <0.01 and *** P <0.001; *ns*, no significant difference). Data are expressed as mean \pm SEM from at least three independent experiments. Statistical analysis was performed by two-tailed Student's *t*-test.



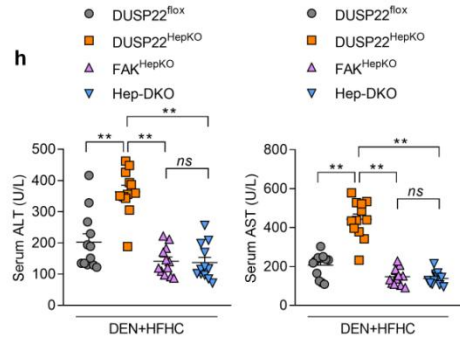
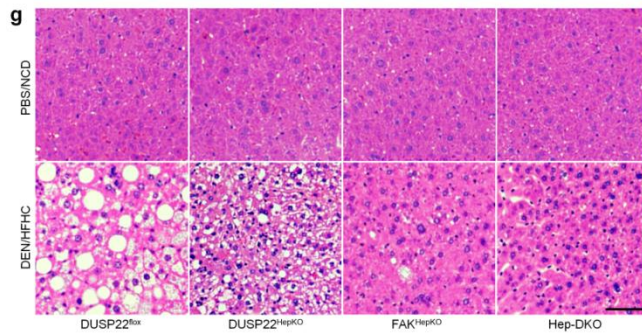
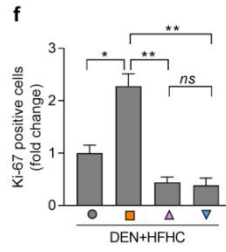
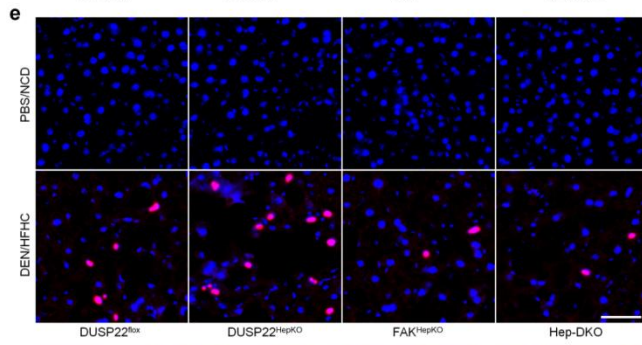
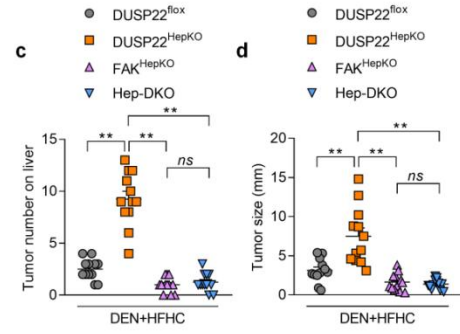
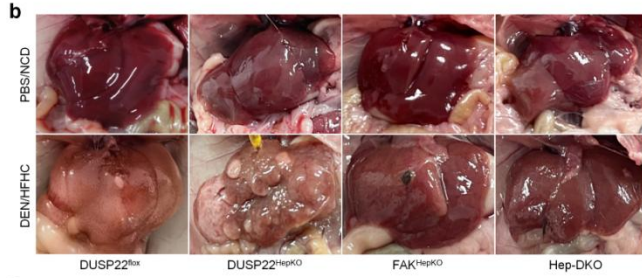
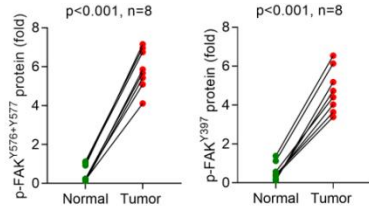
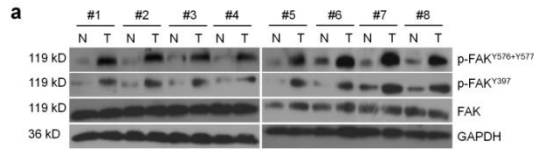
Supplementary Figure 22. FAK is indispensable for the protective function of DUSP22 against HFHC-induced NASH. **a** Schematic diagram of the establishment of LV-shDUSP22-regulated hepatocyte-specific DUSP22 loss-of function in FAK^{HepKO} mice (FAK^{HepKO}/LV-shDUSP22 HFHC) and FAK^{fllox} mice (FAK^{fllox}/LV-shDUSP22 HFHC) halfway through a 24-week HFHC feeding treatment. **b** Western blotting showing DUSP22, p-FAK^{Y576+Y577}, p-FAK^{Y397} and FAK expression in liver of FAK^{HepKO}, FAK^{HepKO}/LV-shDUSP22 and FAK^{fllox}/LV-shDUSP22 mice after HFHC feeding for 24 weeks (n=4 mice per group). **c-i** Measurements of (c) body weight, (d) liver weight, (e) ratio of LW/BW index, (f) blood glucose levels, (g) fasting insulin levels, (h) HOMA-IR index, and (i) serum ALT and AST concentrations in mice from the shown groups (n=12 mice per group) (**P*<0.05 and ***P*<0.01; *ns*, no significant difference). **j** Representative images of H&E staining, Oil Red O staining, Masson trichrome staining, Sirius red staining and immunohistochemistry examination of CD11b in liver sections from the shown groups of mice fed with a HFHC for 24 weeks (n=6 or 12 mice per group, with 10 images for each mouse; Scale bars, 50 μm). **k-o** Results for (k) NAS score, (l) Oil Red O-positive staining, (m) Masson trichrome-positive staining, (n) Sirius red-positive staining, and (o) CD11b-positive cells were analyzed and quantified (n=6 or 12 mice per group) (**P*<0.05, ***P*<0.01 and ****P*<0.001; *ns*, no significant difference). **p** Examination of liver TG, TC and NEFA contents from the indicated groups of mice (n=12 mice per group) (**P*<0.05; *ns*, no significant difference). **q** RT-qPCR results for crucial lipid metabolism- and fibrosis-associated genes as presented in liver of the shown groups of mice (n=4 mice per group) (**P*<0.05 and ***P*<0.01). **r** Representative western blotting of the protein expression of total and phosphorylated IκBα and NF-κB in liver of the indicated groups of mice (n=4 mice per group). **s** Assessments of serum levels of TNF-α, IL-1β, IL-6, MCP-1 and IL-10 from the shown groups of mice (n=12 mice per group) (**P*<0.05 and ***P*<0.01; *ns*, no significant difference). **t** RT-qPCR analysis of several critical inflammation-related genes in liver of the presented groups of mice (n=4 mice per group) (**P*<0.05 and ***P*<0.01). Data are expressed as mean ± SEM from at least three independent experiments. For statistical analysis, **c-p**, and **s** were performed by one-way ANOVA; **q** and **t** were carried out by two-tailed Student's *t*-test.



Supplementary Figure 23. DUSP22 protects against HFHC-induced hepatic dyslipidemia and inflammation. **a,b** Western blotting bands of DUSP22 protein expression levels in liver of HFHC-fed transplanted **(a)** LV-DUSP22 mice, and **(b)** LV-shDUSP22 mice. LV-Ctrl and LV-shCtrl were used as corresponding controls (n=4 mice per group). **c** RT-qPCR results for inflammation-related molecules in liver of the indicated groups of mice (n=6 mice per group) (* P <0.05 and ** P <0.01). **d** RT-qPCR results of lipid metabolism-associated genes in liver of the shown groups of mice (n=6 mice per group) (* P <0.05 and ** P <0.01). Data are expressed as mean \pm SEM from at least three independent experiments. Statistical analysis were carried out by two-tailed Student's t -test.



Supplementary Figure 24. DUSP22 meliorates NASH-HCC cell growth. **a,b** Results for **(a)** RT-qPCR and **(b)** western blotting analysis of DUSP22 mRNA and protein expression levels, respectively, in liver of genetic NASH-HCC mouse models: DEN-treated ob/ob mice (n=12 mice per group). **c,d** Results for **(c)** RT-qPCR and **(d)** western blotting analysis of DUSP22 mRNA and protein expression levels, respectively, in human HCC cell lines (Hep3B, HepG2 and SMMC-7721) and in non-tumor L02 cells. DUSP22 expression in L02 cells was used as a control (n=4 per group) (* P <0.05 and ** P <0.01 versus the expression from L02 group). **e** RT-qPCR results for DUSP22 in HepG2 and SMMC-7721 cells transfected with Ad-shDUSP22 (left) or Ad-DUSP22 (right) for DUSP22 knockdown and over-expression, respectively. Ad-shRNA and Ad-GFP were used as corresponding controls (n=4 per group) (** P <0.01). **f,g** CCK-8 analysis of cell growth in the indicated stable cell lines with **(f)** DUSP22 knockdown or **(g)** over-expression (n=4 per group) (* P <0.05 and ** P <0.01). **h,i** Representative images **(h)** and quantification **(i)** of the proliferation of HepG2 and SMMC-7721 cells transfected with Ad-shDUSP22 or Ad-DUSP22 by EdU assay (n=5 per group, with 10 images per group; Scale bar, 80 μ m) (* P <0.05). **j,k** Representative images **(j)** and quantification **(k)** of the apoptotic cell death of HepG2 and SMMC-7721 cells with DUSP22 knockdown or over-expression by TUNEL staining assay (n=5 per group, with 10 images per group; Scale bar, 80 μ m) (* P <0.05 and ** P <0.01). **l** Representative western blotting and quantification of the protein expression of total and phosphorylated FAK^{Y576+Y577}, FAK^{Y397}, ERK1/2, I κ B α and NF- κ B in SMMC-7721 cells transfected with Ad-shDUSP22 or Ad-DUSP22 as shown (n=4 per group). Data are expressed as mean \pm SEM from at least three independent experiments. Statistical analysis were carried out by two-tailed Student's *t*-test.



Supplementary Figure 25. FAK blockage is involved in DUSP22-inhibited progression of NASH-HCC induced by DEN/HFHC. **a** Western blotting analysis for p-FAK^{Y576+Y577} and p-FAK^{Y397} protein expression levels in individual paired NAFLD-HCC (T) and adjacent normal samples (N) (n=8). **b** Representative images of liver appearances (n=12 mice per group). **c,d** Quantification for **(c)** surface tumor number and **(d)** tumor size in each shown group (n=12 per group) (***P*<0.01; *ns*, no significant difference). **e** Immunofluorescence examination of Ki-67 (Scale bars, 20 μm) in liver sections from the shown groups of mice (n=6 mice per group, with 10 images for each mouse). **f** Number of Ki-67-positive cells was quantified (**P*<0.05 and ***P*<0.01; *ns*, no significant difference). **g** Representative images of H&E staining (Scale bars, 50 μm) in liver sections from the shown groups of mice (n=6 mice per group, with 10 images for each mouse). **h** Serum ALT and AST contents from the indicated groups of mice were examined (n=12 per group) (***P*<0.01; *ns*, no significant difference). Data are expressed as mean ± SEM from at least three independent experiments. For statistical analysis, **a** was performed by two-tailed Student's *t*-test; **c, d, e** and **h** were performed by one-way ANOVA.

Supplementary Tables

Supplementary Table 1. Clinical information of non-steatosis individuals and NASH

Items	patients.	
	Non-steatosis	NASH
All number (n)	16	20
Male (n)	11	11
Female (n)	5	9
Age (years)	35.06 ± 2.00	38.05 ± 2.44
BMI (kg/m ²)	19.56 ± 0.62	29.78 ± 0.61
AST (U/L)	24.79 ± 1.88	54.27 ± 2.21
ALT (U/L)	22.22 ± 2.12	42.28 ± 1.74
TG (mmol/L)	1.71 ± 0.07	2.21 ± 0.09
TC (mmol/L)	3.76 ± 0.12	4.46 ± 0.17
Fasting blood glucose (mmol/L)	5.04 ± 0.19	6.28 ± 0.15
Liver IL-6 mRNA (fold)	1.55 ± 0.06	3.84 ± 0.20
Liver DUSP22 protein (fold)	1.00 ± 0.05	0.34 ± 0.04
Liver TNF- α mRNA (fold)	1.40 ± 0.08	4.61 ± 0.09
LN (μ g/L)	78.31 ± 7.16	158.32 ± 8.32
HA (μ g/L)	37.00 ± 2.81	101.47 ± 5.50
IVC (μ g/L)	70.99 ± 6.44	113.05 ± 5.44
PCIII (μ g/L)	49.31 ± 5.73	116.64 ± 8.41
GGT (U/L)	28.96 ± 2.71	71.83 ± 3.79
AKP (U/L)	86.74 ± 4.83	780.73 ± 7.6

Data are expressed as mean \pm SEM unless otherwise stated. BMI, body mass index; AST, aspartate aminotransferase; ALT, alanine aminotransferase; TG, triglycerides; TC, total cholesterol; LN, laminin; HA, hyaluronuc acid; IVC, collagen type IV; PCIII, type III precollagen; GGT, γ -glutamyl Transpeptidase; AKP, alkline phosphatase.

Supplementary Table 2. Detailed information for non-steatosis individuals and NASH patients.

Items	Sex	Age (Years)	BMI (Kg/m²)	AST (U/L)	ALT (U/L)	TG (mmol/L)	TC (mmol/L)	FBG (mmol/L)	NAS
Non-steatosis	Female	35	19.5	30.3	11.8	1.41	3.23	4.2	0
Non-steatosis	Male	43	15.2	32.1	18.7	1.33	4.71	5.7	0
Non-steatosis	Male	29	19.9	29.5	24.3	2.18	3.7	5.8	0
Non-steatosis	Male	26	19.9	27.0	25.7	1.35	3.42	4.7	0
Non-steatosis	Male	33	19.2	15.5	19.1	2.01	3.66	5.5	0
Non-steatosis	Male	21	17.9	30.7	27.5	1.47	3.73	4.1	0
Non-steatosis	Female	32	18.3	15.0	13.2	1.92	3.22	5.6	0
Non-steatosis	Female	29	18.1	15.2	30.9	1.93	3.25	4.0	0
Non-steatosis	Male	28	20.2	30.8	30.9	1.75	3.56	4.7	0
Non-steatosis	Male	30	19.9	33.8	13.6	1.42	3.91	5.3	0
Non-steatosis	Female	35	15.6	13.7	26.1	1.56	3.38	5.8	0
Non-steatosis	Male	41	18.1	31.8	29.8	1.88	4.08	4.3	0
Non-steatosis	Male	39	23.9	31.3	36.4	1.81	4.15	4.3	0
Non-steatosis	Female	47	23.9	21.4	22.4	1.63	3.47	6.0	0
Non-steatosis	Male	46	22.1	23.0	10.4	2.20	3.96	4.6	0
Non-steatosis	Male	47	21.6	15.6	10.7	1.60	4.78	6.1	0
NASH	Male	33	31.3	37.8	36.3	2.25	3.84	7.1	4
NASH	Female	31	30.3	64.4	57.2	3.54	5.96	7.9	4
NASH	Male	26	28.1	48.0	43.7	1.98	3.64	5.0	5
NASH	Female	32	37.4	59.7	39.9	2.45	4.13	5.2	4
NASH	Female	29	30.9	40.3	32.8	1.67	3.12	5.7	4
NASH	Male	30	28.3	46.6	48.1	2.67	3.71	5.3	5
NASH	Male	45	28.4	59.5	33.6	1.96	4.68	5.0	3
NASH	Male	28	31.5	54.8	37.0	2.33	4.52	6.7	4
NASH	Female	22	30.5	62.0	49.1	2.14	3.16	6.3	6
NASH	Female	35	28.1	62.0	54.5	2.58	4.02	5.9	5
NASH	Male	29	31.3	60.1	31.8	1.98	5.21	6.2	4
NASH	Male	27	29.4	56.9	37.8	1.91	5.9	6.7	4
NASH	Male	45	24.4	42.0	53.7	2.05	4.2	6.6	5
NASH	Female	55	27.3	55.8	33.6	2.11	5.11	6.9	4
NASH	Female	54	31.3	36.6	49.2	2.32	4.89	6.6	4
NASH	Female	54	32.5	44.4	34.7	2.41	4.75	6.3	4
NASH	Male	54	31.2	66.3	42.1	2.14	4.30	6.6	8
NASH	Male	39	28.1	59.2	46.3	2.02	4.71	5.9	6
NASH	Male	47	29.4	68.2	39.8	1.80	4.25	6.3	8
NASH	Female	46	26.3	60.8	44.4	1.97	5.06	6.4	5

FBG, fasting blood glucose; NAS, NAFLD activity score.

Supplementary Table 3. Clinical pathological information of the NAFLD-associated HCC patients.

Patient no.	Gender	Age (years)	Hep B	Hep C	Fatty liver	Diabetes	Hypertension	Dyslipidemia
1	Male	56	Negative	Negative	Yes	Yes	Yes	No
2	Male	69	Negative	Negative	Yes	Yes	Yes	Yes
3	Male	38	Negative	Negative	Yes	No	Yes	Yes
4	Female	72	Negative	Negative	Yes	Yes	No	Yes
5	Female	78	Negative	Negative	No	Yes	Yes	No
6	Male	74	Negative	Negative	Yes	Yes	Yes	No
7	Male	55	Negative	Negative	No	No	Yes	No
8	Male	62	Negative	Negative	No	Yes	Yes	Yes

Hep B, hepatitis B; Hep C, hepatitis C.

Supplementary Table 4. Primer sequences used for RT-qPCR analysis.

Items	Primer sequences (5'→3')
DUSP22 (Homo sapiens)	Forward: AGCAGCGGATTCACCATCTC
	Reverse: TGATGTATGCGATCACCAGTGT
IL-6 (Homo sapiens)	Forward: CCAGGAGCCCAGCTATGAAC
	Reverse: CCCAGGGAGAAGGCAACTG
TNF- α (Homo sapiens)	Forward: CCTCTCTCTAATCAGCCCTCTG
	Reverse: GAGGACCTGGGAGTAGATGAG
IL-1 β (Homo sapiens)	Forward: CCTGCGTGTTGAAAGATGATAA
	Reverse: CTGCTTGAGAGGTGCTGATGTA
IL-18 (Homo sapiens)	Forward: AGAGCGCAATGGTG
	Reverse: GACGCATGCCCTCAA
MCP-1 (Homo sapiens)	Forward: GTCTCTGCCGCCCTTCTG
	Reverse: ACTTGCTGCTGGTGATTCTTCT
CXCR2 (Homo sapiens)	Forward: CATGGAGAGTGACAGCTTTGAA
	Reverse: CTTGTTGATTTCCAGGGATTCTG
CXCL2 (Homo sapiens)	Forward: ATGTCTTTCTTGTAAGGCATACTG
	Reverse: CGAAACCTCTCTGCTCTAACAC
IL-1 α (Homo sapiens)	Forward: AATGACGCCCTCAATCAAAG
	Reverse: TGGGTATCTCAGGCATCTCC
CX3CR1 (Homo sapiens)	Forward: CTTACGATGGCACCCAGTGA
	Reverse: CAAGGCAGTCCAGGAGAGTT
CXCL10 (Homo sapiens)	Forward: GTGGCATTCAAGGAGTACCTC
	Reverse: TGATGGCCTTCGATTCTGGATT
CXCL9 (Homo sapiens)	Forward: CCAATACAGGAGTGACTTGGAAC
	Reverse: TCACTACTGGGTTCCCTTGC
CCL5 (Homo sapiens)	Forward: CAGCAGTCGTCTTTGTCACC
	Reverse: AGGACTCTCCATCCTAGCTCA
CXCL3 (Homo sapiens)	Forward: GCGTATCATTGACACTTCCTGC
	Reverse: CCTTCCAGCTGTCCCTAGAA
CCL4 (Homo sapiens)	Forward: AAGTCTGTGCTGATCCCAGT
	Reverse: CAGGTGACCTTCCCTGAAGA
CD206 (Homo sapiens)	Forward: GCCCGGAGTCAGATCACACA
	Reverse: AGTGGCTCAACCCGATATGACAG
IL-10 (Homo sapiens)	Forward: AGGGCACCCAGTCTGAGAACA
	Reverse: CGGCCTTGCTCTTGTFTTCAC
SREBP1C (Homo sapiens)	Forward: CATGTCTTCGATGTCGGTCAG
	Reverse: TCCTGTTGCCCATATGAAATCA
CYP7A1 (Homo sapiens)	Forward: GACATCATAGCTC TTTACCCAC
	Reverse: GGTGTTCTGCAGTCCTGTAAT
HMGCR (Homo sapiens)	Forward: TACCATGTCAGGGGTACGTC
	Reverse: CAAGCCTAGAGACATAATCATC

ABCG1 (Homo sapiens)	Forward: CCCTGTGGAATGTACCTATGTG
	Reverse: GAGGTGTCCCAAAGATGCAA
CD36 (Homo sapiens)	Forward: AGATGCAGCCTCATTTCAC
	Reverse: GCCTTGGATGGAAGAACAAA
FATP1 (Homo sapiens)	Forward: CCACTTGGATGTCACCACTG
	Reverse: GTGGGACCCTCCAGTAGACA
FABP1 (Homo sapiens)	Forward: ATGAGTTTCTCCGGCAAGTACC
	Reverse: CTCTCCGGCAGACCGATTG
FASN (Homo sapiens)	Forward: GGACCTGACCTGCCGTCTAG
	Reverse: GAGGAGTGGGTGTCGCTGTT
SCD1 (Homo sapiens)	Forward: CTCCACTGCTGGACATGAGA
	Reverse: AATGAGTGAAGGGGCACAAC
DGAT2 (Homo sapiens)	Forward: ATTGCTGGCTCATCGCTGT
	Reverse: GGGAAAGTAGTCTCGAAAGTAGC
ACACA (Homo sapiens)	Forward: TCCAGGCCAGTACGGAATTC
	Reverse: ACTTTCCTCGCCAAACCAGTAG
PPAR γ (Homo sapiens)	Forward: ATGACAGCGACTTGGCAATA
	Reverse: GCAACTGGAAGAAGGGAAAT
PPAR α (Homo sapiens)	Forward: GAGATTCGCAATCCATCGG
	Reverse: CTACATTCGATGTTCAATGC
ACOX1 (Homo sapiens)	Forward: GTCTCCGTCATGAATCCCGA
	Reverse: TGCATGCCAAATTCCCTCA
UCP2 (Homo sapiens)	Forward: TTGGGTTCAAGGCCACAGAT
	Reverse: CCAGCCCCAAGAACTTCAC
CPT1 α (Homo sapiens)	Forward: TCTGCAGTCGACTCACCTT
	Reverse: TCCACAGGACACATAGTCAGG
ACSL1 (Homo sapiens)	Forward: ATCTGCAAGCCAGGAAGAGTC
	Reverse: CTTGCTTGATGCTTTGGTCTGT
α -SMA (Homo sapiens)	Forward: GCTACTCCTTCGTGACCACAG
	Reverse: GCCGTCGCCATCTCGTTCT
COL1A1 (Homo sapiens)	Forward: GTGCTCCTGGTATTGCTGGT
	Reverse: TCCTTGAACACCAACAGGGC
COL3A1 (Homo sapiens)	Forward: TTCGACTTCTCTCCAGCCGA
	Reverse: TCCACTGGCCTGATCCATGT
CTGF (Homo sapiens)	Forward: AGACCTGTGCCTGCCATTAC
	Reverse: ACGCCATGTCTCCGTACATC
GAPDH (Homo sapiens)	Forward: GGAGTCAACGGATTTGGTC
	Reverse: GGCAACAATATCCACTTTACC
DUSP22 (Mus musculus)	Forward: GTTGAAGCAGGAACAAGGT
	Reverse: TTGAGATGGTGTGTCTGC
IL-6 (Mus musculus)	Forward: CAACGATGATGCACTTGCAGA
	Reverse: TCTCTCTGAAGGACTCTGGCT
TNF- α (Mus musculus)	Forward: ACCTGGCCTCTCTACCTTGT

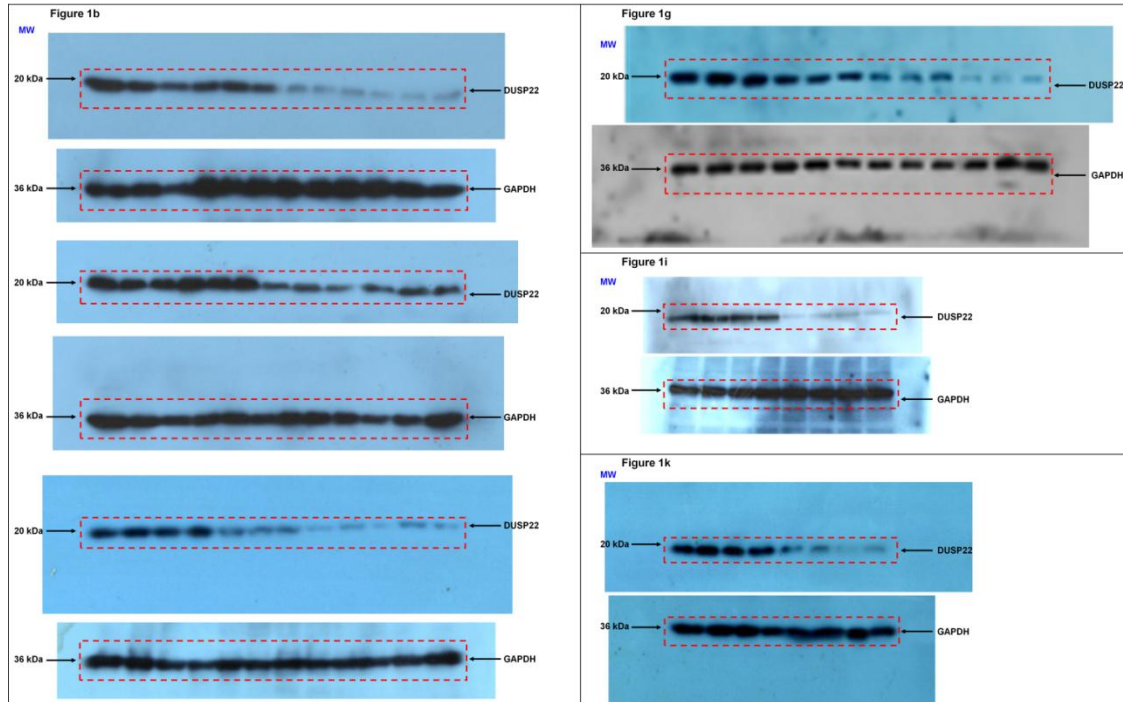
	Reverse: CCCGTAGGGCGATTACAGTC
IL-1 β (Mus musculus)	Forward: GCCACCTTTTGACAGTGATGAG
	Reverse: AGTGATACTGCCTGCCTGAAG
IL-18 (Mus musculus)	Forward: CAAGGCTGGTCCATGCTCC
	Reverse: TGCTATCACTTCCTTTCTGTTGC
MCP-1 (Mus musculus)	Forward: CTGTCACACTGGTCACTCCTAC
	Reverse: CTGTCACACTGGTCACTCCTAC
F4/80 (Mus musculus)	Forward: CGTCAGGTACGGGATGAATATAAG
	Reverse: CTATGCCATCCACTTCCAAGAT
CXCR2 (Mus musculus)	Forward: ATGCCCTCTATTCTGCCAGAT
	Reverse: GTGCTCCGGTTGTATAAGATGAC
CXCL2 (Mus musculus)	Forward: CGGTCAAAAAGTTTGCCTTG
	Reverse: TCCAGGTCAGTTAGCCTTG
IL-1 α (Mus musculus)	Forward: CGAAGACTACAGTTCTGCCATT
	Reverse: GACGTTTTAGAGTTCTCAGAG
CX3CR1 (Mus musculus)	Forward: ATCCAGTTCAGGGAAGGAGG
	Reverse: AGACTGGGTGAGTGACTGGC
CXCL10 (Mus musculus)	Forward: ATGACGGGCCAGTGAGAATG
	Reverse: ATGATCTCAACACGTGGGCA
CXCL9 (Mus musculus)	Forward: TCTGCATCAGTGACGGTAAAC
	Reverse: TGAAGGGCACAGTTTGGAG
CCL5 (Mus musculus)	Forward: TGCTGCTTTGCCTACCTCTC
	Reverse: TCTTCTCTGGGTTGGCACAC
CXCL3 (Mus musculus)	Forward: CAGCCACACTCCAGCCTA
	Reverse: CACAACAGCCCCTGTAGC
CCL4 (Mus musculus)	Forward: TTCTGTGCTCCAGGGTTCTC
	Reverse: CGGGAGGTGTAAGAGAAACAG
CD206 (Mus musculus)	Forward: GGAATCAAGGGCACAGAGTTA
	Reverse: ATTGTGGAGCAGATGGAA
IL-10 (Mus musculus)	Forward: TTTTCACAGGGGAGAAATCG
	Reverse: CCAAGCCTTATCGGAAATGA
SREBP1C (Mus musculus)	Forward: CACTTCTGGAGACATCGCAAAC
	Reverse: ATGGTAGACAACAGCCGCATC
CYP7A1 (Mus musculus)	Forward: CTGGGCTGTGCTCTGAAGTT
	Reverse: TGCTTTCGCAGAAGTAGTGT
HMGCR (Mus musculus)	Forward: ATCATGTGCTGCTTCGGCTGCAT
	Reverse: AAATTGGACGACCCTCACGGCT
ABCG1 (Mus musculus)	Forward: ATCTACGGCTTGGACCGAGA
	Reverse: TGCCAGGACGATGAAATCC
CD36 (Mus musculus)	Forward: AAATAAACCTCCTTGGCCTGA
	Reverse: GCAACAAACATCACCACACC
FATP1 (Mus musculus)	Forward: TGCACAGCAGGTACTACCGCAT
	Reverse: TGCGCAGTACCACCGTCAAC

FABP1 (Mus musculus)	Forward: GCAGAGCCAGGAGAACTTTG
	Reverse: GGGTCCATAGGTGATGGTGAG
FASN (Mus musculus)	Forward: CTGCGGAAACTTCAGGAAATG
	Reverse: GGTTCGGAATGCTATCCAGG
SCD1 (Mus musculus)	Forward: CCTACGACAAGAACATTCAATCCC
	Reverse: ACTCACTGGCAGAGTAGTCGAA
DGAT2 (Mus musculus)	Forward: GGCGCTACTTCCGAGACTAC
	Reverse: TGGTCAGCAGGTTGTGTGTC
ACACA (Mus musculus)	Forward: GGCCAGTGCTATGCTGAGAT
	Reverse: AGGGTCAAGTGCTGCTCCA
PPAR γ (Mus musculus)	Forward: ATTCTGGCCCACCAACTTCGG
	Reverse: TGGAAGCCTGATGCTTTATCCCCA
PPAR α (Mus musculus)	Forward: CAAGGCCTCAGGGTACCACT
	Reverse: TTGCAGCTCCGATCACACTT
ACOX1 (Mus musculus)	Forward: GTCTCCGTCATGAATCCCGA
	Reverse: TGCATGCCAAATTCCCTCA
UCP2 (Mus musculus)	Forward: ACAAGACCATTGCACGAGAG
	Reverse: CATGGTAAGGGCACAGTGAC
CPT1 α (Mus musculus)	Forward: CTCAGTGGGAGCGACTCTTCA
	Reverse: GGCCTCTGTGGTACACGACAA
ACSL1 (Mus musculus)	Forward: TGCCAGAGCTGATTGACATTC
	Reverse: GGCATAACCAGAAGGTGGTGAG
α -SMA (Mus musculus)	Forward: TTCCTTCGTGACTACTGCCG
	Reverse: TATAGGTGGTTTCGTGGATGCC
COL1A1 (Mus musculus)	Forward: CGATGGATTCCCGTTCGAGT
	Reverse: AAGGGTGCTGTAGGTGAAGC
COL3A1 (Mus musculus)	Forward: CCCAACCAGAGATCCCATT
	Reverse: GAAGCACAGGAGCAGGTGTAGA
CTGF (Mus musculus)	Forward: GAGTGTGCACTGCCAAAGAT
	Reverse: GGCAAGTGCATTGGTATTTG
Fibronectin (Mus musculus)	Forward: CACCCGTGAAGAATGAAG
	Reverse: CAGGCAGGAGATTTGTTAG
TGF- β 1 (Mus musculus)	Forward: ATTTGGAGCCTGGACACACA
	Reverse: GAGCGCACAATCATGTTGGA
DUSP3 (Mus musculus)	Forward: GGGTGATGCCAGTTTCT
	Reverse: GATCTCAACGACCTGCTCTC
DUSP8 (Mus musculus)	Forward: TGACCCAAAACGGAATAAGC
	Reverse: AGAGATGCCAGCCAGACAGT
DUSP9 (Mus musculus)	Forward: GGCATCCGCTATATCCTCAA
	Reverse: GGGGATCTGCTTGTAGTGGA
DUSP12 (Mus musculus)	Forward: TCTCTGTGAGCAAAGGCTATT
	Reverse: CTTCGCTGTTGACCCAACTA
DUSP14 (Mus musculus)	Forward: GAGAAGGAGTCCCGACA

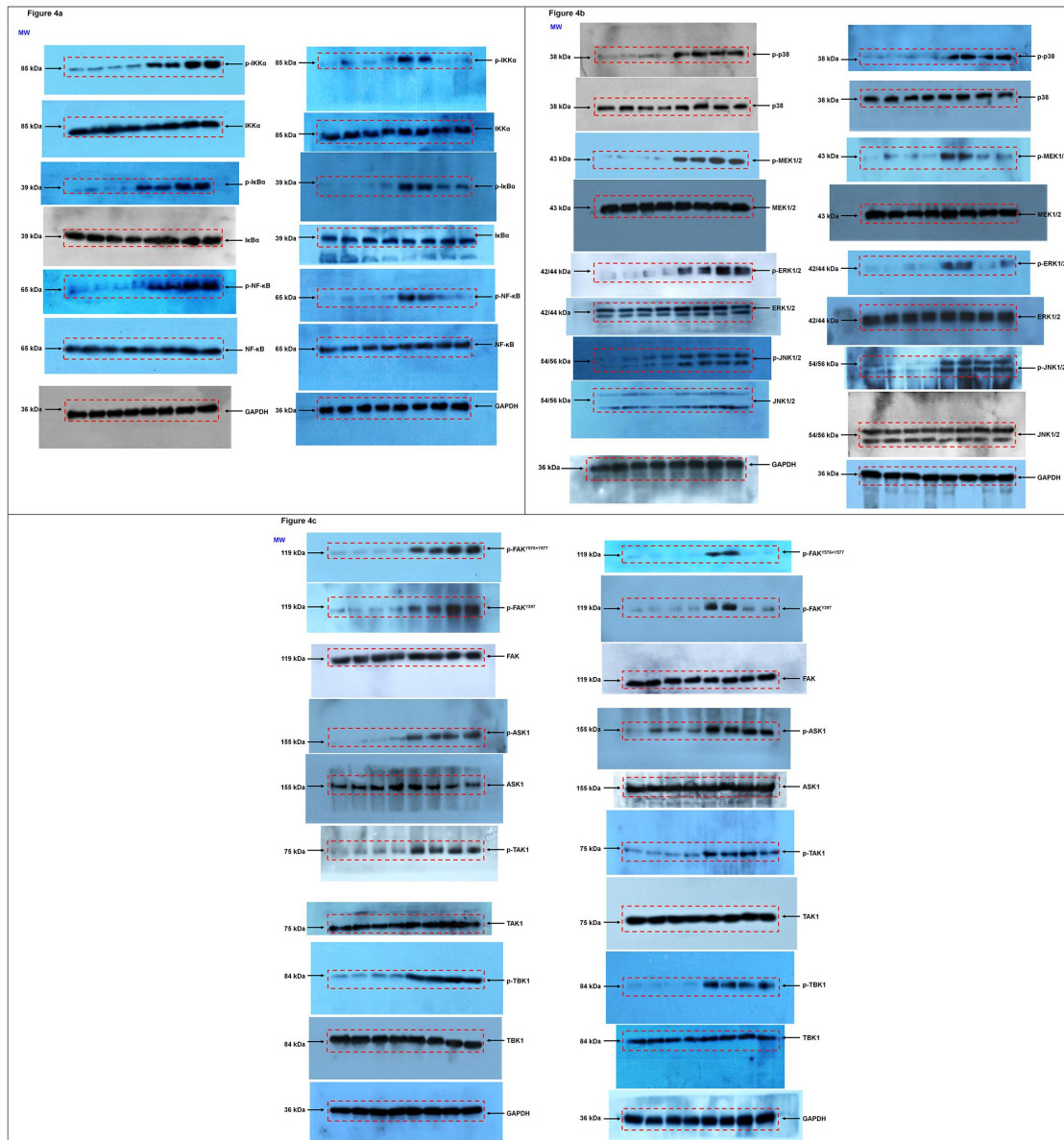
	Reverse: CAGGCAACGCACGTATTTC
DUSP16 (Mus musculus)	Forward: CACTCAGATATTCTGGCTCCC
	Reverse: CTAGACATGGTAGTGGTGATGGC
DUSP26 (Mus musculus)	Forward: ATGCCCTCTGTTACCATCC
	Reverse: CTGTTGTGTGAGGCGTTGAG
GAPDH (Mus musculus)	Forward: GGTGAAGGTCGGTGTGAACG
	Reverse: CCCGTAGGGCGATTACAGTC

Uncropped western blotting bands in the study

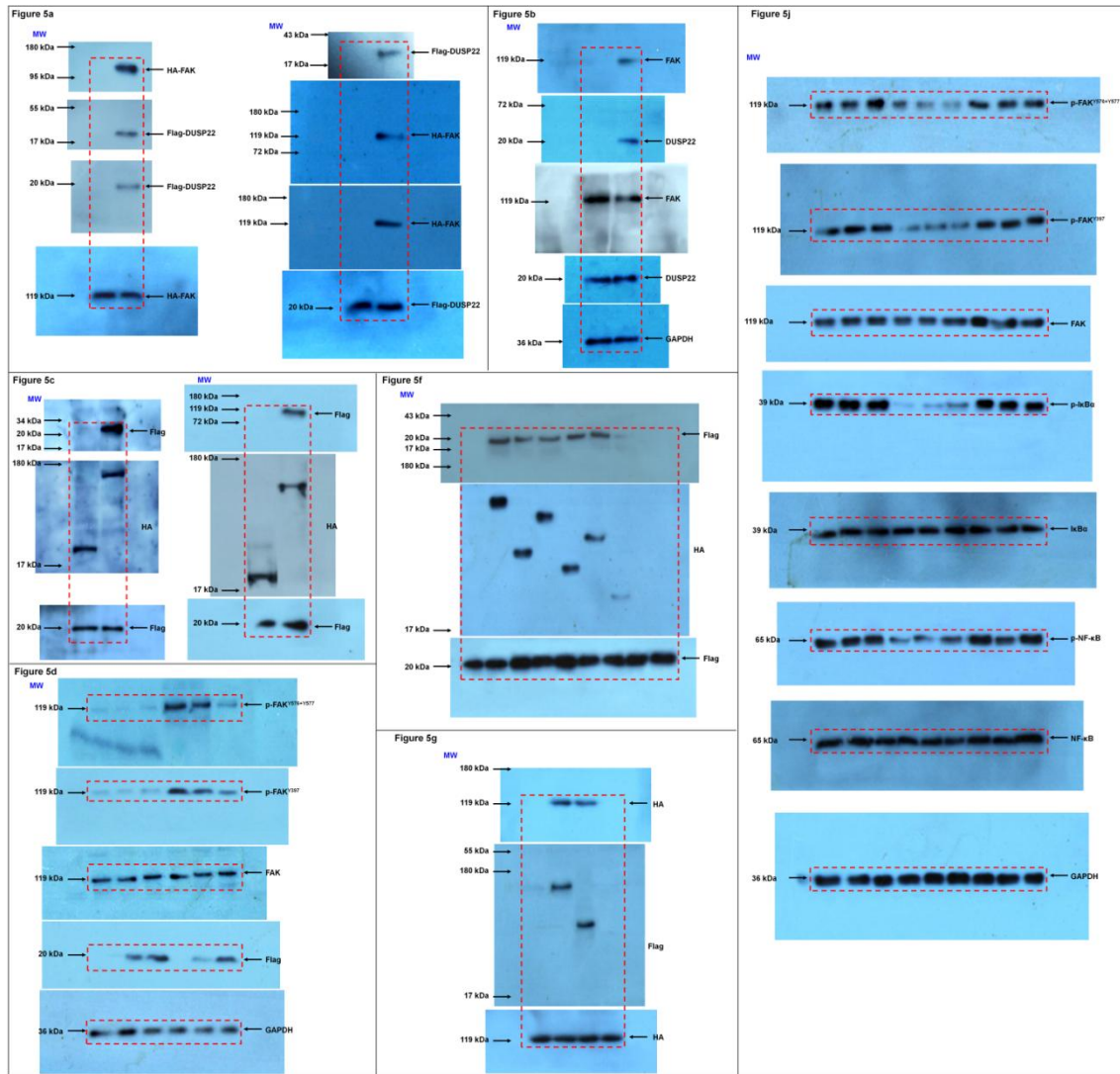
Western blots for figure 1



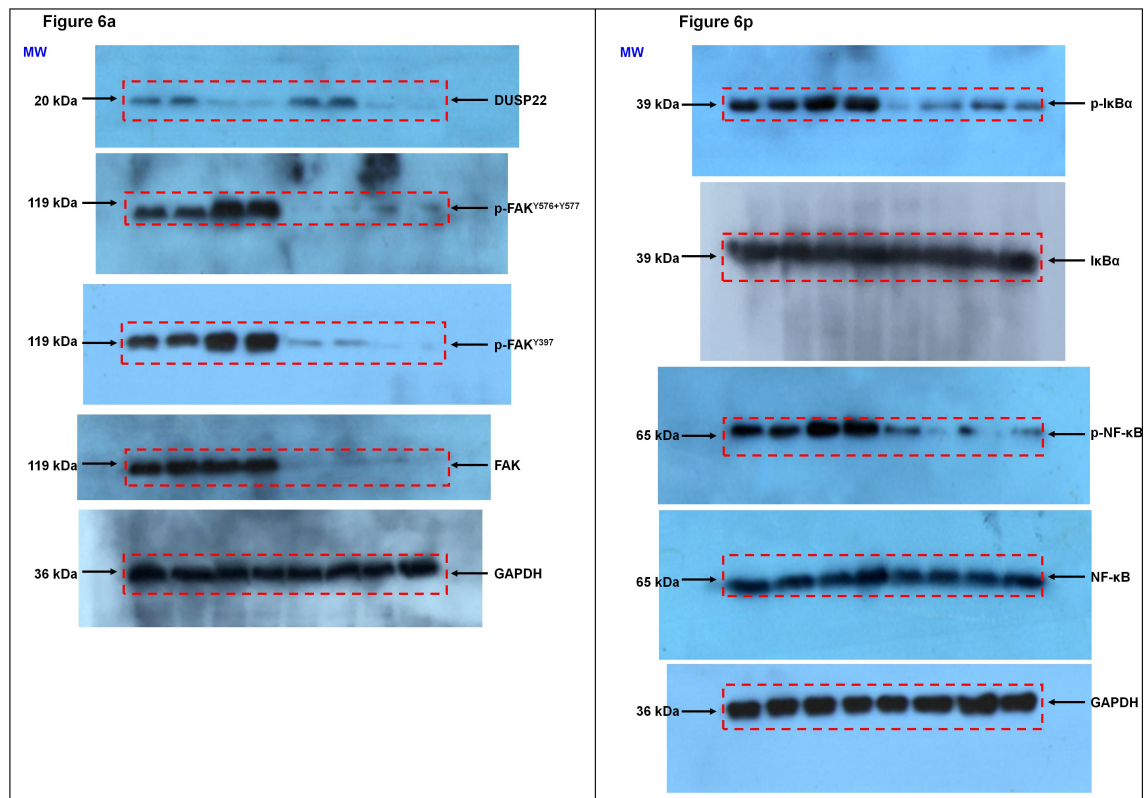
Western blots for figure 4



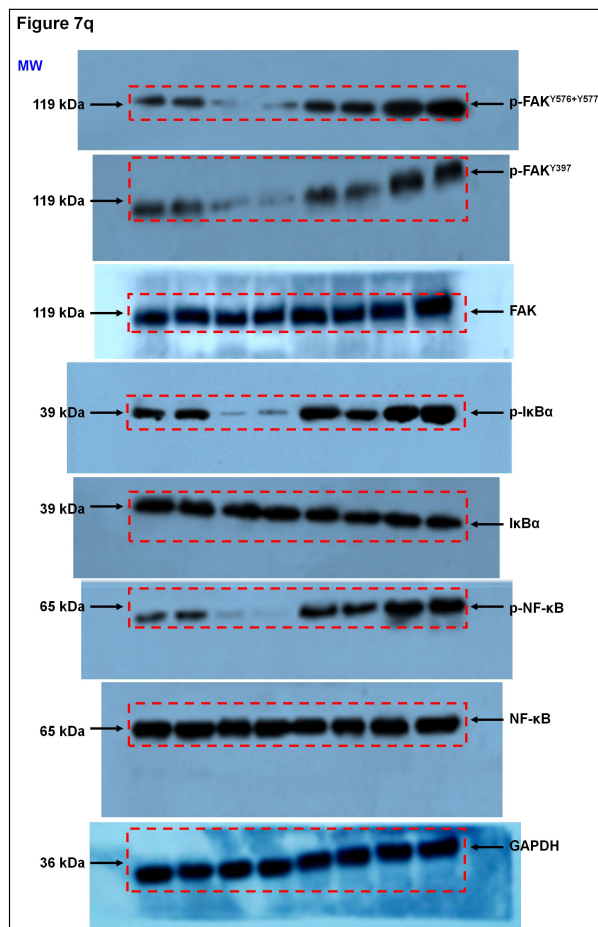
Western blots for figure 5



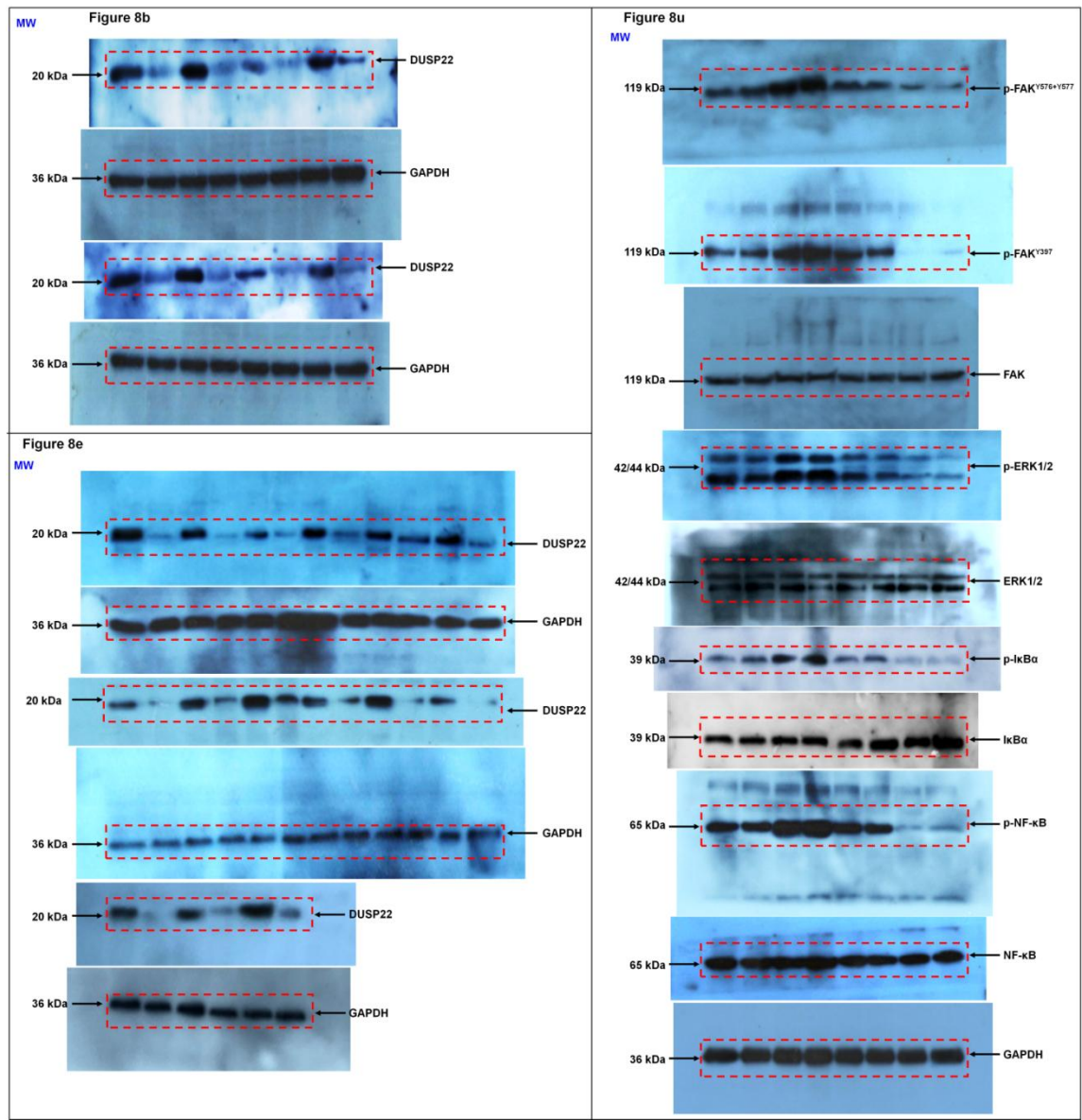
Western blots for figure 6



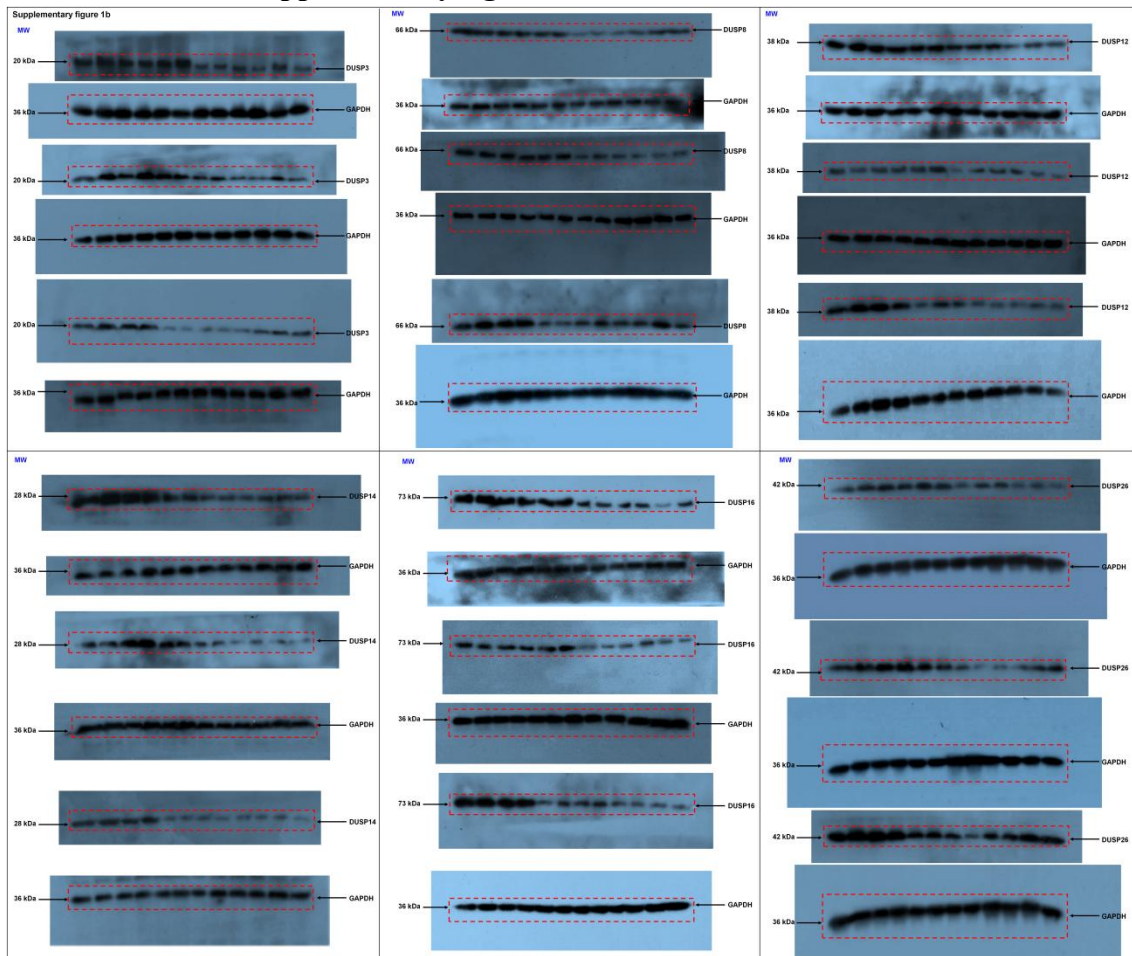
Western blots for figure 7



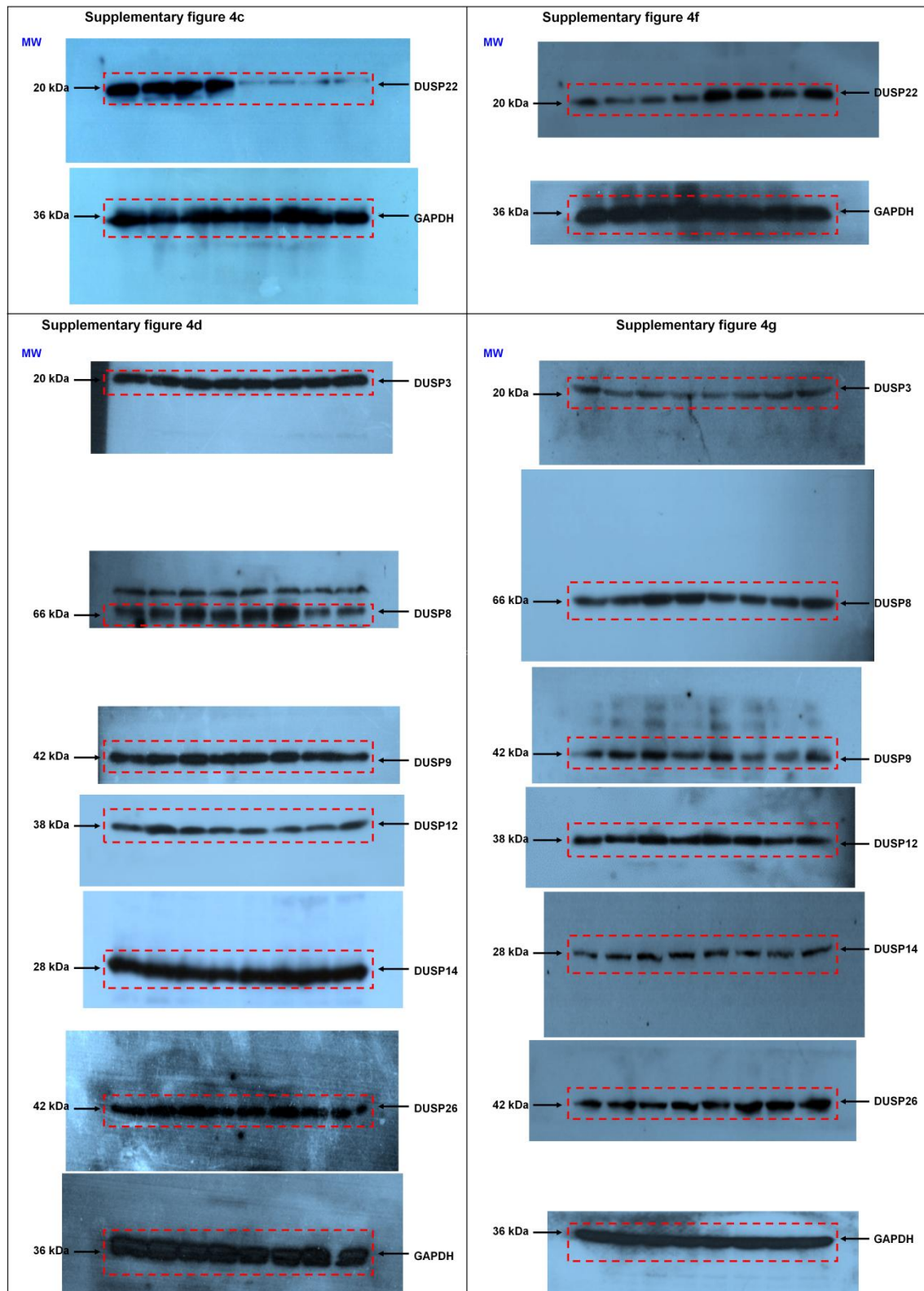
Western blots for figure 8



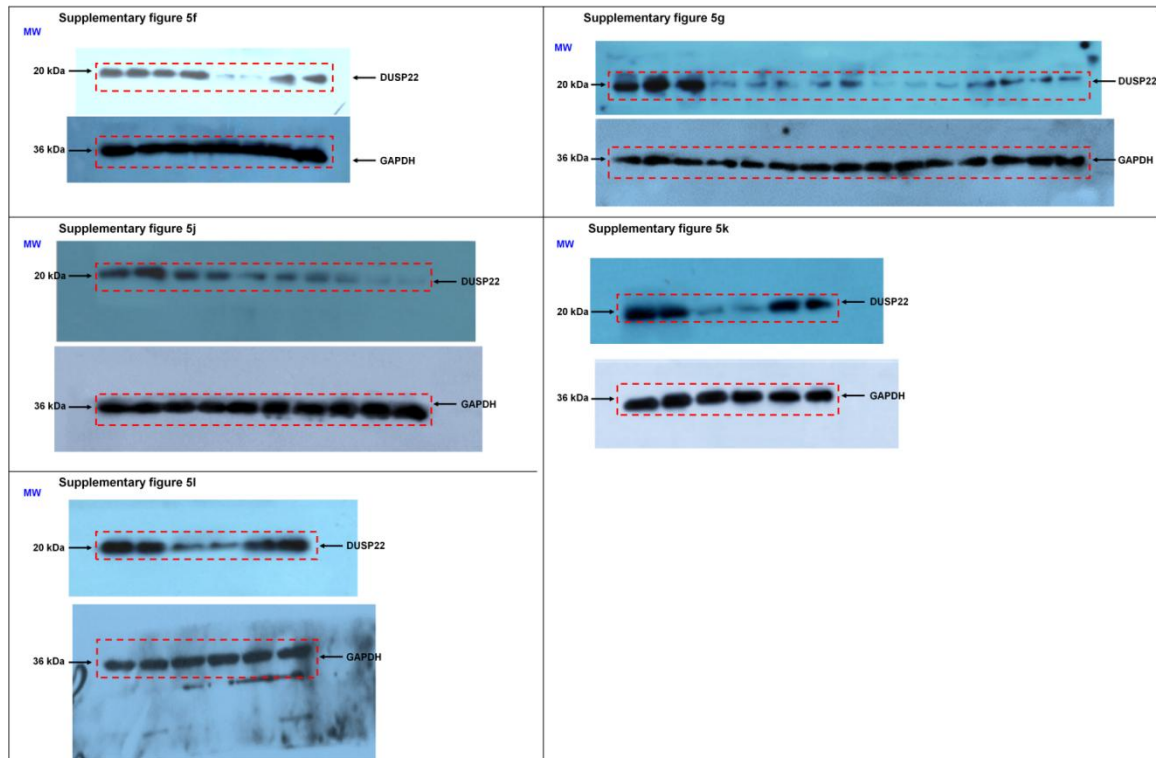
Western blots for supplementary figure 1



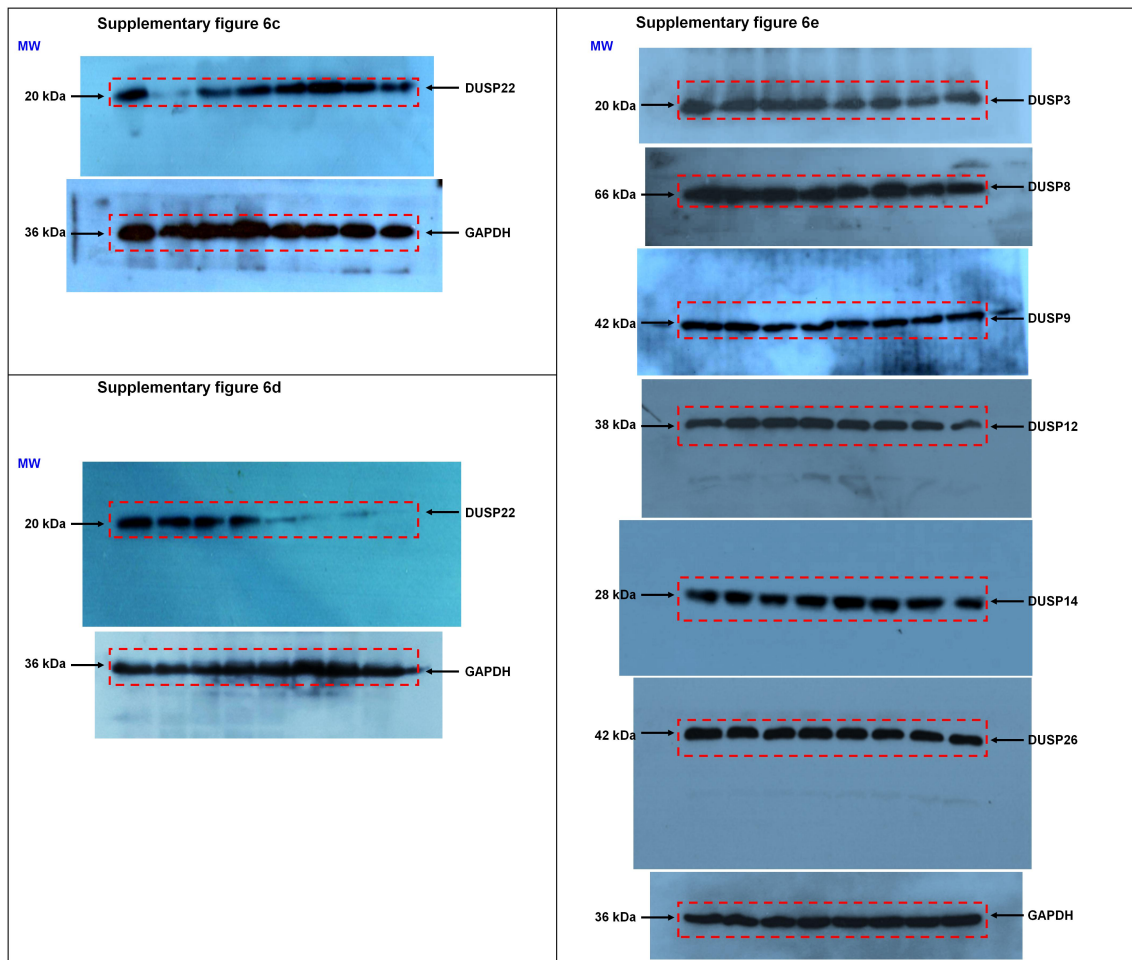
Western blots for supplementary figure 4



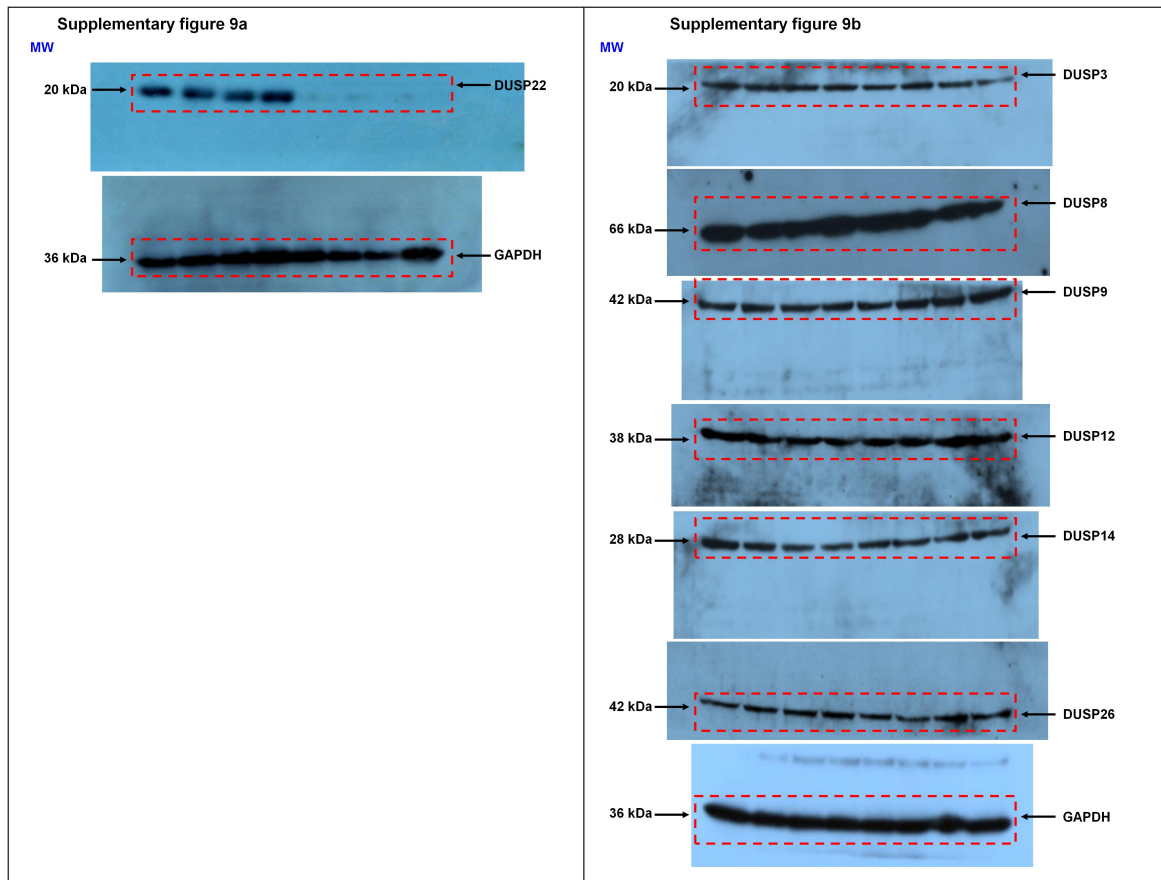
Western blots for supplementary figure 5



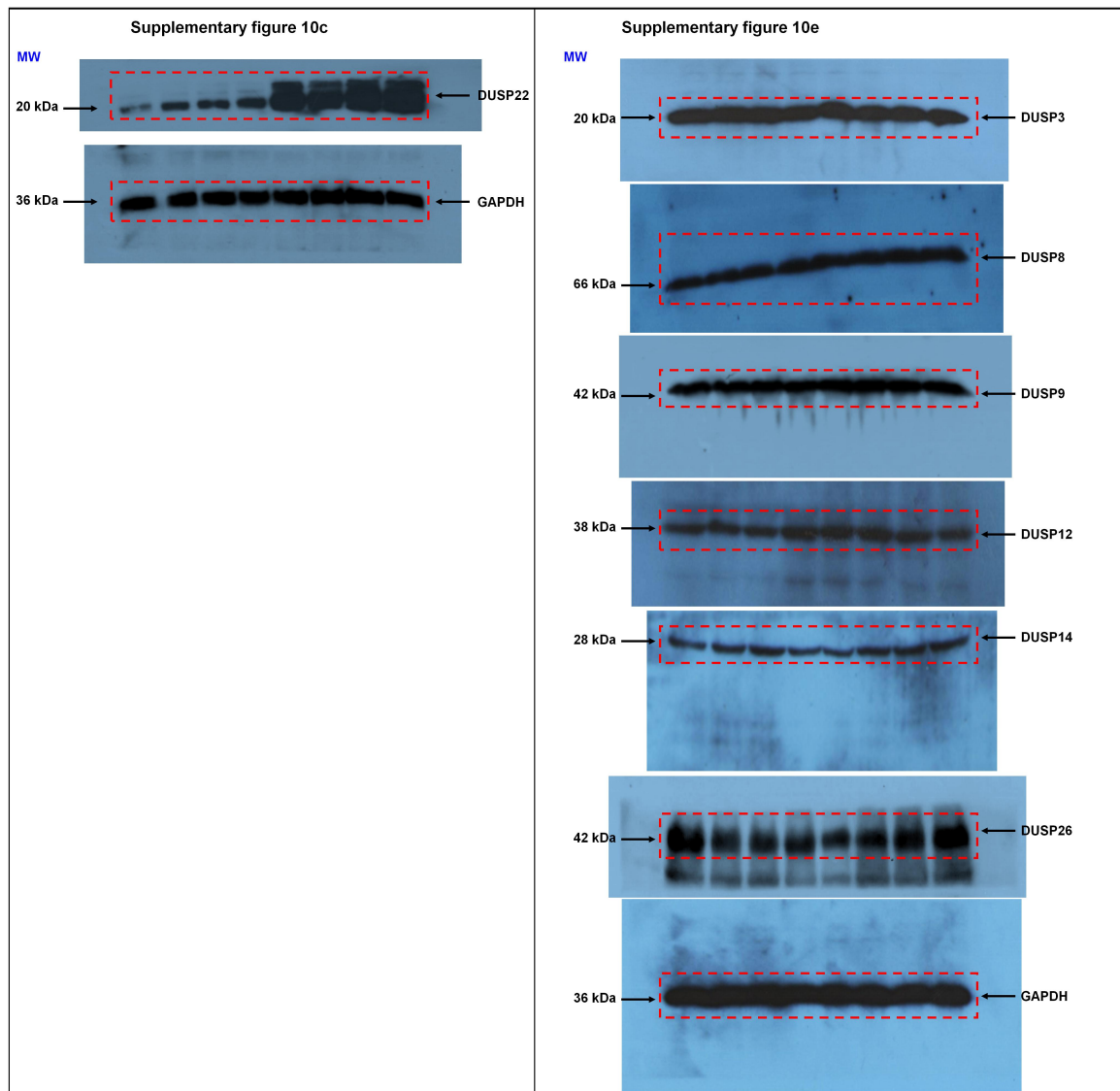
Western blots for supplementary figure 6



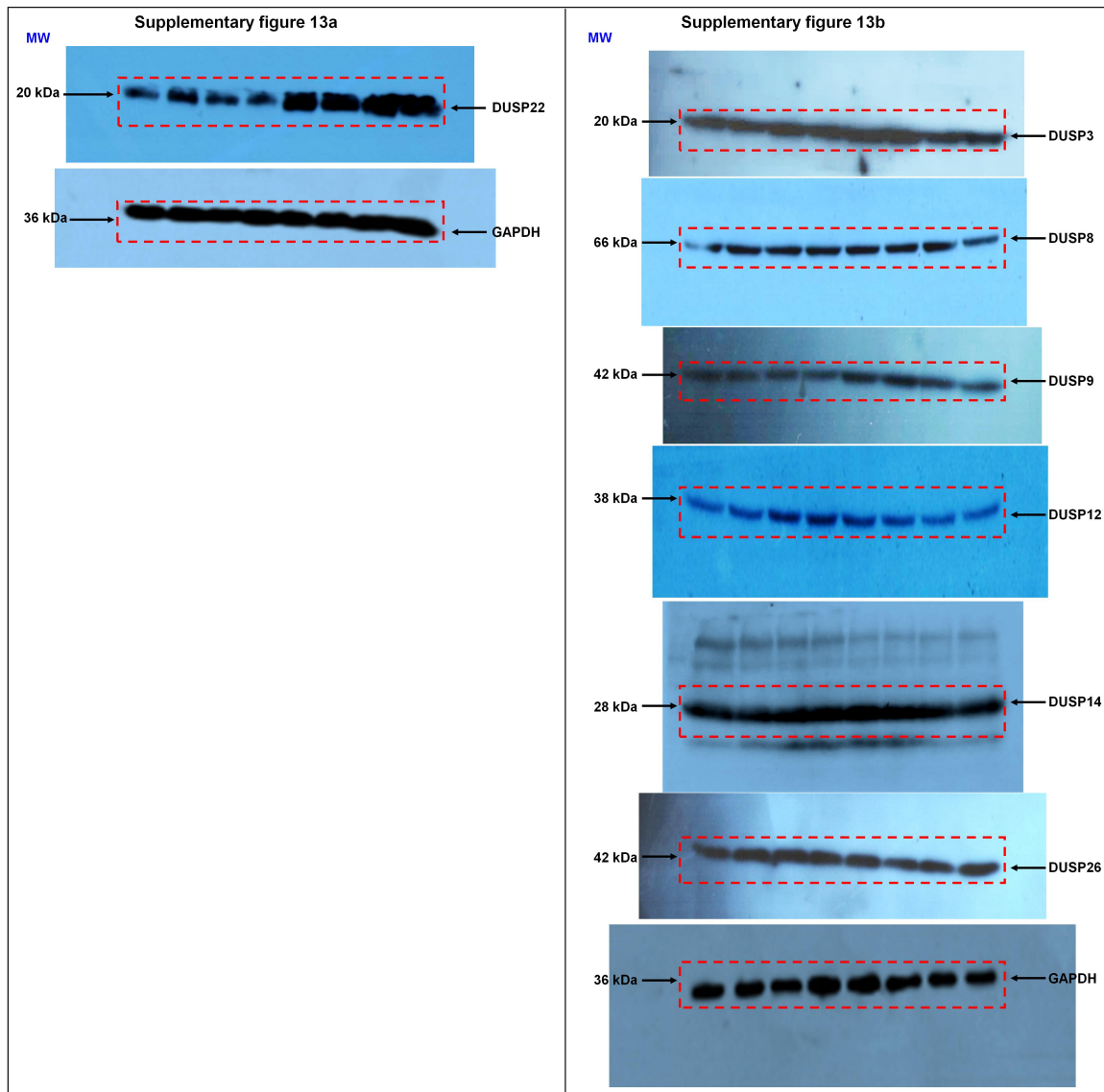
Western blots for supplementary figure 9



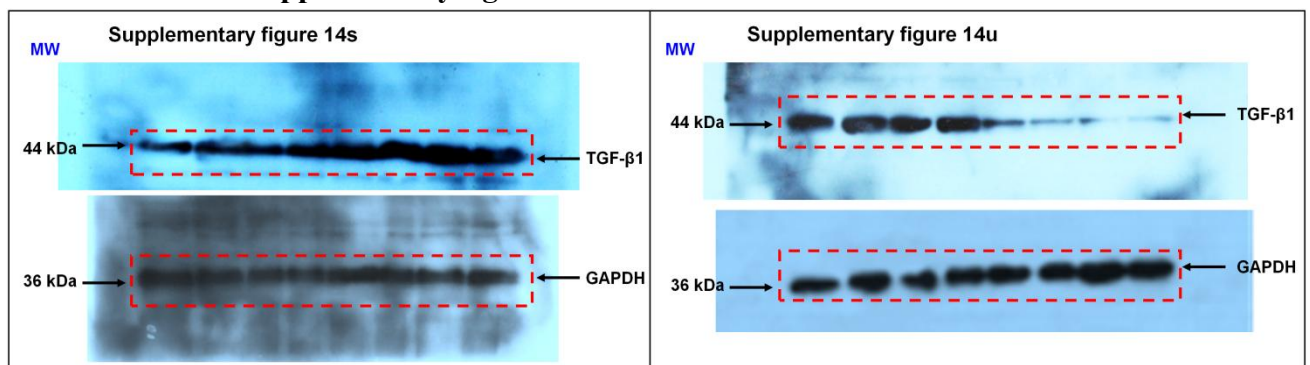
Western blots for supplementary figure 10



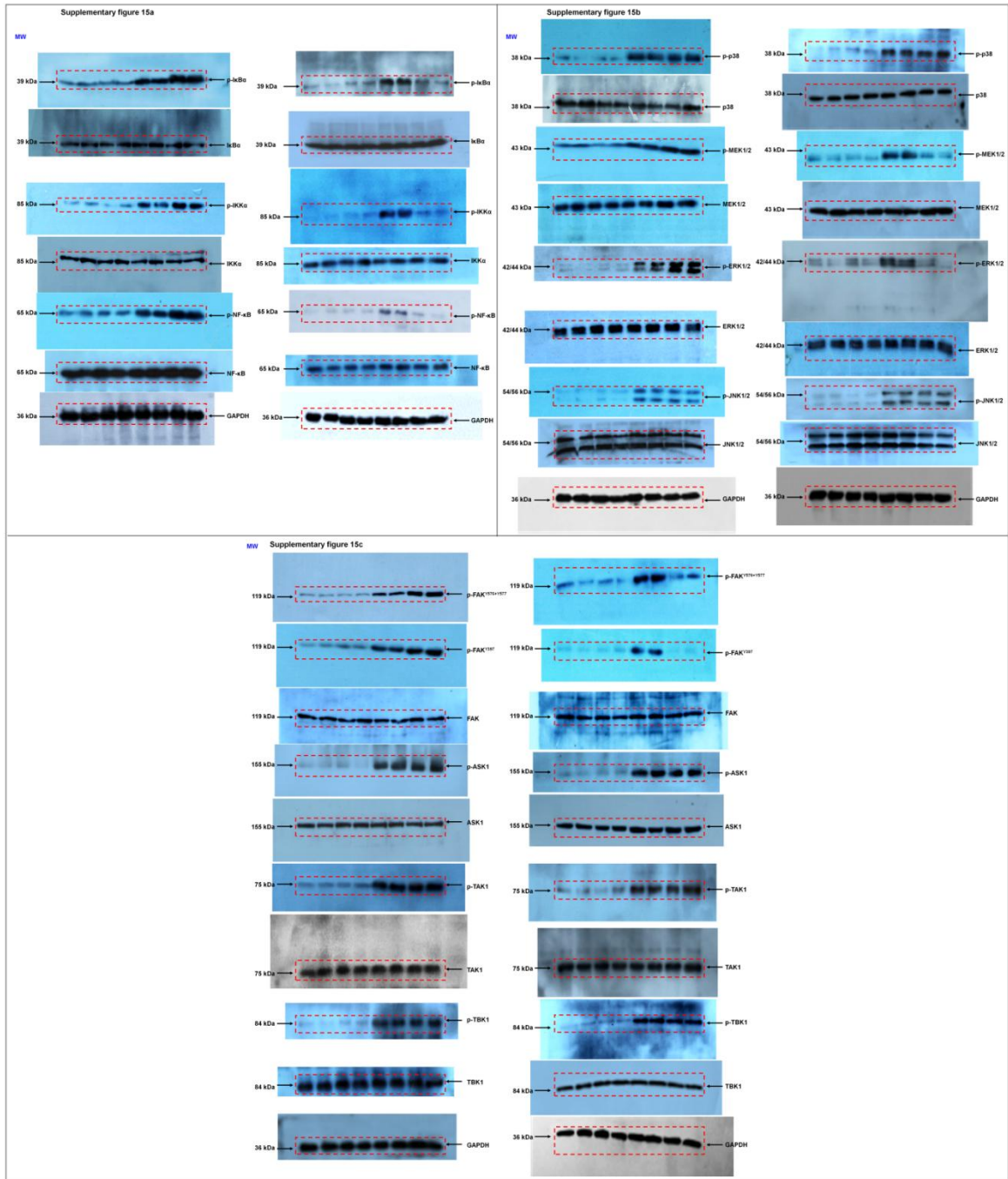
Western blots for supplementary figure 13



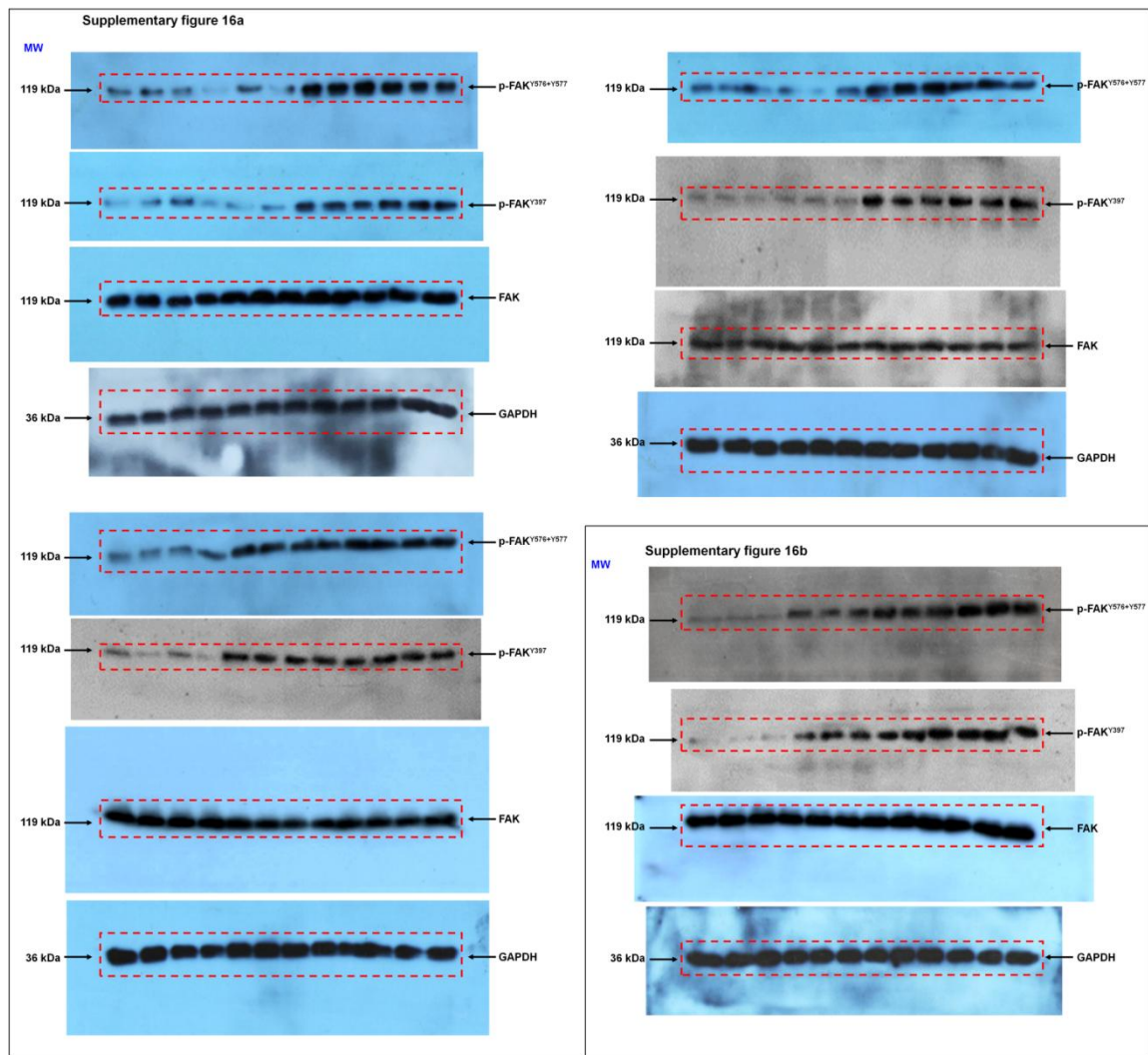
Western blots for supplementary figure 14



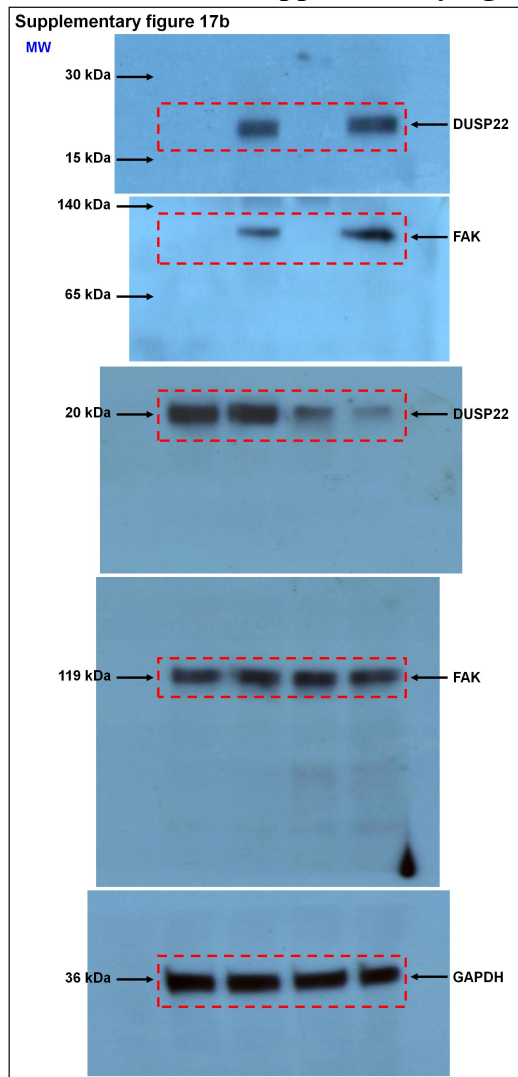
Western blots for supplementary figure 15



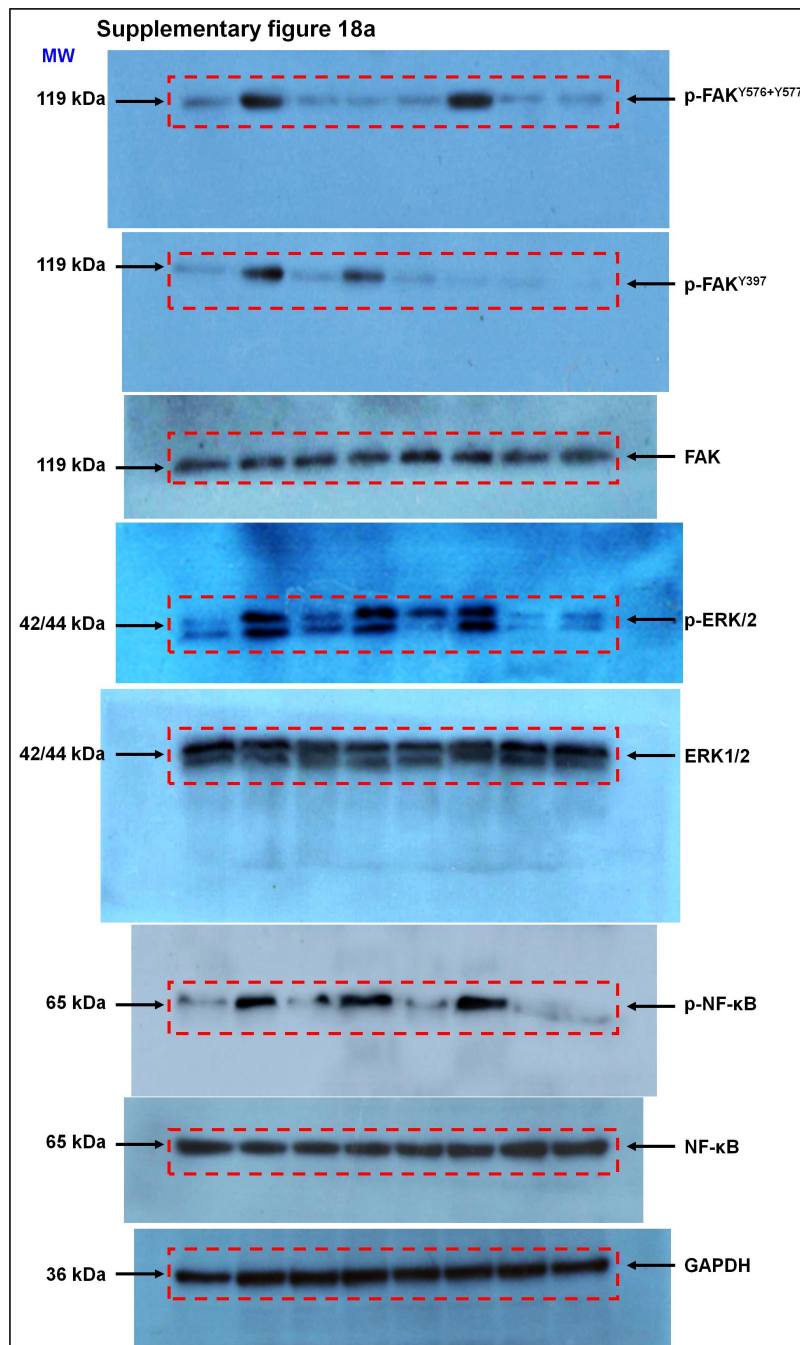
Western blots for supplementary figure 16



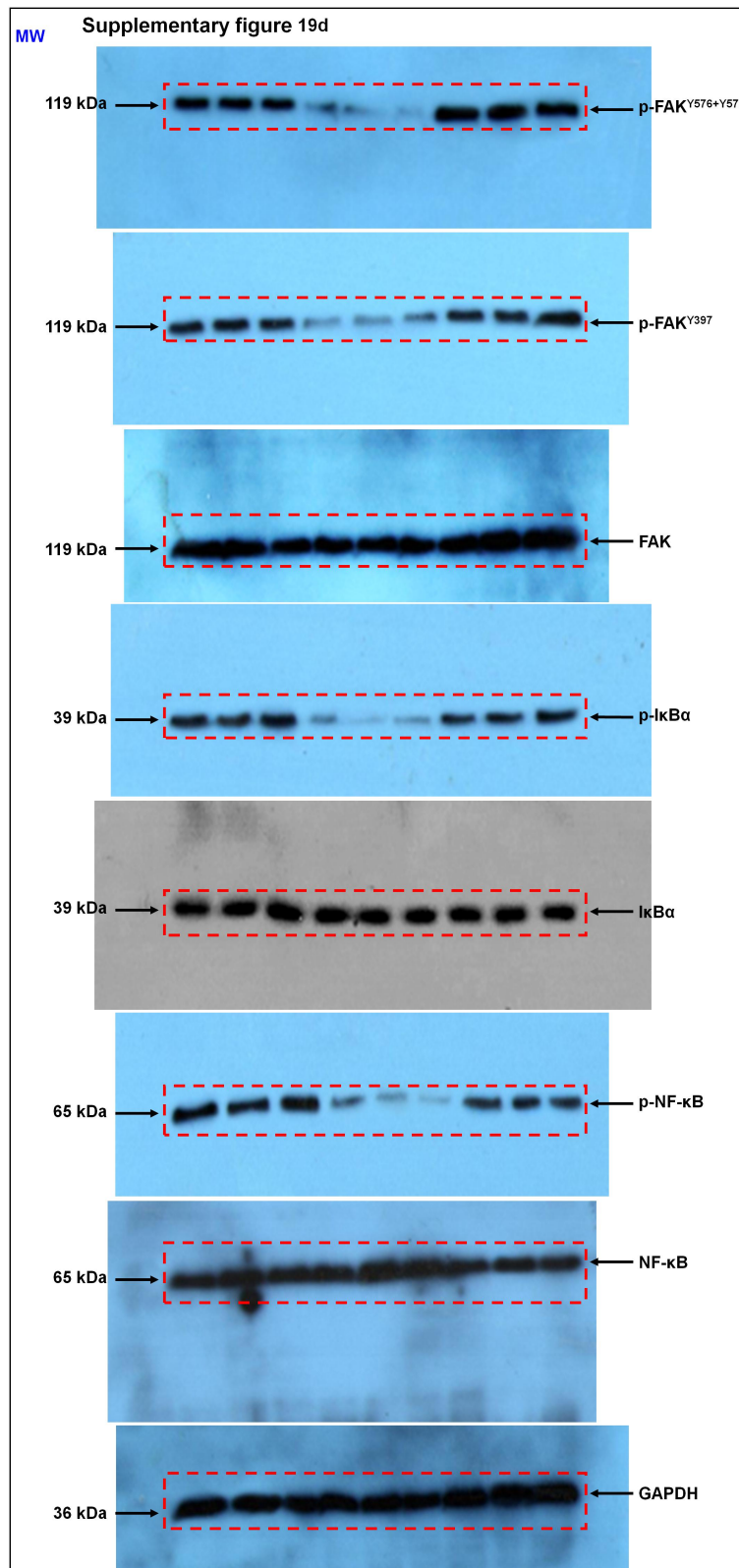
Western blots for supplementary figure 17



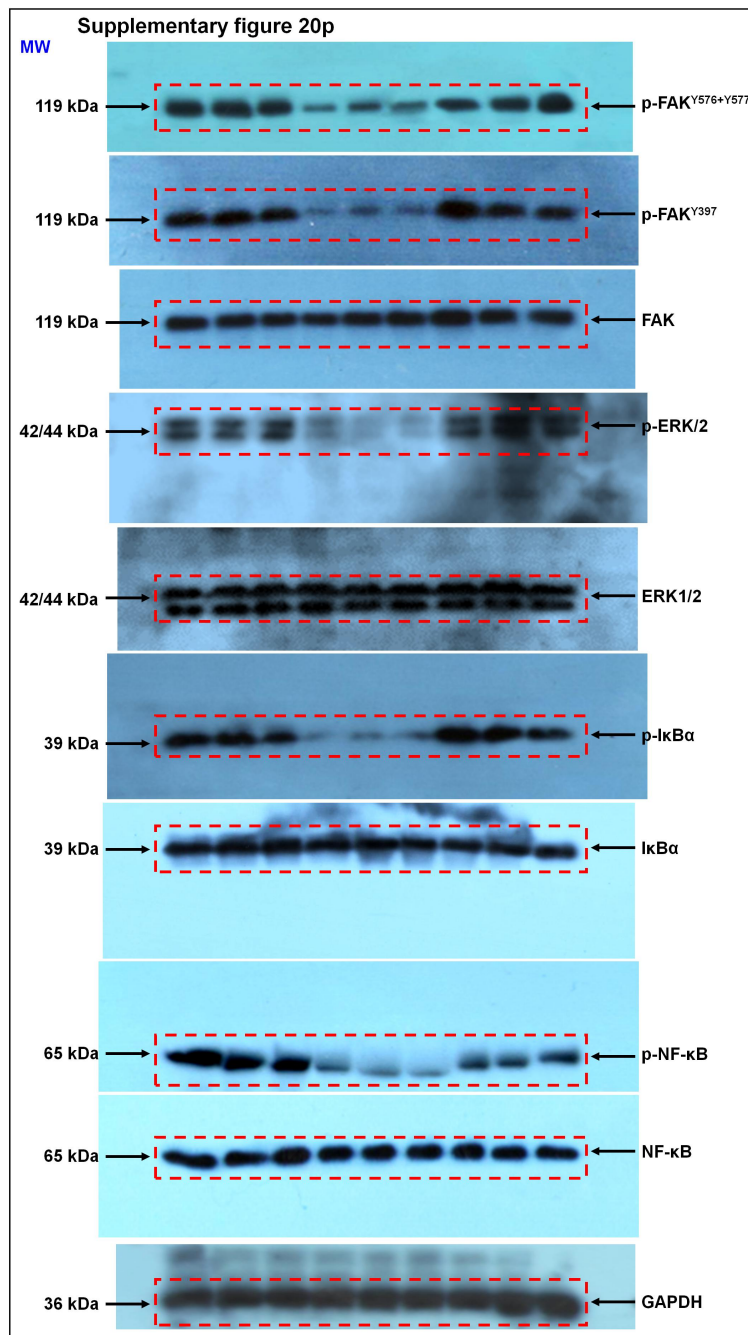
Western blots for supplementary figure 18



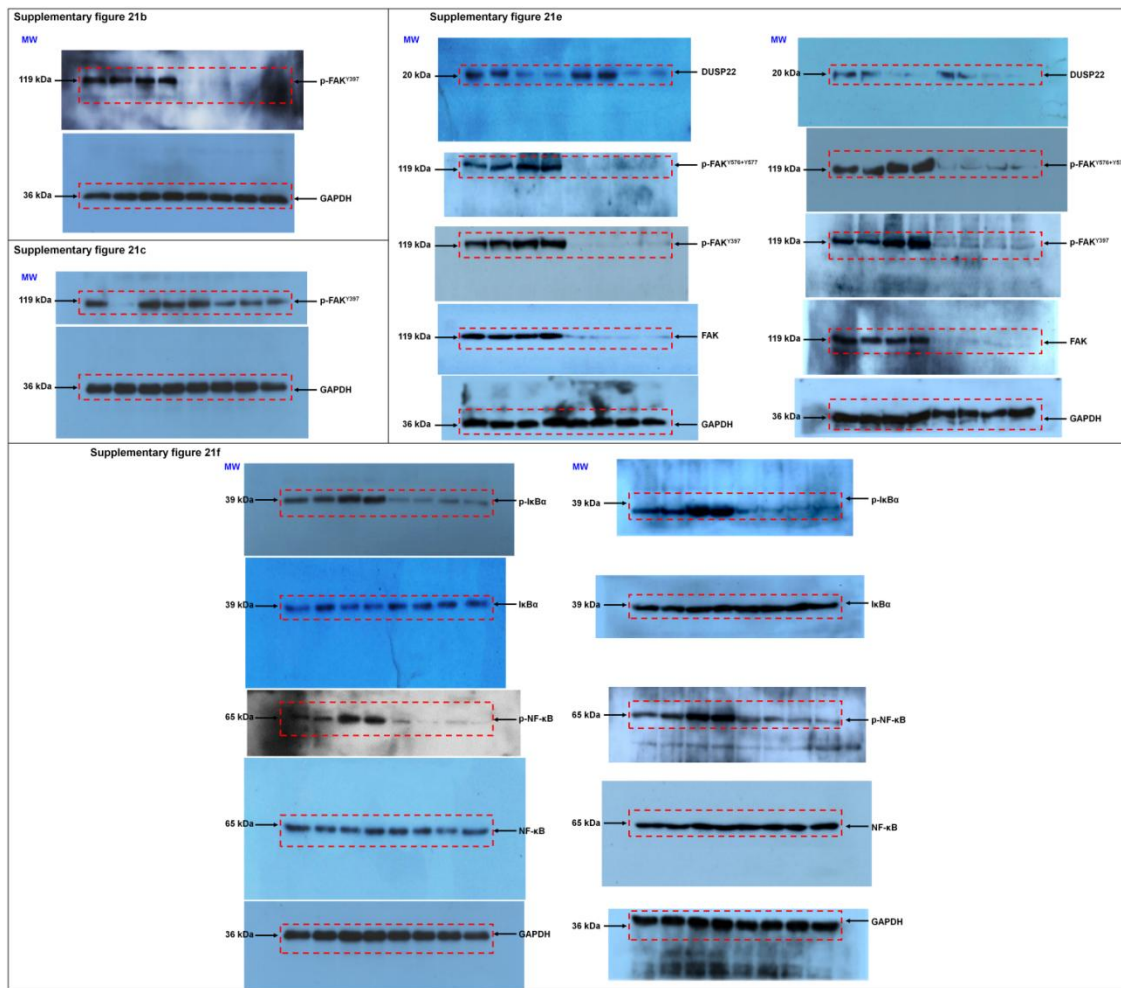
Western blots for supplementary figure 19



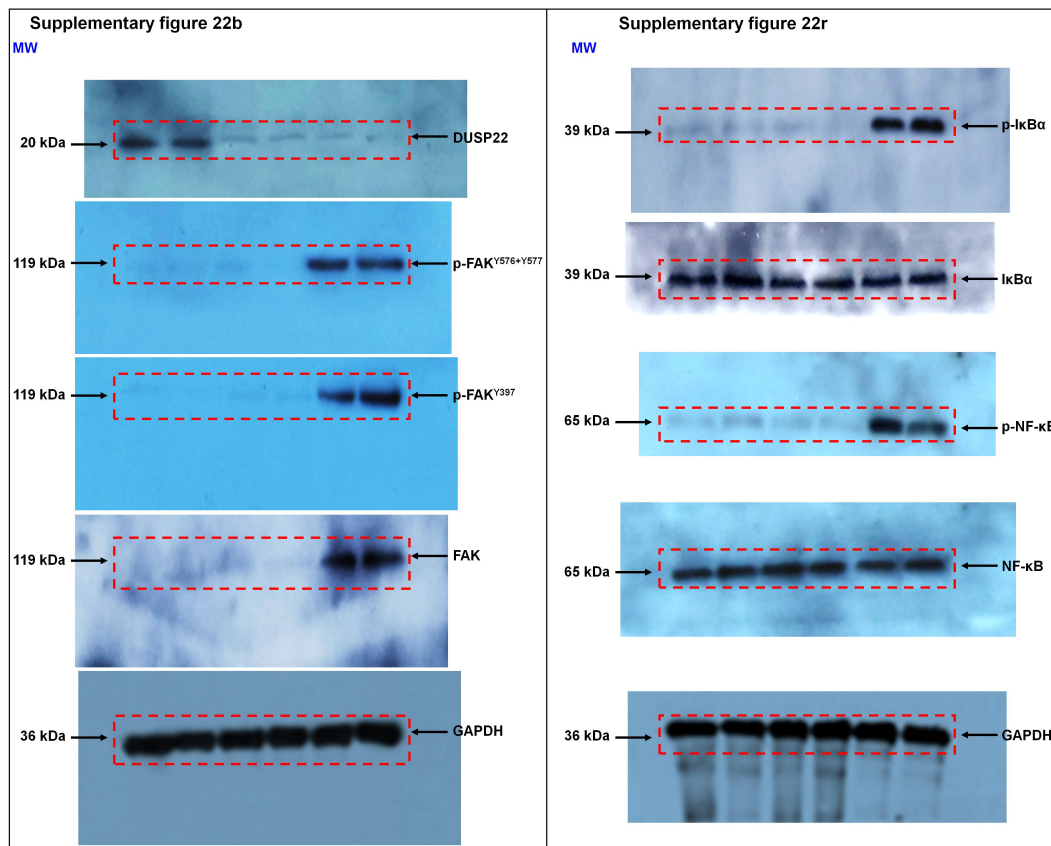
Western blots for supplementary figure 20



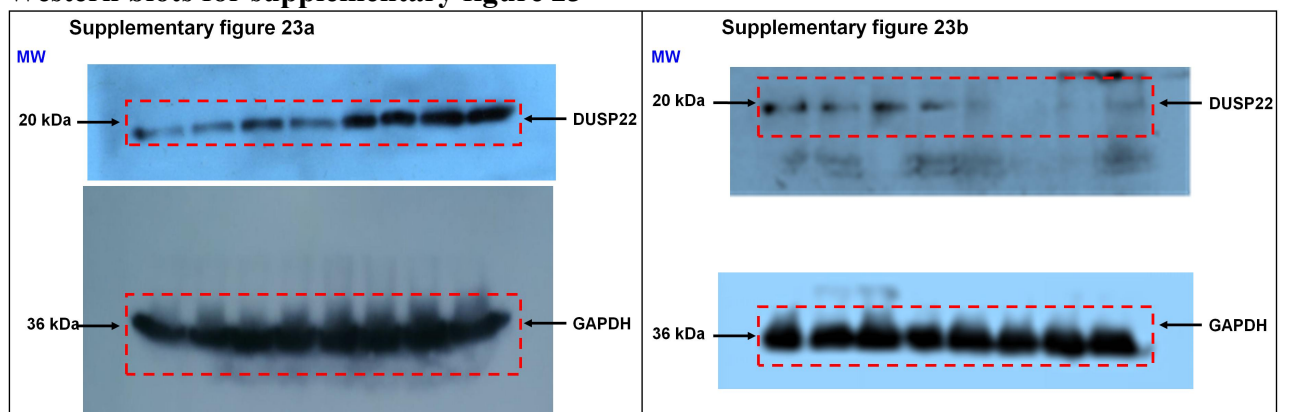
Western blots for supplementary figure 21



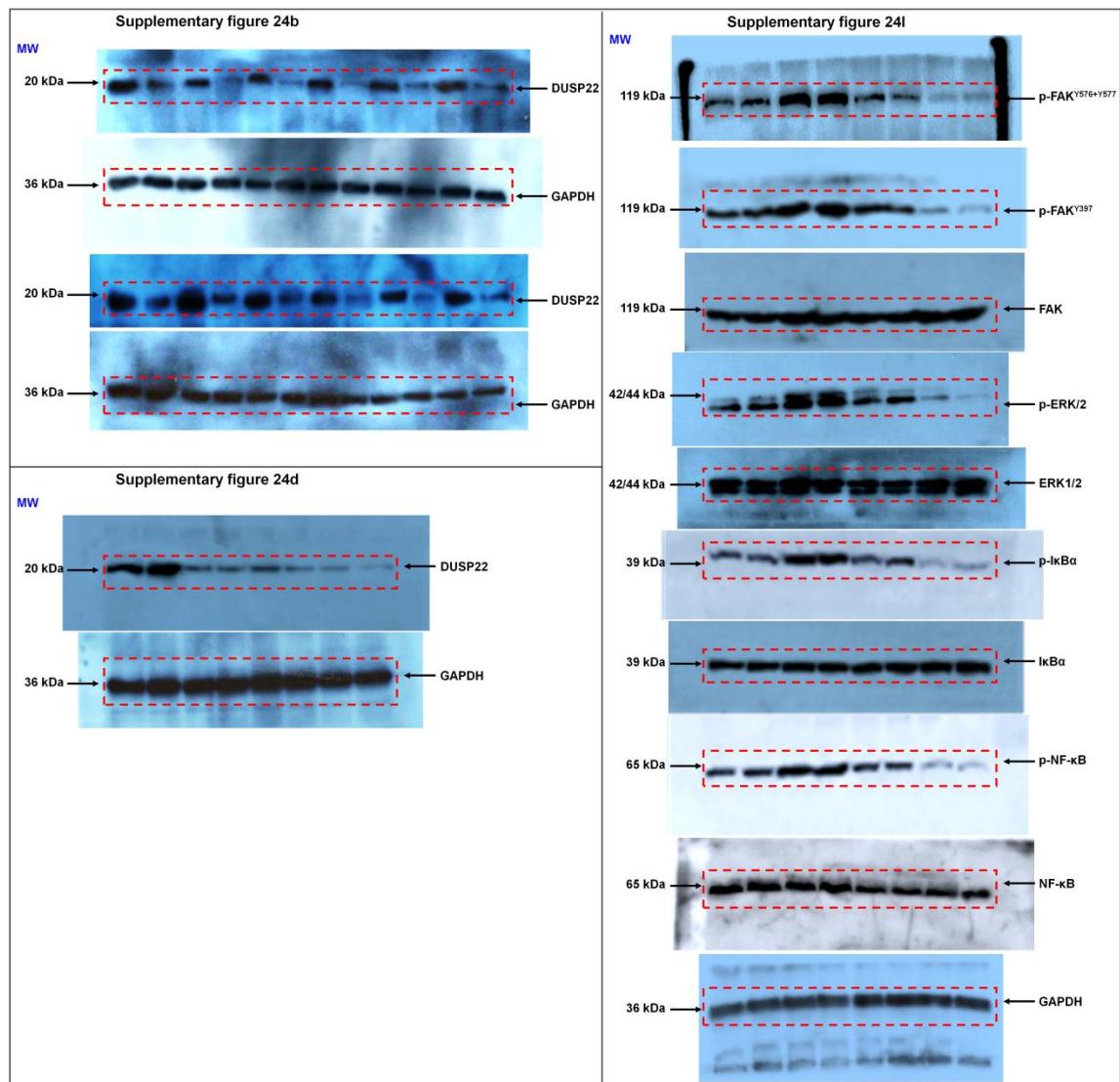
Western blots for supplementary figure 22



Western blots for supplementary figure 23



Western blots for supplementary figure 24



Western blots for supplementary figure 25

